

**Vulnerability mapping in Karst terrains, exemplified in the
wider Cradle of Humankind World Heritage Site.**

By

R.C. Leyland

**Dissertation submitted in fulfilment of the requirements for the degree Magister
Scientia (Environmental and Engineering Geology) in the Department of Geology,
Faculty of Natural and Agricultural Sciences, University of Pretoria, South Africa**

July 2008

Declaration

I, Robert Clive Leyland, hereby declare that the work presented in this dissertation is my own unless referenced otherwise. I also declare that this work has not been submitted at any other institute for any degree, examination or other purpose.

Signed

Date

Abstract

South African karst aquifers are mainly associated with the dolomitic lithologies of the Transvaal Supergroup. Despite the socio-economic and environmental importance of these aquifers, no scientifically based methodology to outline areas that need protection from potential harmful activities exists. Thus an intrinsic resource aquifer vulnerability mapping method for karst terrains in South Africa was developed. The methodology is a modification of the COP aquifer vulnerability mapping method, developed by the Hydrogeology Group of the University of Malaga. The method is predominantly based on the capability of the unsaturated zone to filter or attenuate pollutants by different processes but considers two additional factors that either increase or reduce the protection provided by the unsaturated zone. These are surface conditions that control water flowing towards zones of rapid infiltration, and the temporal availability of a transport agent (rainfall). These three factors are combined to obtain a final vulnerability index, which is spatially visualised using five vulnerability classes (ranging from Very Low to Very High). Modifications to the original COP method include, amongst others, the consideration of rock types commonly found in South Africa, a statistical redefinition of high rainfall (wet) years, a revised consideration of rainfall rates to account for dilution processes and the consideration of older, sediment filled swallow holes.

The method was applied to produce a vulnerability map for Cradle of Humankind World Heritage Site near Krugersdorp, South Africa. The vulnerability map clearly shows the generally inferior but variable aquifer protection in areas characterised by dolomitic lithologies, while surrounding non-karstic areas offer moderate to high resource protection.

The proposed aquifer vulnerability mapping methodology should be used to assess karstic terrains during land use planning and environmental impact assessments. As an easily understandable planning tool the maps can reduce the likelihood of aquifer pollution.

Acknowledgements

I would like to thank the following people and authorities:

Dr Kai Witthüser, supervisor for this study, who provided support, advice and guidance. His endless knowledge on all (geo) hydrological fields proved to be invaluable during the research process.

Professor JL van Rooy, co-supervisor for this study, is also acknowledged for his assistance and guidance.

Professor Ian Meiklejohn and Ms Ingrid Booysen of the Department of Department of Geography, Geoinformatics and Meteorology, University of Pretoria are thanked for there assistance with all matters related to GIS analysis and data capturing.

Mr Martin Holland for his assistance as a fellow MSc student.

The Water Research Commission is acknowledged for making the research possible.

Finally honour and thanks to the one that created the profoundly complex natural systems which we as scientists strive to understand and characterise in simple terms.

Table of contents

| | | |
|-------|--|----|
| 1 | Introduction..... | 1 |
| 1.1 | Motivation..... | 1 |
| 1.2 | Objectives | 2 |
| 2 | Aquifer vulnerability..... | 2 |
| 3 | Karst terrains..... | 5 |
| 3.1 | Origin of karst..... | 5 |
| 3.2 | Characteristics of karst aquifers..... | 6 |
| 3.3 | Groundwater flow in karst aquifers | 10 |
| 4 | Aquifer vulnerability mapping in South African | 10 |
| 5 | The European approach to aquifer vulnerability mapping | 15 |
| 5.1 | The European groundwater vulnerability concept..... | 16 |
| 5.1.1 | Introduction..... | 16 |
| 5.1.2 | The origin-pathway-target model | 17 |
| 5.1.3 | Resource vulnerability vs. source vulnerability..... | 18 |
| 5.1.4 | Groundwater vulnerability in karst areas | 18 |
| 5.2 | Intrinsic vulnerability..... | 18 |
| 5.2.1 | Basic concepts of the European Approach | 18 |
| 5.3 | Specific vulnerability | 20 |
| 5.4 | Hazard mapping | 21 |
| 5.5 | Risk assessment | 22 |
| 5.5.1 | Introduction..... | 22 |
| 5.5.2 | Risk assessment concept..... | 22 |
| 5.5.3 | Risk mapping | 24 |
| 5.6 | Data requirements | 24 |
| 5.7 | Demonstrating the reliability of maps..... | 25 |
| 5.8 | Vulnerability mapping methods..... | 25 |
| 5.8.1 | The PI method..... | 25 |
| 5.8.2 | The VULK analytical transport model and mapping method..... | 26 |
| 5.8.3 | Localised European Approach (LEA) | 27 |
| 5.8.4 | The COP method..... | 28 |
| 5.8.5 | The Time-Input method | 29 |
| 5.9 | Comparative application of the PI and COP methods | 31 |
| 5.9.1 | Introduction..... | 31 |
| 5.9.2 | PI method | 31 |
| 5.9.3 | COP method..... | 32 |
| 5.9.4 | Comparison between PI and COP vulnerability maps..... | 32 |
| 5.9.5 | Hazard mapping | 33 |
| 5.9.6 | Risk mapping | 34 |
| 5.9.7 | Conclusions..... | 35 |
| 6 | Other vulnerability methods | 36 |
| 6.1 | Drastic | 36 |
| 6.2 | German method..... | 36 |
| 7 | VUKA mapping guidelines..... | 37 |

| | | |
|-------|---|----|
| 7.1 | Development of the applied methodology | 37 |
| 7.2 | Overlying layers map | 39 |
| 7.2.1 | O_S sub-score | 39 |
| 7.2.2 | O_L sub-score | 41 |
| 7.2.3 | O score | 45 |
| 7.3 | Precipitation map | 45 |
| 7.3.1 | Pq sub-factor | 45 |
| 7.3.2 | Pi sub-factor | 47 |
| 7.3.3 | P score | 48 |
| 7.4 | Concentration of flow map | 50 |
| 7.4.1 | Scenario 1 | 51 |
| 7.4.2 | Scenario 2 | 57 |
| 7.4.3 | C score | 59 |
| 7.5 | Final vulnerability map | 60 |
| 7.6 | Modifications to original COP method | 60 |
| 7.6.1 | O factor | 60 |
| 7.6.2 | P factor | 62 |
| 7.6.3 | C factor | 62 |
| 7.7 | Utilization of aquifer vulnerability maps | 63 |
| 8 | Aquifer Vulnerability map of the Cradle of Humankind | 65 |
| 8.1 | Physiography, climate and surface drainage | 65 |
| 8.2 | Geological setting | 66 |
| 8.2.1 | General geology | 66 |
| 8.2.2 | Detailed geological description of Chuniespoort Group | 71 |
| 8.3 | Overlying layers map | 74 |
| 8.3.1 | Soil sub-score (O_S) map | 74 |
| 8.3.2 | Lithology sub-score (O_L) map | 77 |
| 8.3.3 | Overlying layers (O) map | 80 |
| 8.4 | Precipitation (P) map | 82 |
| 8.4.1 | Rainfall (Pq) map | 82 |
| 8.4.2 | Temporal distribution (Pi) map | 83 |
| 8.4.3 | Precipitation (P) map | 84 |
| 8.5 | Concentration of flow map | 85 |
| 8.5.1 | Distance to swallow hole (dh) map (Scenario 1 areas only) | 85 |
| 8.5.2 | Slope and vegetation (sv) map (Scenario 1 and Scenario 2 areas) | 86 |
| 8.5.3 | Distance to sinking stream (ds) map (Scenario 1 areas only) | 87 |
| 8.5.4 | Karst development/surface layers (sf) map (Scenario 2 areas only) | 87 |
| 8.5.5 | Concentration of flow (C) map | 88 |
| 8.6 | Final vulnerability map | 90 |
| 9 | Recommendations for future research | 92 |
| 9.1 | Integration with dolomite risk mapping methodologies | 92 |
| 9.2 | Validation of maps | 92 |
| 9.3 | Hazard and risk mapping | 93 |
| 10 | References | 94 |

List of figures

| | |
|--|----|
| Figure 1. Conceptual model of a karst aquifer (Gunn, 1986). | 11 |
| Figure 2. PI Vulnerability map of the Sierra de L bar (Brechenmacher, 2002 in Andreo et al., 2003:186). | 32 |
| Figure 3. COP Vulnerability map of the Sierra de L bar (Andreo et al., 2003:188). | 33 |
| Figure 4. Risk map of the Sierra de L bar (adapted from Andreo et al., 2003). | 35 |
| Figure 5: Diagram of the modified COP method (VUKA) showing the differentiation of the C, O and P factors. | 38 |
| Figure 6. Example of a Land Type Inventory (Macvicar, 1984). | 41 |
| Figure 7. Consideration of different lithologies in the <i>Layer index</i> calculation. | 44 |
| Figure 8. Example of an Overlying layer (O) factor map. | 46 |
| Figure 9: Example of a Precipitation (P) factor map. | 48 |
| Figure 10. Precipitation (P) factor maps for various karst terrains in South Africa. | 50 |
| Figure 11. Examples of swallow holes as seen in aerial photographs. A: Clearly visible feature. B: Feature hidden by dense vegetation, C: New feature not clearly visible on an aerial photograph. | 52 |
| Figure 12. A doline clearly visible in an aerial photograph which acts not as a concentrated recharge point. | 53 |
| Figure 13. Examples of a swallow hole with (A) and without (B) sediment accumulation. | 54 |
| Figure 14. Schematic diagram of a typical karst setting where a swallow hole is blocked with sediment but still linked to the groundwater underneath the sediments (adapted from Trollip, 2006). | 55 |
| Figure 15. Vegetation cover density determined by aerial photograph interpretation. | 56 |
| Figure 16. Extrapolation of surface karst development using aerial photograph interpretation. | 58 |
| Figure 17. Karstic rock areas with different levels of the surface karst development: A: low (<i>fissured carbonate</i>), B: medium (<i>dissolution features</i>) or C: high (<i>developed</i>). | 59 |
| Figure 18: Example of a Concentration of flow (C) factor map. | 60 |
| Figure 19: Example of an aquifer vulnerability map. | 61 |
| Figure 20: Example of A: a Concentration of flow (C) factor map created with conservative <i>dh</i> sub-factor ratings and B: a Concentration of flow (C) factor map created with excessive <i>dh</i> sub-factor ratings. | 64 |
| Figure 21: Location of the Cradle of Humankind World Heritage Site. | 66 |
| Figure 22: Geological map of COHWHS (Obbes, 2000 & own mapping). | 67 |
| Figure 23: Geological map illustrating the distribution of the Transvaal Supergroup (Eriksson & Reczko, 1995). | 69 |
| Figure 24. Soil (<i>O_S</i>) sub-score map for the COHWHS. | 74 |
| Figure 25. Lithology (<i>O_L</i>) sub-score map for the COHWHS. | 78 |
| Figure 26: Overlying layer (O) factor map for the COHWHS. | 81 |
| Figure 27. Rainfall (<i>P_q</i>) sub-factor map for the COHWHS. | 82 |
| Figure 28. Temporal distribution (<i>P_i</i>) sub-factor map for the COHWHS. | 83 |
| Figure 29. Precipitation (P) factor map for the COHWHS. | 84 |

| | |
|--|----|
| Figure 30: Distance to swallow hole (<i>dh</i>) sub-factor map for the COHWHS. | 86 |
| Figure 31: Slope and vegetation (<i>sv</i>) sub-factor map for the COHWHS. | 87 |
| Figure 32: Karst development / surface layers (<i>sf</i>) sub-factor map for the COHWHS. ... | 88 |
| Figure 33: Concentration of flow (C) factor map for the COHWHS. | 89 |
| Figure 34: Aquifer vulnerability map for the COHWHS. | 91 |

List of tables

| | |
|---|----|
| Table 1: Rating and weighting values used for the DRASTIC method in SA (Lynch et al., 1994). | 13 |
| Table 2: Final aquifer vulnerability classes. | 90 |

List of appendices (CD in back cover)

Appendix A: Land Type Inventories of Land Types within the Cradle of Humankind

World heritage Site

Appendix B: Point data used during depth to water map interpolation

Appendix C: Precipitation data for climate stations in the Cradle of Humankind World

Heritage Site Area

Appendix D: Location and sediment fill status of all points identified as swallow holes

1 Introduction

1.1 Motivation

The karstified dolomites of the Chuniespoort Group are capable of sustaining high-yielding boreholes and are the only readily available water resource for many towns, rural areas and farms in the Krugersdorp region. They form a vital component of the water resources needed for the expanding urban and industrial complexes in Gauteng and Rustenburg; hence they are considered as one of the most important aquifers in South Africa (Barnard 2000). Despite its importance no scientific based outline of areas that need protection from potential harmful activities, and areas where such activities would constitute a minor risk to the natural resources and sources exists.

The present pressure on urban development onto dolomite areas are a major concern regarding the safety of residents and will also create an enormous potential source of pollution to the dolomitic aquifers underlying these areas. The concept of vulnerability mapping may also be an important decision tool when expansion of urban areas onto dolomitic land must be evaluated. For this reason a karst terrain vulnerability mapping procedure, taking into account the international knowledge gained in karst vulnerability mapping as well as the specific conditions of the South African dolomites, soils and climatic conditions has been developed. The vulnerability mapping concept may be expanded in the future to include the surface stability (potential for sinkholes and dolines) or the vulnerability against draughts if the resource is used as a regular or emergency water supply.

This report contains

- a summary of the international literature on aquifer vulnerability mapping in karst terrains (sections 2 to 6),
- a detailed description of the methodology for the compilation of aquifer vulnerability maps in South Africa (section 7) and
- a discussion of the maps created for the Cradle of Humankind World Heritage Site (section 8) and recommendations for future research (section 9).

1.2 Objectives

It is hoped that the findings of this research and the aquifer vulnerability mapping methodology that has been produced are utilized to produce aquifer vulnerability maps of karst terrains during land use/development planning investigations and that these maps are then used to prevent the development of more vulnerable areas or at least limit the type of development in such areas so that a low risk of aquifer contamination exists. In this way the research will help to preserve our important karstic groundwater resources. Furthermore it is hoped that this research will open the doors on further karst aquifer vulnerability research and awareness which are both lacking in South Africa.

2 Aquifer vulnerability

The National Research Council (NRC) defines groundwater vulnerability to contamination as “the tendency or likelihood for contaminants to reach a specified position in the groundwater system after introduction at some location above the uppermost aquifer” (NRC, 1993 in Lynch et al., 1994:239). Polluted aquifers are very difficult and expensive to clean and therefore a proactive approach to groundwater protection is economically and technically more viable (Parsons & Jolly, 1994 in van Schalkwyk & Vermaak, 2000:5-4).

Four main groups of contaminant sources are typically considered for vulnerability mapping: Municipal (e.g. sewer leakage), agricultural (e.g. animal wastes), industrial (e.g. pipeline leaks) and mining (e.g. acid mine drainage) sources (Sililo et al., 2001). Sililo et al. (2001) provide a summary of the various pollutant types, impacts and health risks associated with each such source.

The aquifer vulnerability concept is based on the assumption that the physical environment may provide a degree of protection against contaminants entering the ground surface (Vrba & Zaporozec, 1994 in van Schalkwyk & Vermaak, 2000:5-6). Natural attenuation of pollutants occurs when the pollutants pass through the vadose zone and physical, chemical and biological interactions between the material present in the vadose zone and the pollutants result in the reduction of the pollutant concentrations. It

therefore follows that a potential natural attenuation depends on both, the pollutant properties as well as the properties of the vadose zone (Sililo et al., 2001).

The vulnerability of an area depends not only on the contaminant attenuation capacity of the vadose zone, but also on the travel time of infiltrating water and contaminants as well as on the relative quantities of contaminants that can reach the groundwater. All 3 of these factors are a function of geological and hydrogeological attributes like subsoils overlying the groundwater, type of recharge (point or diffuse) and thickness of the vadose zone (Sililo et al., 2001).

The prediction of groundwater vulnerability should therefore be based on the determination of above-mentioned attributes for the area concerned. Many different methods of groundwater vulnerability determination have been developed and have been subdivided by Barber et al. (1993 in Sililo et al., 2001:3.1) into four different classes: Empirical, Deterministic, Probabilistic and Stochastic methods.

- Empirical methods are based on the combination of maps of various physiographic attributes by assigning a numerical index or score to each of the attributes considered (e.g. soil type, groundwater level etc) to arrive at a final rating for the area. Empirical methods are by definition based on experience and professional judgment.
- Deterministic approaches use simplified analytical algorithms to arrive at e.g. a Leaching Potential Index (LPI) expressed in terms of transport velocity, depth to groundwater and potential decay.
- Probabilistic and Stochastic methods require more complex numerical solutions of the governing transport equations and statistical approaches to determine the combination of factors that determine the vulnerability of an aquifer (Sililo et al., 2001).

All methods require different types of data. In general, methods using more detailed knowledge of the system being assessed are considered to be more accurate. However, complex and detailed data may not be available, or economically obtainable, for an area and simpler methods are justified. Barber et al. (1993, in Sililo et al., 2001:3.4) list the following data requirements for vulnerability assessment schemes:

- Meteorological data (required to estimate the natural recharge and as such the amount of infiltration).
- Land surface data e.g. topography and vegetation cover (required to estimate the runoff and infiltration characteristics).
- Vadose zone data (required to arrive at a transport model for the contaminants and to determine the infiltration rate).
- Saturated zone data (required for source vulnerability assessment as lateral transport within the groundwater body must be considered).
- Pollutant properties (required for specific vulnerability assessments as these properties affect transport of different contaminants).
- Soil layer data (used by Sililo et al. (2001) to deduce groundwater vulnerability based on soil properties only).

Ideally vulnerability assessment methods should include a consideration of the hydraulic properties of subsurface material and the use of a qualitative description of the aquifer medium (Aller et al., 1987, Berg & Kempton 1988, Keefer & Berg 1990, Van Stempvoort et al., 1993, Navulur et al., 1995 in Beskesi & McConchie, 2002:324). However, due to the lack of available data many regional vulnerability assessments either use qualitative descriptions of the aquifer medium, based on information from geological maps and well drillers' reports (Keefer and Berg 1990; Van Stempvoort et al. 1993 in Beskesi & McConchie, 2002:324), as a proxy for hydraulic conductivity, or do not consider hydraulic conductivity at all (Reynders, 1994 in Beskesi & McConchie, 2002:324).

The aim of an aquifer vulnerability assessment is to protect groundwater quality by providing development planners, regulators and all water authorities with a simple means of incorporating groundwater into their planning decisions (Campbell, 2004). By presenting such decision makers with aquifer vulnerability maps, vulnerable areas can be avoided during future developments or sites in vulnerable areas can be engineered in such a way to avoid contamination (van Schalkwyk & Vermaak, 2000).

So far no karst specific aquifer vulnerability mapping studies have been conducted in South Africa. In Europe a comprehensive study know as COST Action 620

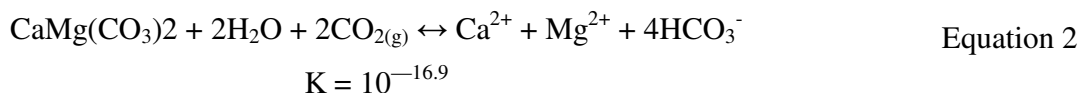
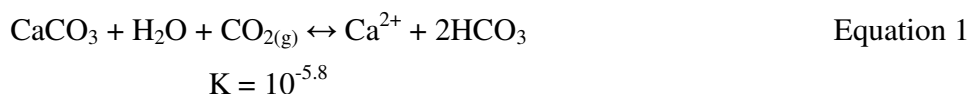
has been completed with the aim of developing an approach to “vulnerability and risk mapping for the protection of carbonate (karst) aquifers” (Zwahlen, 2003). This is the most comprehensive available study focussed on aquifer vulnerability in karst terrains.

3 Karst terrains

3.1 Origin of karst

Karst features mainly occur in carbonate rocks, limestone and dolomite, and in such formations the associated features are considered as true karst. Evaporite formations (e.g. gypsum and anhydrite) and sometimes quartzite formations can, when special geochemical processes occur, also develop karst phenomena, but are not considered true karst (Bakalowics, 2005). Because of the unique nature of true karst systems, only karst in carbonate rocks will be considered in this report. Carbonate rocks occupy about 12% of the planet’s dry, ice-free land (Ford and Williams, 1989 in Bakalowics, 2005:149) and may be one of the most important aquifer formations in the world (along with alluvium). Despite the complexity and number of unknown associated with the karst medium, it is certainly one of the most suitable aquifers for a joint patrimonial protection and exploitation of its resources. One significant result of karstification is the development of highly permeable zones of large storage capacity, capable of sustained groundwater extraction from high-yielding boreholes. However the heterogeneity of karst aquifers makes it difficult to quantify and predict the movement of groundwater and contaminants through and/or between different aquifer zones.

Karst is commonly considered to be the result of the solution of carbonate rocks (referred to as “karstification”). When infiltrating rainwater is in equilibrium with the carbon dioxide in the atmosphere (~0.035%) and the soil zone (up to a few %), it forms a weak carbonic acid (H_2CO_3). This weakly acidic water causes the dissolution of the carbonate minerals while circulating through a dolomitic succession. The final result is the development of open cavities and caves. The weak acid reacts with the carbonate rocks according to the set of equilibrium reactions, as shown in Equation 1 (calcite) and Equation 2 (dolomite).



Flowing water exports the products of the dissolution process resulting in underground voids that progressively organise into a hierarchical structure (known as the conduit system or karst network) in the vadose and the phreatic zone. Karst therefore develops only if there is a possibility of dissolving carbonate rock (i.e. the existence of a solvent) and groundwater flow determined by a hydraulic gradient exists (Bakalowics, 2005).

Geologically karstification is very rapid process and different approaches (Bakalowicz 1975; Atkinson et al. 1978; Dreybrodt 1998) have shown that a few thousand years (generally less than 50 ky) are sufficient for the development of an integrated karst network. As a result of the short development time carbonate aquifers exist in a range of forms ranging from fractured, non-karstic aquifers to truly karst aquifers. Between these two extremes all the intermediate stages of karst conduit development can be found.

3.2 Characteristics of karst aquifers

The term karst describes a terrain generally underlain by limestone or dolomite, in which the landforms are formed by the dissolution of rock (karstification) and in which the drainage is underground in fissures, conduits and caves enlarged by solution (IAH, 1999). Karst networks are highly heterogeneous and different from all other heterogeneous media, even the fracture medium from which they originate. Drogue (1974), Grillot (1977) and Razack (1980) (all in Bakalowics, 2005:151) agree that a karst network pattern is predetermined by the fracture pattern with the main conduits developing along the main faults and fractures and the smaller conduits developing on fissures. Most karst hydrogeologists however assume that the karst network is different from the fracture pattern. Karst processes “select” some of the original discontinuities,

fractures, joints, bedding planes or macro-porosities, and develop a hydraulic continuum from surface to spring. This heterogeneity progressively becomes organized into a hierarchy in the same way a fluvial system does. Conduits in karst networks are classically several meters wide and kilometers long and flow conditions within these conduits may be identical to those in surface rivers, with free surface flow and high velocities as well as flow rates. Confined flow conditions may also commonly occur in phreatic conduits during flood seasons (Bakalowics, 2005).

In the phreatic zone, karst networks locally result in very high hydraulic conductivities in the aquifer and these areas function as a drainage-pipe network, draining out groundwater stored in the phreatic zone and water flowing through the vadose zone. In porous and fractured media aquifers the storage capacity is associated to well-known types of voids and may be assessed by geological and hydraulic methods. However, hydrogeologists disagree about storage conditions in karst aquifers with the following three main models of organization of groundwater flow in the phreatic zone (Bakalowics, 2005):

- **Groundwater is stored in the rock matrix**, i.e. primary and secondary rock porosity. According to Drogue (1974), Mudry (1990) and Kiraly (1997) this model assumes that the phreatic zone is hydraulically continuous, with a relatively low permeability and the karst aquifer is considered as a double-continuum medium with the saturated matrix porosity drained by conduits.
- **Groundwater is stored in karstic voids** that develop around the conduits and are connected to them by high water head loss zones. According to Mangin (1994 in Bakalowics, 2005:151), the strong permeability contrast (several orders of magnitude) between the matrix and conduits results in an absence of exchanges and makes the storage in the matrix negligible. The phreatic zone is therefore hydraulically discontinuous. Marsaud (1996 in Bakalowics, 2005:151) represents the karst phreatic zone to be made up of pipes draining drums.
- **Groundwater storage in the phreatic zone does not exist** and the karst network drains groundwater from the vadose zone. In this model, the epikarst with its local and seasonal saturated part plays an important role in storage.

Depending on the rock texture and structure and the geological history of the formation, typically one of these models dominates. The epikarst acts as an exchange zone between the bio-atmosphere and the karst itself, storing groundwater locally and seasonally in a perched saturated zone. The recharge occurs either directly into the infiltration zone from points breaking the epikarst (sinkholes and swallow holes) or through the epikarst. The saturated part of the epikarst delays the diffuse infiltration by percolating through vertical cracks at its base but also discharges by overflow into vertical conduits during the rainy season (Bakalowics, 2005).

The classical hydrogeological approaches used to deduce aquifer properties are generally ineffective in karst aquifers because of their inability to show the existence of conduits. In the classical hydrogeological approach a detailed description of the geological framework (especially the fracturing distribution) was considered as the most efficient way to characterize a karst network. However Eraso (1986 in Bakalowics, 2005:154) showed that such an approach is not sufficient as groundwater flow follows preferential pathways based on both the connectivity of the discontinuities and the hydraulic gradient existing between the recharge and discharge area. Later case studies showed the difficulty or even the impossibility in inferring the karst network structure from the geological framework and fracturing distribution (Bakalowics, 2005). An alternative approach is to analyse karst system functioning from hydrodynamics (Mangin, 1974, 1984; Marsaud, 1996), hydrothermics (Andrieux, 1976), and various natural tracers (Plagnes, 1997; Rouch, 1980; Bakalowicz, 1979; Bakalowicz et al. 1974). Currently most karst hydrogeologists investigate carbonate aquifers by using a combination of some of these methods.

The unique properties that need to be considered in karst terrains are (Zwahlen 2003):

- Each karst system has its own individual characteristics.
- Karst systems are highly heterogeneous and anisotropic and therefore the interpolation and extrapolation of field data is problematic for karst areas.
- Karst groundwater is recharged by two methods, diffuse infiltration through the soil and concentrated point recharge via dolines and swallow holes.

- Lateral surface or subsurface flow has to be expected in areas covered by low permeability layers (e.g. tributaries to a stream sinking into the karst aquifer via a swallow hole) and as such the protective function of the overlying layers may be bypassed.
- The presence of an epikarst zone has to be expected and this can function both as a water storage zone (which increases the natural protection of the system) and a concentration of flow zone (which increases the vulnerability of the system). The structure and function of the epikarst zone are difficult to assess, as a large portion of it is not visible at the land surface.
- Karstic aquifers are dual porosity aquifers (due to fractures and solution voids), but can frequently be triple porosity aquifers due to the additional presence of inter-granular pores (matrix). Groundwater storage takes place in pores and fractures, while conduits act as drains. The combination of both extremely fast and slow flow components within a karst system results in contaminants being transported very fast or stored for a very long time.
- Karst systems are characterised by fast and strong hydraulic reactions to hydrologic events and the temporal variations of the groundwater table often reach several tens of meters. In addition to this the groundwater table in karst systems is often discontinuous and difficult to evaluate.
- Karst catchments are extremely complex, often extremely large and hydraulically connected over long distances. Tracer tests have shown some flow paths of karst springs to cross each other and the catchments of karst springs to often overlap.

The chemical properties of karst systems are also fairly unique in that the carbonate medium present in karst areas restricts the mobility of reactive contaminants such as phosphate (which precipitates as apatite) and heavy metals (that can precipitate as carbonate species). Acid rains or waters (e.g. acid rock drainage) are quickly buffered by the carbonate medium and the pH value of water in karst aquifers, despite its low variability due to the buffer effect of the carbonate medium, can together with Redox-potential (E_h) play a role in the solubility of inorganic metals (Zwahlen, 2003).

3.3 Groundwater flow in karst aquifers

Karst aquifers are often characterised by a dual or triple porosity, comprising of solutional voids, fractures and the rock matrix (intergranular pores). While the fractures and the rock matrix provide predominately storage potential, the conduits act as drains. Hence a fast advective transport of contaminants with significant tailing effects similar to fractured aquifers can be expected emphasizing the vulnerability of karst aquifers. An epikarst zone (if present) either allows diffuse infiltration of surface water, or concentrates the surface water flow into vertical conduits such as fractures and fault zones (Figure 1). Where sinkholes or swallow holes are present, they break and bypass the epikarst zone (Bakalowicz, 2005). Theoretical and practical problems associated with karst aquifers result from this duality of the aquifer recharge, storage and discharge processes (e.g. Pinault et al., 2001; Kiraly, 2003; Scanlon et al., 2003).

4 Aquifer vulnerability mapping in South African

Scientific investigations of the karst regions in South Africa started in the early sixties (De Kock, 1964; Brink & Partridge, 1965). Since then many investigations have been carried out by geologists, hydrologists and geomorphologists. Therefore, different approaches prevailed in karst studies, each with their own concepts and methods. On the one hand, karst evolution and the cycle of karst development associated with the regional dolomite have long attracted attention from South African geologists (Marker, 1972; Martini & Kavalieris, 1976; Marker, 1980; Wolmarans, 1986; Martini et al., 2003).

On the other hand, investigations on the groundwater potential of the regional dolomite emerged when more groundwater was needed for the growing population and the impact of the gold mining activities needed to be addressed. This led to numerous large-scale and widespread groundwater investigations carried out by Enslin & Kriel (1967), Fleisher (1981), Foster (1984); Bredenkamp et al., (1986), Kuhn (1986), Bredenkamp (1995) and Barnard (1997).

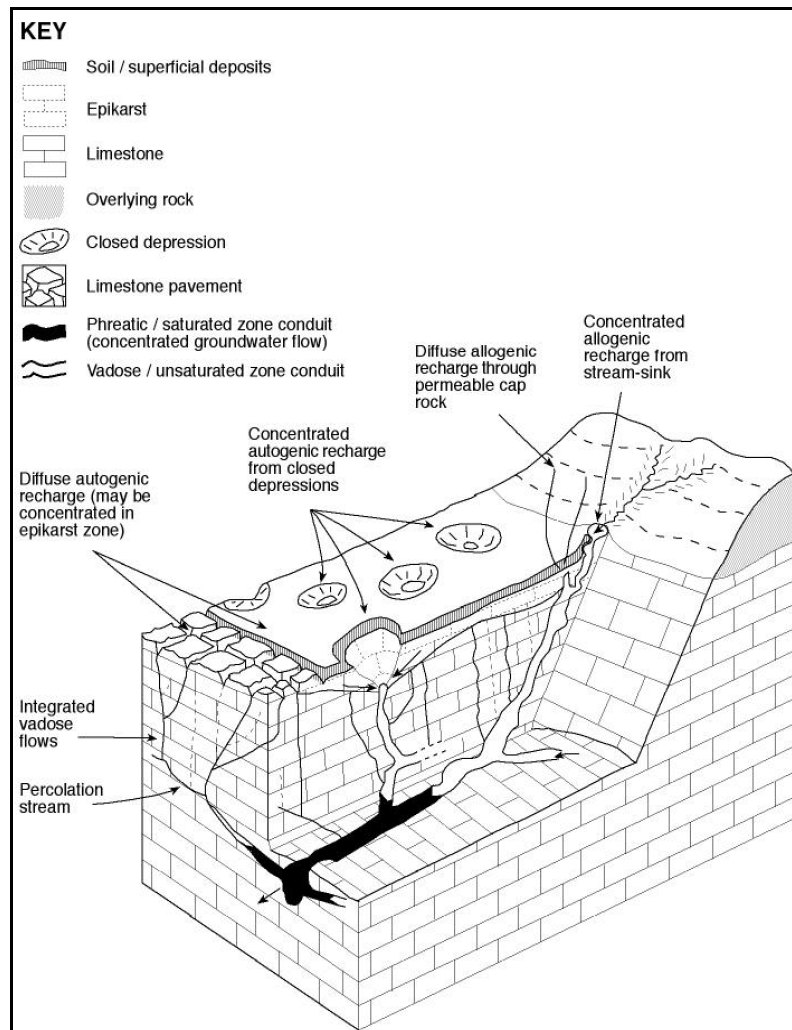


Figure 1. Conceptual model of a karst aquifer (Gunn, 1986).

Lynch et al. (1994) produced a national-scale groundwater vulnerability map of southern Africa using the DRASTIC methodology (see section 6.1). The rating values used as well as the weighting values for each of the parameters are shown in Table 1. Lynch et al. (1994) did not include the hydraulic conductivity (CR) parameter in their vulnerability analyses as at the time of the study they believed the information that was available on hydraulic conductivity values for Southern Africa was insufficient. They also mention that DRASTIC does have some limitations and that these are contained in the vulnerability map of Southern Africa. They give the following non-comprehensive list of physical parameters that have a strong influence on the groundwater vulnerability, but are neglected by the DRASTIC methodology: fracturing & faulting, effects of

precipitation intensity and duration, soil reactivity, anisotropy and heterogeneity of the soil, the vadose zone and the aquifer hydraulic conductivity.

Due to the fact, that not all data sets required for the vulnerability assessment were available, many assumptions were made during the creation of the various layers in the GIS (Lynch et al., 1994). For example, the factor weightings used during this study (Table 1) were those agreed upon for the USA and therefore may not be applicable to local conditions. However, Lynch et al. (1994) noted that since the results of the method are used as means of comparing the relative vulnerability between different areas, the weightings used are justifiable. However, no attempts were made to validate the vulnerability map of Southern Africa.

As a result of the large area mapped and the assumptions made in the DRASTIC evaluation process, the produced map shows large areas of equal vulnerability and can't be used for practical applications. With respect to the usefulness of this map for determining the vulnerability of karst areas, it is important to note that the impact of the vadose zone rating (*IR*) was assigned a single value for all areas underlain by dolomite irrespective of the actual thickness or properties of the vadose zone. This will obviously not be a true reflection of the vulnerability of dolomite areas as the properties of the vadose zone may differ significantly within these areas. The need for local scale aquifer vulnerability mapping is thus illustrated by the shortcomings of the national scale map produced by Lynch et al. (1994).

According to Sililo et al. (2001) this is the only type of vulnerability assessment method that has been applied in South Africa. They also note that this map can only be used as a preliminary reconnaissance tool and not for a site-specific assessment of aquifer vulnerability. They attribute this to the assumptions and generalizations made during the production of this map. The actual vulnerability of an area may be totally different from the assigned values. It is for this reason, that smaller scale maps, which show more accurately the true vulnerability of areas and can be used as decision making tools, should be produced (Sililo et al., 2001).

Table 1: Rating and weighting values used for the DRASTIC method in SA (Lynch et al., 1994).

| Depth to groundwater (<i>DR</i>) | | Net recharge (<i>RR</i>) | |
|---|--------|--|--------|
| Range (m) | Rating | Range (mm) | Rating |
| 0-5 | 10 | 0-5 | 1 |
| 5-15 | 7 | 5-10 | 3 |
| 15-30 | 3 | 10-50 | 6 |
| >30 | 1 | 50-100 | 8 |
| | | >100 | 9 |
| Aquifer media (<i>AR</i>) | | Soil media (<i>SR</i>) | |
| Range | Rating | Range | Rating |
| Dolomite | 10 | Sand | 8-10 |
| Intergranular | 8 | Shrinking and/or aggregated clay | 7-8 |
| Fractured | 6 | Loamy sand | 6-7 |
| Fractured & weathered | 3 | Sandy loam | 5-6 |
| | | Sandy clay loam and loam | 4-5 |
| | | Silty clay loam, sandy clay and silty loam | 3-4 |
| | | Clay loam and silty clay | 2-3 |
| Topography (<i>TR</i>) | | | |
| Range (% slope) | | | Rating |
| 0-2 | | | 10 |
| 2-6 | | | 9 |
| 6-12 | | | 5 |
| 12-18 | | | 3 |
| >18 | | | 1 |
| Impact of the vadose zone (<i>IR</i>) | | | |
| Range | | | Rating |
| Gneiss, Namaqua metamorphic rocks | | | 3 |
| Ventersdorp, Pretoria, Griqualnd West, Malmesbury, Van Rhynsdorp, Uitenhage, Bokkeveld, Basalt, Waterberg, Soutpansberg, Karoo (northern), Bushveld, Olifantshoek | | | 4 |
| Karoo (southern) | | | 5 |
| Table Mountain, Witteberg, Granite, Natal, Witwatersrand, Rooiberg, Greenstone, Dominion, Jozini | | | 6 |
| Dolomite | | | 9 |
| Beach sands and Kalahari | | | 10 |
| Parameter weightings | | | |
| <i>D_w</i> | | | 5 |
| <i>R_w</i> | | | 4 |
| <i>A_w</i> | | | 3 |
| <i>S_w</i> | | | 2 |
| <i>T_w</i> | | | 1 |
| <i>I_w</i> | | | 5 |
| <i>C_w</i> | | | 3 |

Foster (1987) believes that the vulnerability of an aquifer to pollution (normally due to anthropogenic activities) is directly linked to the following factors:

1. The accessibility of the saturated zone to penetration of mobile contaminants.
2. The physicochemical retention or reaction of pollutants resulting in attenuation.
3. Manner of pollutant disposition.
4. Physicochemical mobility and persistence of the pollutants.

The WRC has funded the study of the above-mentioned factors in various research projects. Van Schalkwyk & Vermaak (2000) investigated factor 1 in a WRC funded project focussing on the hydrogeological properties of soils and rocks in the vadose zone that affect aquifer recharge and pollution. Factors 2 and 4 were studied in a WRC funded project, that investigated the contaminant attenuation capacity of soil/aquifer systems focusing on the vadose zone (Sililo et al., 2001). They presented a provisional groundwater vulnerability classification system based on two criteria. The first of these criteria is the “hydraulic attenuation” which is given a rating from 1 (maximum hydraulic attenuation) to 5 (minimum hydraulic attenuation) based on the physical properties of the soil in the area. The second criterion is the “chemical attenuation”, which is given three ratings (for cationic, anionic and organic contaminants) from 1 (maximum chemical attenuation) to 5 (minimum chemical attenuation) based on the soil type (Sililo et al., 2001). Qualitative ratings/descriptions to soil horizons, materials and features, that are diagnostic criteria in the South African soil classification system, are allocated.

The ratings from the two criteria are combined by one of the following approaches to arrive at a vulnerability rating for the area concerned:

- Combining the two ratings (using the average of the three chemical attenuation ratings)
- Selection of the most critical of the two ratings (the higher attenuation cancels out the lower attenuation/higher risk rating)
- A hybrid approach based on both of these approaches (e.g. average of scores obtained by each approach).

Sililo et al. (2001) mention that their proposed groundwater assessment strategy is based on the assumption that most rock formations (and some unconsolidated deposits) are sufficiently fractured for preferential flow to dominate the recharge process and for rock-water interaction to be negligible. The soil-water interaction will be the dominant influence on the groundwater composition and contamination. This method of determining aquifer vulnerability is not specifically designed for karst areas and does not take into account the unique properties of karst terrains.

A WRC research project “Improved methods for aquifer vulnerability assessments and protocols (AVAP) for producing vulnerability maps, taking into account information on soils” (WRC Project K5/1432) has been completed. However, no karst specific focus existed within the AVAP program and as such the need for the development of a local karst aquifer vulnerability mapping method was identified.

5 The European approach to aquifer vulnerability mapping

The Directorate General for Science, Research and Development of the European Commission set up a specific working group in the frame of COST Organization (Cooperation in Science and Technology), COST Action 620, active from 1997 to 2003 in order to develop an approach to “vulnerability and risk mapping for the protection of carbonate (karst) aquifers”. Experts participating in this Action soon realised that the philosophies behind the existing European methods were often very different due to variations in legislative backgrounds that influenced not only the practical implementation of individual methods, but also the conceptual approach to deal with vulnerability (Zwahlen, 2003).

Three working groups were set up within Action 620. The first working group developed a scientific approach to the mapping of intrinsic vulnerability of karst groundwater. The intrinsic vulnerability of an aquifer system, by definition independent of the properties of specific contaminants, is solely a function of the geological, hydrogeological and hydrological properties thereof. The second working group established a system to characterise the vulnerability of groundwater to specific contaminants or groups of contaminants, i.e. the specific vulnerability of aquifer systems. Specific vulnerability takes both, the properties of the system and those of the

contaminants into account to determine the specific attenuation processes of contaminants in the aquifer.

The third working group concentrated on hazard and risk mapping. Hazards are defined as activities and land-use practices that pose a threat to groundwater (e.g. industrial activities). Risk maps are obtained by synthesising the information presented on both hazard and vulnerability maps.

Zwahlen (2003), stresses that though the vulnerability maps, created using the devised methods are a vital tool to protect karst aquifers, they remain a simplification of reality. Extrapolation and interpretation of data sets over relatively large areas, as well as the occasional use of data of unknown quality are factors contributing to the degree of simplification. However, the validation process, which considers the success of the map to reproduce prevailing hydrogeological conditions, compensates the simplification problem to a large degree (Zwahlen, 2003).

5.1 The European groundwater vulnerability concept

5.1.1 Introduction

The European Water Directive (2000) requires the characterisation of all groundwater bodies in member states in order to assess their uses and the degree to which they are at risk. The initial characterisation requires member states to consider all existing hydrological, geological, pedological, land-use, discharge, abstraction and other data to characterise the general character of the overlying strata in the catchment area from which the groundwater body receives its recharge and as such the degree of risk that the body is at (Zwahlen, 2003). Those groundwater bodies, which have been identified as being 'at risk', must be assessed more precisely considering the following:

- Geological and hydrogeological characteristics of the groundwater body.
- Characteristics of the superficial deposits and soils.
- Associated surface systems with which the groundwater body is dynamically linked.
- The directions and exchange rates of water between the groundwater and surface systems.
- Sufficient data to calculate the long-term annual average rate of overall recharge.

Due to the qualitative and often subjective nature of vulnerability assessments a need for the establishment of clearly identified reference criteria to be used for quantification, comparison and validation purposes of vulnerability concepts exists. The concept of groundwater vulnerability is generally based on the assumption that the physical environment is capable of providing some level of natural protection of groundwater against human impacts, especially with regard to contaminants entering the subsurface environment (Vrba & Zaporozec 1994, in Zwahlen, 2003:5). Vulnerability is defined as a relative, non-measurable, dimensionless property and the following subdivisions proposed by Vrba & Zaporozec (1994, in Zwahlen, 2003:5):

- **Intrinsic vulnerability** of groundwater to contaminants takes into account the geological, hydrological and hydrogeological characteristics of an area, but is independent of the nature of the contaminants and the contamination Scenario.
- **Specific vulnerability** takes into account the properties of a particular contaminant or group of contaminants in addition to the intrinsic vulnerability of the area.

Vulnerability maps combine various complex hydrogeological properties in an integrated comprehensible way and areas with the same vulnerability are displayed on the map in a uniform way. Such vulnerability maps should be easy to interpret and can then be used as a practical tool for land-use planning, protection zoning and risk assessment. The main disadvantage of using a qualitative approach to vulnerability is that a property, which is not precisely defined, cannot be derived unambiguously from measurable quantities (Zwahlen, 2003).

5.1.2 The origin-pathway-target model

The concept of groundwater vulnerability used by ACTION 620 is based on an origin-pathway-target model for environmental management, similar to the source – pathway – receptor concept of Risk-Based Corrective-Action (ASTM 1995). During vulnerability mapping it is assumed that the **origin** of the contamination is at the land surface but it is however possible that some contaminants are released below the surface (e.g. a leaking sewer system). A **pathway** is the flow path that a potential contaminant follows from its point of release (the origin), through the system, to the point that has to

be protected (target). The **target** (receptor) is the water, which has to be protected (see section 5.1.3).

5.1.3 Resource vulnerability vs. source vulnerability

For **resource** protection the groundwater surface in the aquifer is the target and in the case of confined or artesian hydraulic conditions the target is identical to the top of the aquifer under consideration and not to the potentiometric surface (Zwahlen, 2003). The pathway considered in resource protection consists hence of the vertical passage through the layers above the groundwater surface (unconfined aquifer) or surface of the aquifer (confined aquifer). For **source** protection the water in a well or spring is the target and the pathway therefore includes additionally the mostly horizontal flow route within the aquifer.

5.1.4 Groundwater vulnerability in karst areas

Although the concept of groundwater vulnerability is relevant to all types of aquifers (granular, fractured and karst), karst aquifers have unique properties which should be taken into account during a vulnerability assessment. Karst aquifer vulnerability assessment methods are usually either methods especially dedicated to karst or methods that although applicable to all aquifer types contain special methods to be used when being applied to karst areas. Due to the often intermediate conditions between a purely fractured / granular and karstified carbonate aquifer, coexistence of several aquifer types in one catchment as well as the higher acceptance of a general applicable methodology by decision-makers COST 620 decided on the later option.

5.2 Intrinsic vulnerability

5.2.1 Basic concepts of the European Approach

Three aspects must be considered in the determination of the intrinsic vulnerability of groundwater (Daly et al., 2002 in Zwahlen, 2003:17):

1. Advective transport time from the origin to the target.
2. Physical attenuation (e.g. by dispersion, dilution and dual porosity effects).
3. Relative quantity of contaminants that can reach the target (this is included as a portion of the contaminants may never reach the target due to leaving the catchment via surface runoff).

Vulnerability mapping therefore requires the assessment of those properties of an area that control these aspects. The first aspect (advective transport time) is mainly controlled by permeability, effective porosity, hydraulic gradient and distance between origin and target. If the advective transit time is large there is more time to react to a contamination event and since most specific processes of contaminant attenuation are directly or indirectly dependent on the travel time (e.g. mortality of bacteria) an increase in travel time also results in improved natural attenuation processes (Zwahlen, 2003). The second aspect (physical attenuation) results in a decrease in the concentration of the contaminant and the final aspect (quantity reaching the target) is controlled by the effective or relative recharge.

The so-called “European Approach” of intrinsic vulnerability assessment of karst aquifers takes the following factors into account:

1. The overlying layers (O) factor represents the biologically active zone of the soil profile that occurs between the ground surface and the water table. It is often the most important factor determining vulnerability of groundwater to contamination.
2. The concentration of flow (C) factor represents the degree to which precipitation is concentrated towards areas where rapid infiltration and subsequent bypassing of the overlying layers is possible.
3. The precipitation regime (P) factor considers the annual precipitation as well as the frequency, duration and intensity of extreme events that influence the type and quantity of infiltration. The factor is especially important to consider on a regional scale (Zwahlen, 2003).
4. Karst network development (K factor) is only important in source vulnerability determination where horizontal flow in the aquifer is considered. The K factor is used to represent a range of karst network possibilities ranging from non-karstified carbonate rocks with limited inter-granular porosity to karst aquifers with fast active conduit systems.

The O, C and K factors represent the internal characteristics of the system, while the P factor represents an external stress applied to the system. When resource vulnerability mapping is being done, the factors O, C and P should be taken into

consideration and only when source vulnerability mapping is performed should the factor K be taken into account as well. The European approach is only a conceptual framework for determining aquifer vulnerability and as such it does not contain any detailed guidelines, tables or formulas. Different groups within COST 620 used this basic concept of the European approach and converted it into quantitative methods applicable to the particular karstic terrain in which they were working (see section 5.8).

The O, C and K factors represent the internal characteristics of the system, while the P factor represents an external stress applied to the system. When resource vulnerability mapping is being done the factors O, C and P should be taken into consideration and only when source vulnerability mapping is performed should the factor K be taken into account as well. The European approach is only a conceptual framework for determining aquifer vulnerability and as such it does not contain any detailed guidelines, tables or formulas. Different groups within COST 620 used this basic concept of the European Approach and converted it into quantitative methods applicable to the particular karstic terrain in which they were working (see section 5.8).

5.3 Specific vulnerability

Specific resource maps reflect a more detailed potential migration picture of a particular contaminant. Intrinsic vulnerability maps generally display a worst case Scenario and fail to take into account the positive attenuation effects deriving from specific contaminant properties such as retardation and degradation and therefore may overestimate the vulnerability of an area. Retardation results in a decreased mobility and migration rate of contaminants but cannot reduce contaminant load. Retardation does however result in additional time for degradation to occur (Zwahlen, 2003). Degradation is the permanent loss of contaminant load from a water system and results in lowered concentration at the target. Both of the above mentioned processes benefit aquifer protection and reduce vulnerability even if the contaminant is not fully attenuated and as such specific vulnerability is nearly always lower than or at least equal to the intrinsic vulnerability of a particular area.

5.4 Hazard mapping

Considering the *origin-pathway-target* model, the risk of contamination of groundwater depends on:

- the hazard posed by a potentially polluting activity (equivalent to origin),
- the intrinsic vulnerability of groundwater to contamination (equivalent to pathway),
- the potential consequences of a contamination event (the target is the groundwater).

For groundwater protection an assessment of the risks posed by existing and **future** human activities and the responses to the risk (measures designed to mitigate and manage the risk) is required (Zwahlen, 2003). Zwahlen (2003) proposes the following steps to analyse and map hazards in a study area:

- Definition and inventory of hazards (potential source and degree of harmfulness of a contamination resulting from human activities, subdivided in infrastructural, industrial and agricultural activities)
- Hazard data requirements (nature of the activity, type and amount of harmful substances present as well as status of installations and plants).
- Rating and weighting of hazards (classification of hazards that is suitable for the formulation of possible groundwater protection zones or measures. Cost 620 provides general recommendations to be used judging the potential degree of harmfulness of different types of hazards).
- Graphical interpretation (hazard maps should show some other important attributes like the name and a short description of each hazard).
- Data evaluation (hazard attributes that permit a rigorous data quality control and assurance and a distinction between measured, statistical, extrapolated and estimated data).
- Production of hazard maps ('unclassified' hazard maps show only the relevant geographical location information whereas 'classified' hazard maps are based on a hazard index computation).

5.5 Risk assessment

5.5.1 Introduction

Risk is generally the probability that in a certain timeframe an adverse outcome will occur in a person, a group of people, plants, animals or ecology of a specified area that is exposed to a particular dose or concentration of a hazardous agent. The risk associated with harmful substances depends both on the level of toxicity and on the level of exposure and typically risk analysis focuses on natural resources, like air, water and soil, which are essential to all life forms (Zwahlen, 2003).

With regard to groundwater COST 620 provides definitions for risk and risk assessment as follows:

- **Risk:** The possible contamination from a hazardous event that embodies both probability and consequences defined as the likelihood or expected frequency of a specified adverse consequence on groundwater. It is not intended to be an absolute measure but rather a means of relative measure or comparison and can be defined by the product of the probability of an event and the consequential damage.
- **Risk assessment:** The evaluation process for estimating the potential impact of a chemical, biological or physical agent on groundwater. Risk assessments have to take into account the likelihood of an impact, the intensity with which the impact affects the groundwater (both determined during the risk intensity assessment) and the sensitivity of groundwater with respect to the impact (determined during the risk sensitivity assessment).

5.5.2 Risk assessment concept

Risk assessments can be divided into two stages with the first (risk intensity assessment) determining the intensity of a hazardous event, on the specific target, by considering all the factors that are possibly damaging. The second step (risk sensitivity assessment) determines the results of such impacts on the target with respect to the target's sensitivity to changes coming from outside (takes into consideration the target's ecological and economic value). These two steps may then be combined according to a

certain mathematical procedure (Fedra & Weigkricht, 1995, Kovar & Nachtnebel, 1993 in Zwahlen, 2003:108) to complete the risk assessment.

Risk intensity assessments for groundwater consists of two tasks (Forster & Hirata, 1988, Lobo-Ferreira, 2000, NEPC 2000, Daly & Drew, 2000 in Zwahlen, 2003:109): The hazard assessment dealing with the possible origins of contamination and the likelihood of a release as well as the estimation of all the processes that can lead to a reduction of the contamination before it reaches the target, i.e. the vulnerability of the target. The starting point is usually the development of a conceptual hydrogeological model of sufficient accuracy to describe the migration of contaminants to a potential target. A quantitative or at least semi-quantitative estimation describing the portion (or concentration) of contaminants reaching the target must be obtained by a risk intensity assessment.

The contamination of groundwater starts where contaminants reach the phreatic surface. The damage caused by a contamination has to be included in the risk assessment and depends on the extension of the plume and the distribution of the contaminants in the plume, which in turn depend on potential attenuation processes. The target at risk generally consists of only a part of the whole groundwater body (Zwahlen, 2003).

The sensitivity of groundwater to a contamination impact is therefore influenced by all factors that might minimize the harmfulness of the contaminants with regard to the target. The reduction of both the ecological and the economical value of the groundwater must be considered during such a **risk sensitivity assessment** (Scholles, 1997, U.S.EPA, 1996, Zakharova, 2001 in Zwahlen, 2003:111).

The total risk identified by a risk assessment enables decision-makers to reach decisions e.g. on the type of protection measures that would be most appropriate. Zwahlen (2003) recommends using the following three risk indices:

- Risk intensity index (RII): provides a relative measure for the intensity of the hazardous impact resulting from the likelihood of the hazard and the vulnerability of the target.

- Risk sensitivity index (RSI): provides a relative measure for the sensitivity with which the groundwater reacts to the impact and the resulting damage expressed in terms of ecological and economical values.
- Total risk index (TRI): summarises the effects of all influencing factors analysed in the risk assessment procedure.

5.5.3 Risk mapping

Due to scale and resolution effects the selection of a suitable scale is most important and depends on the objectives for which the map shall be used (Zwahlen, 2003). Geographic information systems (GIS) are powerful tools for spatial analysis but simulation models are more useful tools for complex and dynamic analysis (but in turn lack the spatial analysis functions that a GIS offers).

The complete risk assessment map shows the distribution of risk classes defined by the range of the TRI (total risk index) and is used by decision makers, land use planners, water utilities or the interested public. The supporting maps are the risk intensity map (RII) (together with its two basic maps, the hazard and the vulnerability map) and the risk sensitivity map (RSI) (Zwahlen, 2003). Any of these maps may be accompanied by single factor map such as a map showing the thickness of unsaturated zone, groundwater flow direction or time of break-through.

The calculation of the risk intensity index may consider the hazard and vulnerability indices by using a matrix concept (Foster, 1987; Magiera, 2002; Daly & Misstear, 2002 in Zwahlen, 2003:115) or by using a mathematical approach to combine intrinsic vulnerability and hazards.

5.6 Data requirements

Under normal circumstances data from numerous sources are utilized. Uncertainties contained in the source map (geology, soils, landuse, etc.) are amongst others important sources of errors. Different resolutions and uncertain quality of data affect the reliability of the final map negatively. Appropriate validation methods during the mapping process are required to estimate the reliability of any vulnerability map (Zwahlen, 2003).

5.7 Demonstrating the reliability of maps

Groundwater vulnerability maps are conservative simplifications of prevailing hydro-geological conditions and are often expressed in terms of a conceptual model that embraces the hydrogeological theories being employed to produce the vulnerability map. It is therefore necessary to test the validity of both, the conceptual model as well as the usefulness of the vulnerability map at specific locations. It is advisable to develop a method to verify and validate the quality of the final product as part of the mapping method.

Verification procedures are the quality assurance of a particular method and include logical and procedural checks to calculations. It can include a comparison with other methods. Validation procedures include the analysis of observations (hydrographs, chemo-graphs, isotopes or tracer experiments), the use of analytical or numerical models, any calculation, test or investigation performed within the study area that is independent of the used vulnerability method. The principle of validating one model using another model is a difficult concept, but it can increase the degree of confidence (Zwahlen, 2003).

5.8 Vulnerability mapping methods

5.8.1 The PI method

Introduction

The PI method was developed within the scope of COST 620 at the Department of Applied Geology (AGK), University of Karlsruhe, Germany (Goldscheider et al. 2000a, b) According to Goldscheider (2003) the PI method was first applied and compared with other methods in the Engen test site, Swabian Alb, Germany (Sturm 1999, Klute 2000, Goldscheider et al. 2000a in Goldscheider, 2003:144). By 2003 the method and modification of it had been applied in 12 karst systems in 7 European countries (Goldscheider, 2003).

General concept

The PI Method is a GIS-based approach to mapping intrinsic groundwater vulnerability with special consideration of karst aquifers (Goldscheider, 2003). It is based on an origin (hazard on ground surface) – pathway (layers between ground and groundwater surface) – target (groundwater table in the uppermost aquifer) model. If the

resource vulnerability map is intersected with a map showing the flow route in the aquifer towards a spring or well, it can also be used for source vulnerability mapping. The acronym stands for the two factors considered by the method (**P**rotective cover and **I**nfiltration conditions).

The protective cover (P) describes the protective function of the layers between the ground surface and the groundwater table (soil, subsoil, non karst rock and unsaturated karst rock) and therefore is equivalent to the O factor (overlying layers) of the European Approach. The P factor is calculated according to a modified version of the German (GLA) method (Hölting et al., 1995), with P = 1 referring to a very low degree of protection and P = 5 referring to very thick and protective overlying layers.

The infiltration conditions (I factor) describe the degree to which the protective cover is bypassed due to swallow holes and sinking streams. The factor is equivalent to the C factor of the European Approach and is given as 1 if the infiltration occurs diffusely and 0 if the protective cover is completely bypassed. The catchment of a sinking stream is assigned a value between 0 and 1, depending on the proportion of lateral flow components present.

The spatial distribution of the protection factor PI or π , obtained by multiplying the P and I factors, is shown on the final vulnerability map. Small I and P maps should be printed as insets on the vulnerability map to show how the vulnerability of a particular area is influenced by the two independent factors (Goldscheider, 2003). The π factor ranges between 0.0 (low degree of natural protection and high vulnerability) and 5.0 (high degree of natural protection and low vulnerability). All areas on each of the three maps are assigned to one of five classes symbolised by five colours ranging from red for high risk to blue for low risk.

5.8.2 The VULK analytical transport model and mapping method

Introduction

VULK is an analytical computer programme, which was developed at the Hydrogeology Center of Neuchâtel (CHYN) as a tool for intrinsic vulnerability assessment (Jeannin et al. 2001 in Cornation et al., 2003:155). The acronym VULK stands for **V**ULnerability and **K**arst. The conceptual framework comprises a simple

method for transfer time mapping for both resource and source vulnerability. The computer programme allows for calculating contaminant transport at selected points but further development aims at coupling VULK with a GIS, so that it will be possible to create attenuation maps showing the maximum concentration of a potential contamination event. The mathematical background of VULK is described in detail by Jeannin et al. (2001 in Cornation et al., 2003:155).

General concept

The basic idea of VULK is to model the breakthrough curve at a defined target resulting from an instantaneous release (Dirac input) of conservative contaminants at a given point (origin) within the system (usually located on the land-surface). Transport within the system is modelled with a 1-D single- or dual-porosity analytical advective-dispersive transport solution of a non-reactive solute under steady-state flow conditions (Cornation et al., 2003). Up to 5 compartments along the pathway between the origin and the discharge point (target) are considered as separate sub-systems. The modelled breakthrough curve allows the determination of the transfer time, duration and concentration level of a potential contamination event at the given point and therefore the characterisation the groundwater vulnerability at the given point.

The soil, subsoil, non-karst rock and unsaturated karst rock are taken into account for resource vulnerability assessments, for source vulnerability assessments the saturated zone of the karst aquifer is considered as well. Therefore VULK uses the O (overlying layers) and K (karst network development) factors of the European Approach, but does not consider the concentration of flow (C factor) in the catchment of sinking streams (Cornation et al., 2003). Sub-systems are coupled by means of successive convolutions (i.e. the output of one system is the input of the next one). Dilution processes can also be taken into account and the user can select the number of sub-systems and a single- or dual-porosity approach in order to match the actual situation.

5.8.3 Localised European Approach (LEA)

Introduction

The ‘Localised European Approach’ (LEA) was developed by S. Dunne with D. Drew at Trinity College Dublin (Dunne, 2003a). This method may be used as an

alternative to the PI method and is a straightforward approach that does not use a numerical index. The research was conducted in field areas in the UK (four in England and two in South Wales) with the hydrological settings and data availability of the UK in mind (Dunne, 2003a). The general concept coincides with the European Approach to intrinsic resource vulnerability mapping (i.e. the overlying layers (O factor) and the concentration of flow (C factor) are taken into account.

General concept

An area's vulnerability is classified according to the O factor (overlying layers) into one of six classes, ranging from "very low" to "extreme". The method assumes that runoff usually originates from a small, but relatively consistent part of the watershed known as the contributing area. Once the contributing area has been delineated for a specific body of surface water the HOST (Hydrology of Soil Types) classification system is used to deduce the pathway taken by rainfall (i.e. dominantly vertical or lateral) (Boormand et al., 1995 in Dunne 2003a:162). Dolines and their recharge areas (50 m buffer zone) as well as the 10m buffer zones around sinking streams are classified as extremely vulnerable (Dunne, 2003a). Similarly, areas with surface karst features are classified as zones of extreme vulnerability. The vulnerability of all other areas depends only on the overlying layers.

5.8.4 The COP method

Introduction

The COP method was developed by the Hydrogeology Group of the University of Malaga (GHUMA) and was supported by the Spanish Ministry of Research and Science (PB98-1397 and REN2002-01797/HID Projects) and the Research Groups of the Junta de Andalucía (RNM-139 and RNM-308) (Vías et al., 2003). The proposed method has been tested on two carbonate aquifer pilot sites in southern Spain with different climatological, hydrogeological and geological (lithological, tectonic and geomorphological) characteristics. Both sites have previously been investigated using other vulnerability mapping methods, allowing a comparison of the methods.

General concept

The COP method assumes that contaminant transport depends predominately on the ability of water to move through the aquifer and that the contaminant infiltrates from the surface by means of rainfall. COP is an acronym derived from the initials of the three vulnerability factors considered. The O factor indicates the capability of the unsaturated zone, by means of various processes, to filter out or attenuate contamination and thus reduce its adverse effects. The C and P factors are used as modifiers that correct the degree of protection provided by the overlying layers (O factor). The C factor takes into account the surface conditions that control water flowing towards zones of rapid infiltration and can alter the protection capacity of groundwater described by the O factor to any degree between nullifying it (C factor = 0) and not altering it (C factor = 1). The P factor considers the characteristics of the transport agent in the unsaturated zone, i.e. precipitation. Since the influence of precipitation on vulnerability is not as great as that of the flow concentration, the value of the P factor ranges from 0.4 to 1. While the P and O factors can be used to evaluate the vulnerability of any type of aquifer, the C factor is specific to karst aquifers (Vías et al., 2003).

The three factors are multiplied to obtain the final vulnerability index and classified into five classes ranging from Very Low to Very High. The higher classes are assigned mainly depending on the influence of the C factor. The Very Low class refers to zones in which the C and P factors have little influence on protection.

5.8.5 The Time-Input method

Introduction

The Time-Input method's main factors are the travel-time (**TIME**) from the surface to groundwater and the amount of precipitation (**INPUT**) as groundwater recharge. The weighting is empirical and gives the travel-time a slightly higher importance than the groundwater recharge. Unlike the other schemes vulnerability is expressed in real time and input values in real quantities instead of dimensionless numbers. The method was applied in a forested mountainous dolomite area in Austria (Kralik & Keimel, 2003).

General concept

The Time-Input method is based on three main preconditions: Potential contaminants are believed to behave similarly to an ideal tracer and move more or less like the infiltrating water (specific vulnerability assessment is not considered). Secondly the main target of a vulnerability assessment is the surface of the uppermost groundwater body (i.e. resource protection) as this enables a consistent investigation of the total recharge area. For the protection of particular wells or springs (source protection), the distance to the source and the lateral movement in the saturated zone are considered. Finally the “mean bad conditions” of a hydrological year are assessed preferentially and therefore the mean conditions of periods with fairly rapid travel-times and a high input of water are investigated (extreme events are not considered) (Kralik & Keimel, 2003). Vulnerability is expressed as travel time (**TIME**) classes (measured in seconds [s]) which are modified by the correction factor (**INPUT**) based on groundwater recharge measured in millimeters per year [mm].

To obtain the first main factor (travel-**TIME**) the thickness of each layer (overlying unconsolidated deposits and the different bedrock strata) is divided by its hydraulic conductivity. Additional information on faults and karstification is incorporated into the assessment. Each stratum’s mean hydraulic conductivity has to be estimated considering faults, the inclination of bedding planes towards the groundwater and karstification features like swallow holes and karrenfields.

Low recharge quantities have high correction factors, thus increasing time and lowering vulnerability and vice versa. However, when high input significantly dilutes a quantitatively limited contaminant to concentration levels below the regulatory limit or toxicity values correction factors must also be used in the opposite direction as those used when high input is assumed to create a higher vulnerability. The **INPUT**-factor depends on the amount of precipitation, the solar radiation input, the slope inclination and aspect, the vegetation, the type and thickness of the soil and the catchment area and is expressed as groundwater recharge in mm/year (calculated using a simple water balance equation).

As this assessment scheme uses real physical values of time and input, the evaluation of its main factors can be undertaken using different techniques (e.g. the

analysis of isotope or natural tracers or water balance calculations). The limitation of the method is obviously the data availability. Although the method was tested in a relatively complicated mountainous dolomite karst area it can be applied (with minor modifications) to porous aquifers (Kralik & Keimel, 2003).

5.9 Comparative application of the PI and COP methods

5.9.1 Introduction

The PI and COP method were applied to produce intrinsic vulnerability, specific vulnerability as well as hazard and risk maps for a karst aquifer in southern Spain and the obtained maps were subsequently compared (Andreo et al., 2003).

The Sierra de Líbar covers a surface area of 103 km² between the provinces of Malaga and Cádiz, Andalusia, Spain and is characterised by a high seasonal rainfall, with a mean precipitation of over 1500 mm per year. Jurassic dolomites and limestones, and Cretaceous marls and marly limestones underlie the area which is characterised by steep slopes and plateau-shaped mountain ridges (Andreo et al., 2003). A large variety of well-developed karst landforms, including karrenfields, vertical shafts and poljes with swallow holes, and caves are present in the area (Delannoy, 1987 in Andreo et al., 2003:184).

5.9.2 PI method

The evaluation of the P and I factors for this site was proposed by Brechenmacher (2002 in Andreo et al., 2003:184) and a sub-factor F was used to describe the degree of fracturing and epikarst development. P values of zero were assigned to large areas due to the presence of strongly developed epikarst, which is not sealed by soil and/or clayey sediments and the vulnerability in these areas is consequently classified to be “Very High”. A “Very High” vulnerability was also assigned to the inner areas of the poljes where the slopes exceeded 3.5 %, as these areas are drained by surface runoff that bypass any surface layers via swallow holes (Andreo et al., 2003).

“High” vulnerability areas are the inner areas of the poljes where the slope is less than 3.5% and where no water fluxes are generated towards the swallow holes as well as areas where Quaternary materials outcrop, over Jurassic limestones, due to the extreme permeability of these materials. Figure 2 gives the intrinsic vulnerability map obtained by applying the PI method at the test site.

5.9.3 COP method

The final COP vulnerability map (Figure 3) shows “High” vulnerability in most of the system and this is related to the high degree of karstification of the carbonate outcrop (which favours rapid infiltration). The differences in vulnerability (between “High” and “Very High” categories) within the carbonate outcrop arise from the presence of very specific conditions of factors O or C (Andreo et al., 2003). The poljes of the central part of the aquifer were classified as being of “Very High” vulnerability due to the presence of swallow holes that bypass the protective capacity of the unsaturated zone of the aquifer. The areas classified as “High” vulnerability are Jurassic limestone and dolomite outcrop areas where the thickness of the unsaturated zone exceeds 250 m and the slope is greater than 8%.

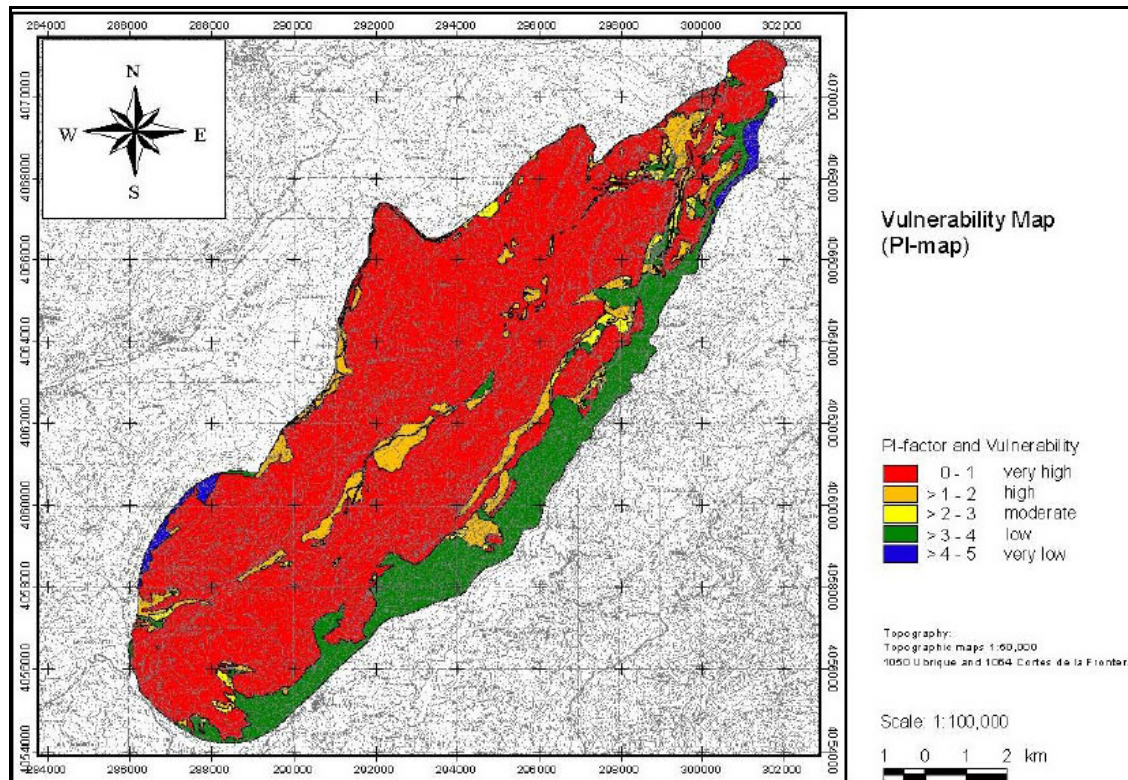


Figure 2. PI Vulnerability map of the Sierra de Líbar (Brechenmacher, 2002 in Andreo et al., 2003:186).

5.9.4 Comparison between PI and COP vulnerability maps

While the PI and COP method use different numbers of factors and different theoretical concepts for the rating of each factor and its sub-factors, the produced maps

show only minor differences. Zones classified as “high vulnerability” by the PI method may be classified as “very high vulnerability” by the COP method or vice versa, but no extreme classification errors (e.g. one method classifying area as low vulnerability while other method classifies same area as high vulnerability) were identified. The COP method appears to be a more detailed assessment method as it takes more factors into account. This results in different degrees of vulnerability being identified in areas where the PI method classified the entire area as one vulnerability class.

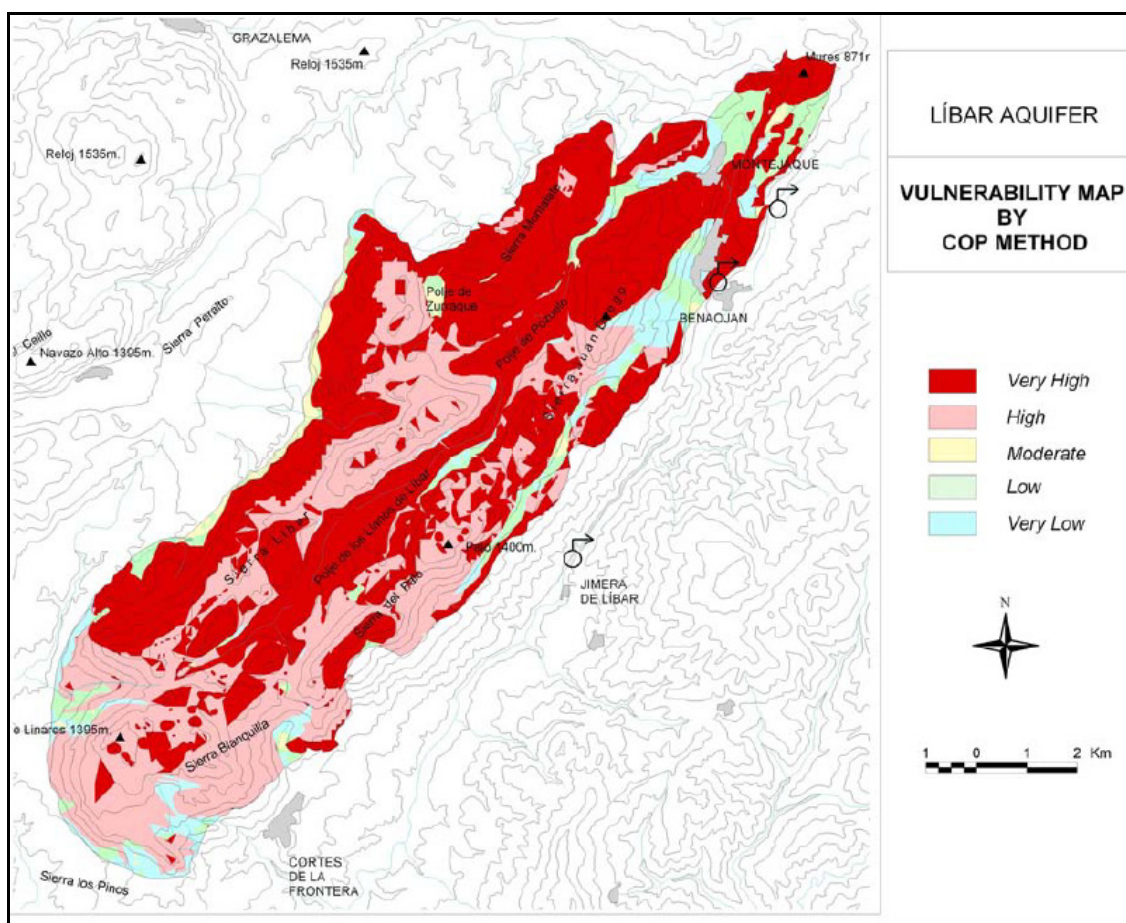


Figure 3. COP Vulnerability map of the Sierra de Lívar (Andreo et al., 2003:188).

5.9.5 Hazard mapping

The infrastructure of the test site e.g. villages, roads and railway lines as well as solitary houses and buildings were mapped and the hazards visited in the field to assess their properties with respect to the quantity of relevant substances. Any reduction factor

and further hazards were mapped simultaneously. The required data were often unavailable and the ranking and reduction factor were estimated on the basis of the relative size and the technical conditions of the hazard. For geographically overlapping hazards the highest value was chosen. The ranking value of the hazards (Q_N) ranges between 0.8 and 1.2 and as no information was available relating to the probability of a contamination event for any of the mapped hazards a value of one was used for the reduction factor (R_F). However a reduction factor of 0.5 was used for the graveyards.

Due to the rural characteristic of the test site the Hazard Index classification ranges only between 16 and 54, out of the possible range from 0 to 120, consequently the hazards were classified as “No” or a “Very Low” hazard levels. Livestock husbandry in the area has caused groundwater point contamination in the past and even though there are few industrial activities, the hazard map in combination with the vulnerability map is very useful for risk assessments to avoid further contamination of the groundwater (Andreo et al., 2003).

5.9.6 Risk mapping

The risk assessment methodology for the test site Sierra de L'bar is almost identical to that proposed by Morris & Foster (2000 in Andreo et al., 2003:196). Risk is described as the risk of groundwater pollution from each hazard when its contamination load is released and the risk maps therefore show the risk to groundwater pollution of each mapped hazard in the sense of resource protection (Andreo et al., 2003).

Morris & Foster (2000, in Andreo et al., 2003:196) and Foster & Hirata (1988, in Andreo et al., 2003:196) calculate the risk by overlaying the intrinsic vulnerability map (constructed with the PI-Method) and the hazard map. Due to the fact, that the PI factor and the Hazard Index are inversely related, the risk value is defined as the product of them. The risk assessment implies that even hazards with a low or very low hazard level could produce a “Very High” risk level if the vulnerability is very high and vice versa. The hazards in the test area are generally of the least dangerous type (villages in the northeast and feedlots in the poljes in the central region). However, the vulnerability of most of the area is classified as “high” or “extreme” due to the intensive karstification of

the outcropping limestones. The risk distribution (Figure 4) shows a differentiated spatial classification as compared to the PI vulnerability map (Figure 2).

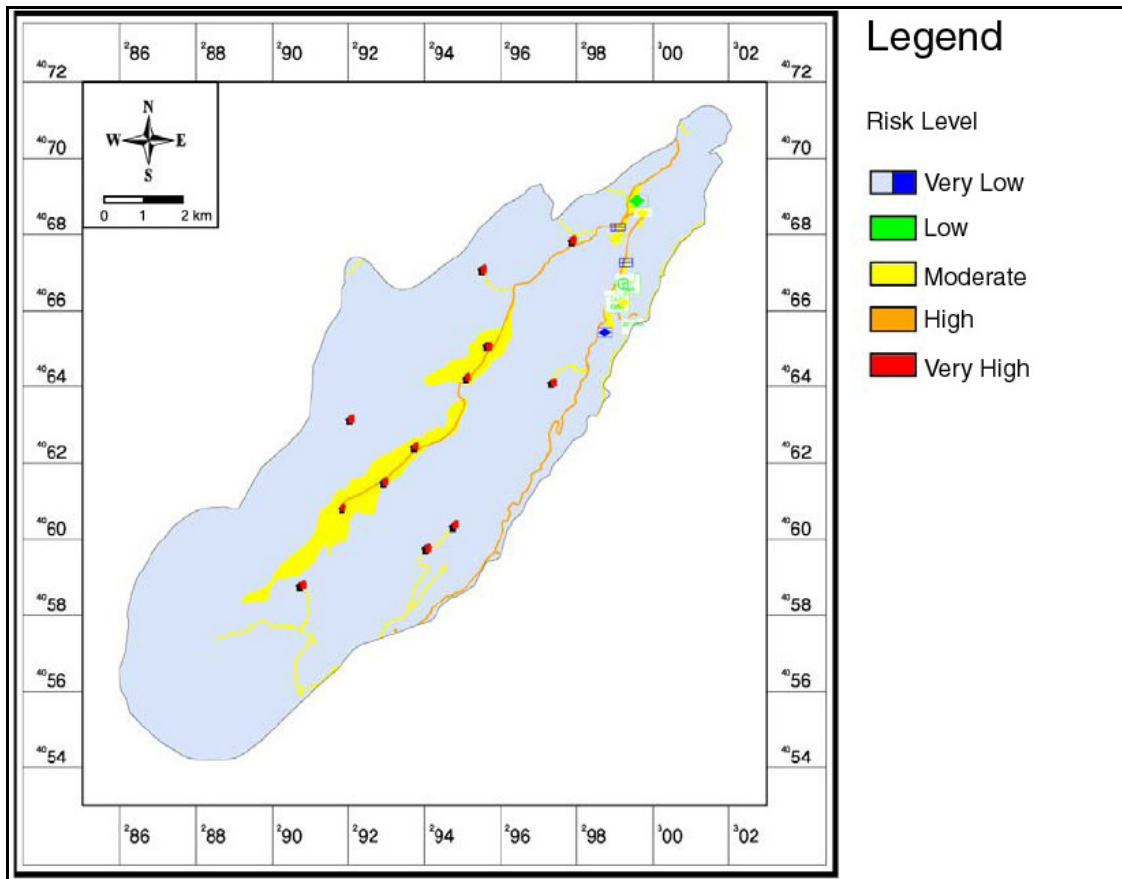


Figure 4. Risk map of the Sierra de Líbar (adapted from Andreo et al., 2003).

5.9.7 Conclusions

The Sierra de Líbar case study illustrates the fact that the final risk map does not include all the information that might be required by an end user. For example, a land-use planner using the final risk map will know that the existing situation at the margins of the mountains poses low or moderate risk to groundwater, but to ascertain the risk posed by future developments, the planner would also require access to the intrinsic vulnerability map and/or the appropriate specific vulnerability maps (Andreo et al., 2003).

6 Other vulnerability methods

6.1 Drastic

DRASTIC is a weighting and rating system that was developed by the United States Geological Survey in the mid 1980's (Aller et al., 1987 in Dunne, 2003b:295). The method utilises seven parameters: depth to groundwater table (D), net recharge (R), aquifer media (A), soil media (S), topography (T), impact of the vadose zone media (I), hydraulic conductivity of the aquifer (C). The parameters are combined by the use of Equation 3 to obtain the DRASTIC index which can then be used to identify areas that are more likely to be vulnerable to groundwater pollution relative to other areas.

$$\text{Drastic index} = DRD_w + RRR_w + ARA_w + SRS_w + TRT_w + IRI_w + CRC_w \quad \text{Equation 3}$$

Where : *DR* is depth to groundwater table rating

RR is net recharge rating

AR is aquifer media rating

SR is soil media rating

TR is topography rating

IR is impact of the vadose zone media rating

CR is hydraulic conductivity of the aquifer rating

D_w is depth to groundwater table weighting

R_w is net recharge weighting

A_w is aquifer media weighting

S_w is soil media weighting

T_w is topography weighting

I_w is impact of the vadose zone media weighting

C_w is hydraulic conductivity of the aquifer weighting

The method seems to be best suited for regional assessments (1:50 000 and 1:100 000 scales) and has been applied in a large number of countries worldwide (Aller et al., 1987, Lynch et al., 1994) as well as in South Africa (Lynch et al., 1994, see section 4).

6.2 German method

The German State Geological Surveys (GLA) and the Federal Institute of Geosciences and Natural Resources (BGR) established a method for assessing the protective function of the layers above the groundwater surface (von Hoyer & Söfner, 1998 in Dunne, 2003b:295). The German method places considerable emphasis on travel time as a measure of the effectiveness of overlying layers to protect underlying groundwater and the protective function is therefore dependent on the main factors

controlling the travel time (the thickness of each stratum and the properties of the material). The protective cover includes all strata between the ground surface and the piezometric surface (i.e. topsoil, subsoil and unsaturated bedrock, both karstic and non-karstic). The protective function of the topsoil is assessed according to its effective field capacity, that of the subsoil by considering grain-size distribution and that of the unsaturated bedrock according to lithology and the degree of fracturing and karstification where relevant. The method does not consider flow concentration, i.e. it assumes diffuse infiltration and vertical percolation through the unsaturated zone.

7 VUKA mapping guidelines

This section is a comprehensive guideline to the intrinsic resource aquifer vulnerability mapping method developed to be used in karst terrains within South Africa.

7.1 Development of the applied methodology

The applied methodology is a modification of the COP aquifer vulnerability mapping method, developed by the Hydrogeology Group of the University of Malaga (GHUMA) (Vías et al., 2003). This method is based on the determination of the protection offered by the unsaturated zone of the aquifer against a contaminant event and indicates the capability of the unsaturated zone to filter or attenuate contamination by different processes and thus to reduce its adverse effects (Vías et al., 2003). Two other factors that modify the degree of protection provided by the overlying layers (the O factor) are then considered. These are the C factor, which takes into account the surface conditions that control water flowing towards zones of rapid infiltration, and the P factor, which considers the characteristics of the agent (water), that transports the contaminants through the unsaturated zone. The three factors are multiplied to obtain a final vulnerability index, which is classified into five vulnerability classes, ranging from *Very Low* to *Very High*. A map of each of the main factors is produced using a flow diagram that dictates the sub-factor ratings that need to be deduced based on the available information (Figure 5).

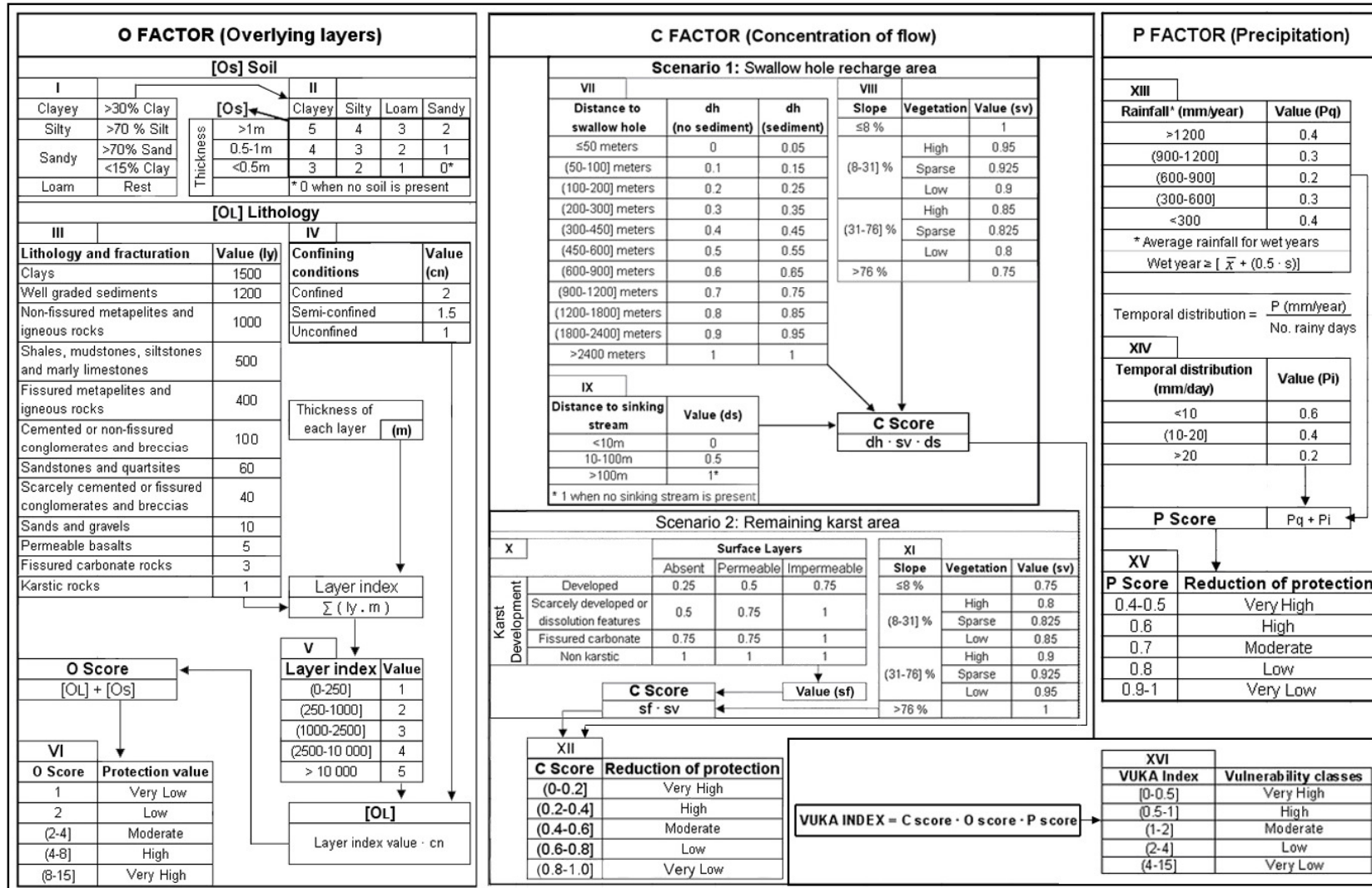


Figure 5: Diagram of the modified COP method (VUKA) showing the differentiation of the C, O and P factors.

7.2 Overlying layers map

The overlying layer map is created by assigning two sub-scores to all areas being mapped. These sub-scores are the *soil* (O_S) and the *lithology* (O_L) sub-scores (tables I to V in Figure 5). The sum of these two sub-scores is referred to as the O score and represents the degree of aquifer protection by the overlying layers in the mapping area.

7.2.1 O_S sub-score

The soil sub-score is determined by the type of soil cover (soil grading) (table I of Figure 5) and the depth of the soil (table II of Figure 5). A thicker soil layer results in an increased likelihood of physical and chemical contaminant attenuation occurring as the water passes through the soil. The O_S sub-score values therefore increase with increasing soil thickness. A similar increase of O_S values exists for soils that are finer grained. This is due to the fact that finer grained soils have generally a lower hydraulic conductivity and therefore increasing the travel time of water through the soil. Finer grained soils also generally contain more clay with an increased adsorption capacity for ionic contaminants are lower therefore the vulnerability of the aquifer.

Soil mapping should be performed to determine the O_S sub-score and this process should include the collection of representative soil samples of major soil horizons for grading analysis. However, due to the often regional scale at which vulnerability mapping is likely to be performed it is advised that land system/land facet mapping or land type/terrain unit mapping (Partridge, 1994) techniques be utilized in order to extrapolate field mapping data from type areas across the entire mapping area. A digital soil map created using either the land system/land facet mapping or land type/terrain unit mapping technique will result in accurate data of both soil type and soil depth.

In the case of feasibility studies and vulnerability studies on catchment level, the process of soil mapping will be extremely expensive even if land system/land facet mapping techniques are utilized. In these cases the South African Land Type maps (Government Printer/Agricultural Research Council-Institute for Soil Climate and Water) can be used as a data source of lower accuracy. Land Type maps show the distribution of different *Land Types* across an area. Within each *Land Type* there are different *Terrain units* and these in turn consist of a collection of soil-rock complexes known as *Soil*

series' or *Land classes* (Summarized in the Land Type Inventories accompanying each map) (Figure 6). Each *Terrain unit* is defined by a range of slope gradients, slope lengths and a slope shape. Based on these parameters the distribution of different *Terrain units* within each *Land Type* can be determined using GIS analysis. Using a digital terrain model (DTM) the slope shape of all areas within the mapping area can be determined using, for example, the TOPOSHAPE function in IDRISI 32[®] or CURVATURE function in ARC GIS[®], while the slope gradients can be obtained using, for example, the TIN SLOPE function in ARC GIS[®]. By overlaying slope gradient and slope shape layers and relating it to the relevant Land Type Inventory a *Terrain unit* layer can be created for each *Land Type*. Figure 6 is an example of how *Land Type* Ab12 is characterized by four *Terrain units* with *Terrain unit 1* being all areas where the slope is between 0% and 7% and the slope shape is convex.

Based on the *soil series*' present (as summarized in the accompanying Land Type Inventories) a soil depth and soil type is then assigned to each *Terrain unit*. This process is not always straight forward as a *Terrain unit* can contain more than one *soil series*. For example *Terrain unit 1* (Figure 6) contains five different *soil series*'. However 91% of the area within *Terrain unit 1* consists of just two of the five *soil series*. In this example both the *soil series*' are characterized by loam soils that have a clay content of 15-25% and a depth of 100-200m, therefore these properties can be assigned to *Terrain unit 1*.

A significant problem of this approach as opposed to soil mapping is that *Terrain units* may contain multiple dominant *soil series*' with soil types and/or depths that fall within different *Os* sub-score classes (table I and II of Figure 5). In such cases a precautionary approach should be used and the worst case Scenario (i.e. lowest soil depth and lowest clay content) should be assigned to the *Terrain unit*.

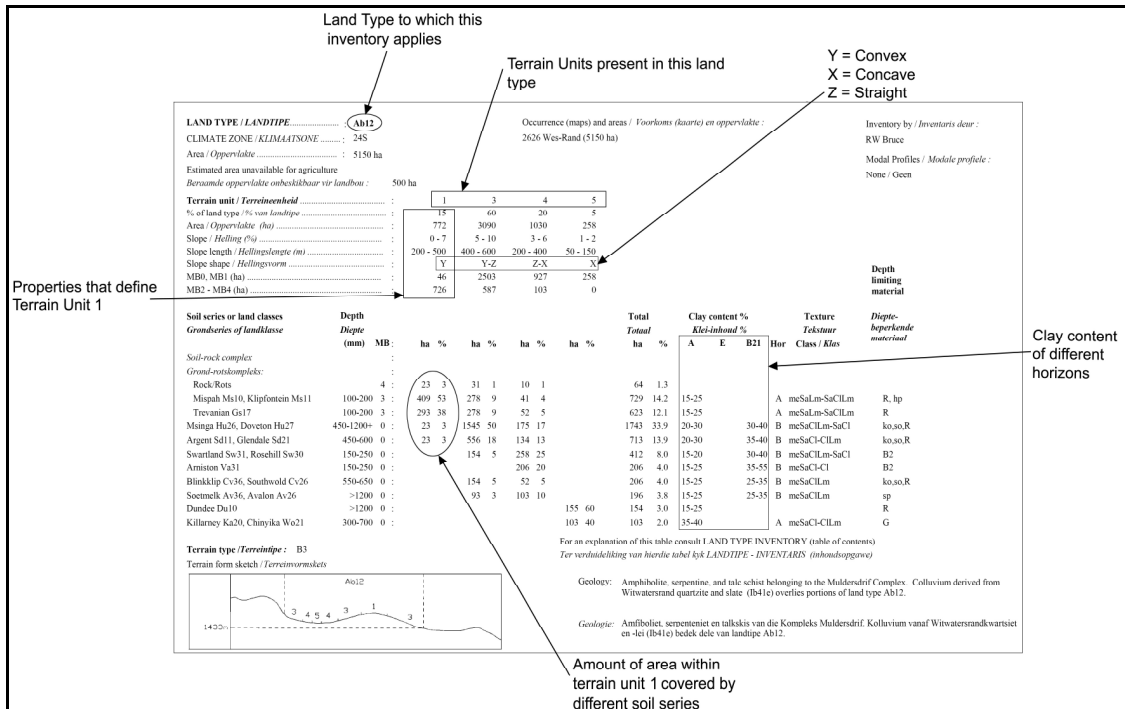


Figure 6. Example of a Land Type Inventory (Macvicar, 1984).

Special attention must be paid to the data available in the Land Type Inventory as some *soil series* have a reported clay content for A horizons, while other series have clay contents data for both A and B2 horizons. In the latter case the highest clay content should be considered, as the high clay content horizon will determine the infiltration rate of water and therefore the protective function of the soil.

The reported soil depth in the Land Type Inventory is not always the depth to bedrock but rather the depth to the “material which markedly restricts water and/or root penetration” (Macvicar, 1984:14). However, since such materials will reduce the vertical migration of water the depths reported in the Land Type Inventories are suitable to be used as the soil depth.

7.2.2 O_L sub-score

The lithology sub-score is determined by the depth to the water table (“m” in Figure 5), the *lithology and fracturation (ly)* sub-factor (table III of Figure 5) and the *confining conditions (cn)* sub-factor (table IV of Figure 5).

Water table depth

A GIS layer defining the depth of the water table below ground surface is required and a detailed hydrocensus should be performed for the entire mapping area. This means that every borehole in the area (Department of Water Affairs and Forestry and private boreholes) should be visited and an up to date depth to ground water measurement should be recorded. Once this has been completed, further drilling of monitoring boreholes might be necessary in areas where no boreholes are present or where steep phreatic surface gradients are expected and critical for the assessment.

In the absence of a hydrocensus the only readily available data source that contains groundwater depth data will be the National Ground Water Archive/Database (NGDB) provided by the Department of Water Affairs and Forestry (DWAF). This database is however extremely inconsistent and often contains clusters of apparently different boreholes (10 or more) spaced meters apart, that have significantly different water depths. In addition many boreholes only have water depth data for more than 4 decades ago. The use of NGDB data is therefore at this stage not recommended and if used, intense “cleaning” of data is required.

The ground water depth data can then be extrapolated using a GIS to arrive at a model of the depth to water table. Ultimately this extrapolation should be based on the relationship between altitude and water depth in the observed borehole data (Bayesian interpolation). However in Karst regions the double porosity nature of the aquifer often results in heterogeneous changes in water surface elevation and as such a significant relationship between water depth and elevation can not always be determined. In such cases a weighted extrapolation method, such as kriging or the inverse distance weighting method can be used. Where dolomite “compartments” are clearly understood and their boundaries are defined the point data within each compartment should be extrapolated separately.

l_y sub-factor

The lithology and fracturation sub-factor considers the type of rock and the degree of fracturation present within each of the overlying layers. Clays and well graded sediments are given very high *l_y* sub-factor ratings as these will have very low hydraulic

conductivities when compared to rocks and as such retard the transmission of pollutants to the underlying aquifer significantly. Since sands and gravels (poorly graded coarse sediments) have a high hydraulic conductivity and will not retard water flow significantly a much lower *ly* sub-factor rating (2 orders of magnitude less) is assigned to such materials. Rocks are assigned *ly* ratings based on their average hydraulic conductivities. This results in intact (non-fissured) metamorphic and igneous rocks and fine grained sedimentary rocks having higher ratings with their fissured equivalents having reduced ratings. Coarse to intermediate grained sedimentary rocks and their metamorphic equivalents have intermediate ratings (once again fissured equivalents have lower ratings) while highly conductivity rocks such as permeable basalts and karstic rocks have low ratings.

The largest scale, digitally available geological map, should be used to assign *ly* values (table III of Figure 5) to the mapping area. In situations where different scale maps are available for different parts of the mapping area, these maps may be combined with each other to the best degree possible. All maps should be randomly checked during field investigations to determine their accuracy.

Once lithology sub-factor (*ly*) values (table III of Figure 5) have been assigned to each lithology within the mapping area, the structural setting must be considered to compensate for areas where the surface lithology is not the only lithology between the surface and the water table. An example is a thin surface layer which does not extend to the water table and more than one lithology (*ly*) sub-factor and thickness must be assigned. Another example is where the lithologies are dipping at such an angle that on the down dip side of the contact more than one lithology will be present vertically above the water table (Figure 7). Within such areas the thickness of each layer obviously varies. The calculation of these layer's thicknesses depends on the scale of the map being produced and the dip of the strata. If the scale and dip (i.e. small scale and/or steep dip) results in these areas being very small a simplified calculation, in which each of the overlying lithologies is assigned as a thickness equal to 50% of the water depth, will be sufficient. When large scale maps are used and/or a shallow dip is present, the area underlain by two lithologies will be more significant and should be divided into two or more sub areas representing different thickness ratios of the two layers.

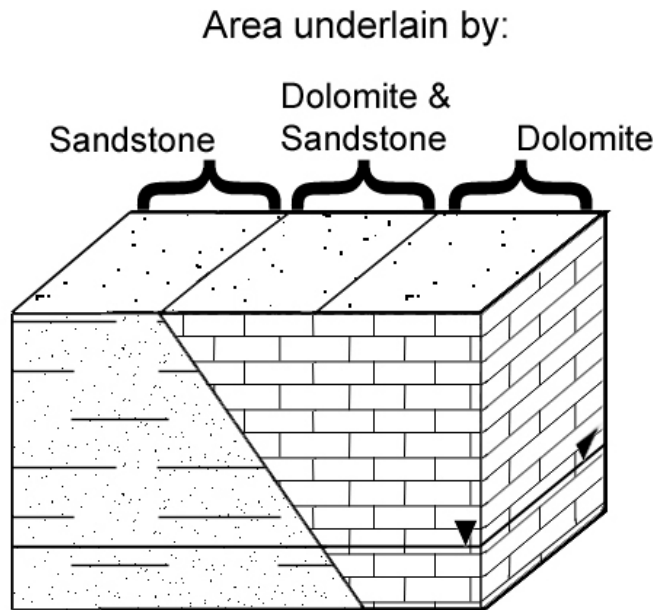


Figure 7. Consideration of different lithologies in the *Layer index* calculation.

cn sub-factor

The entire area being mapped must be assigned a confining conditions (*cn*) sub-factor value (table IV of Figure 5). This is done by determining what layers overlie the aquifer and whether the aquifer is confined (overlain by an aquiclude), semi-confined (overlain by an aquitard) or unconfined (not overlain by a different lithology). Based on these observations a GIS layer showing the distribution of different confining conditions is created. Confined aquifers are assigned a *cn* sub-factor rating of 2 which doubles the O_L sub-score for such an aquifer. This is due to the fact that if an aquiclude overlies an aquifer any infiltrating water will only reach the aquifer when it has migrated horizontally to unconfined or semi-confined parts of the aquifer. This horizontal migration of the water results in an increased travel time and higher amounts of natural attenuation of any contaminants present before the water reaches the aquifer. Since aquitards allow the transmission of water at very low rates when compared to an aquifer (and therefore allow more time for pollutant attenuation to occur) a *cn* sub-factor rating of 1.5 is assigned to semi-confined aquifers.

Combination of layers

The lithology and fracturation layer is overlain with the water depth layer in a GIS and the *Layer index* is then calculated as the sum of the products of each layer above the water table's *ly* sub-factor value and its thickness Equation 4).

$$Layer\ index = \Sigma (l_y \cdot m) \quad \text{Equation 4}$$

Once all areas are defined by a *Layer index*, table V (Figure 5) is used to represent each area by a *Layer index value*. The *Layer index* value layer is then overlain with the Confining conditions layer (*cn* sub-factor) and their product yields the O_L sub-score value for the entire mapping area.

7.2.3 O score

The O_S and O_L sub-score layers are overlain in a GIS and the sum of the two sub-scores is then calculated to yield the final O score for the entire mapping area. O Scores range from 1 to 15 and table VI (Figure 5) is used to interpret the O Scores into varying levels of aquifer protection. The illustration of the different O Scores within a mapping area (the O Map) shows how the different soils and lithologies provide varying degrees of protection within a mapping area (e.g. Figure 8).

7.3 Precipitation map

The precipitation layer map is created by assigning two sub-factors to the mapping area, the *rainfall* (Pq) (mm/year) and the *temporal distribution* (Pi) (mm/day) sub-factors (tables XIII to XIV of Figure 5). The sum of these two sub-factors is referred to as the P score and represents the degree to which the natural aquifer protection (O factor) is reduced due to the rainfall regime in that area.

7.3.1 Pq sub-factor

The rainfall sub-factor is determined based on the average rainfall for wet years. A wet year is defined as a year in which the total rainfall exceeds or equals the long-term *arithmetic average rainfall plus 0.5 times its standard deviation* (table XIII of Figure 5).

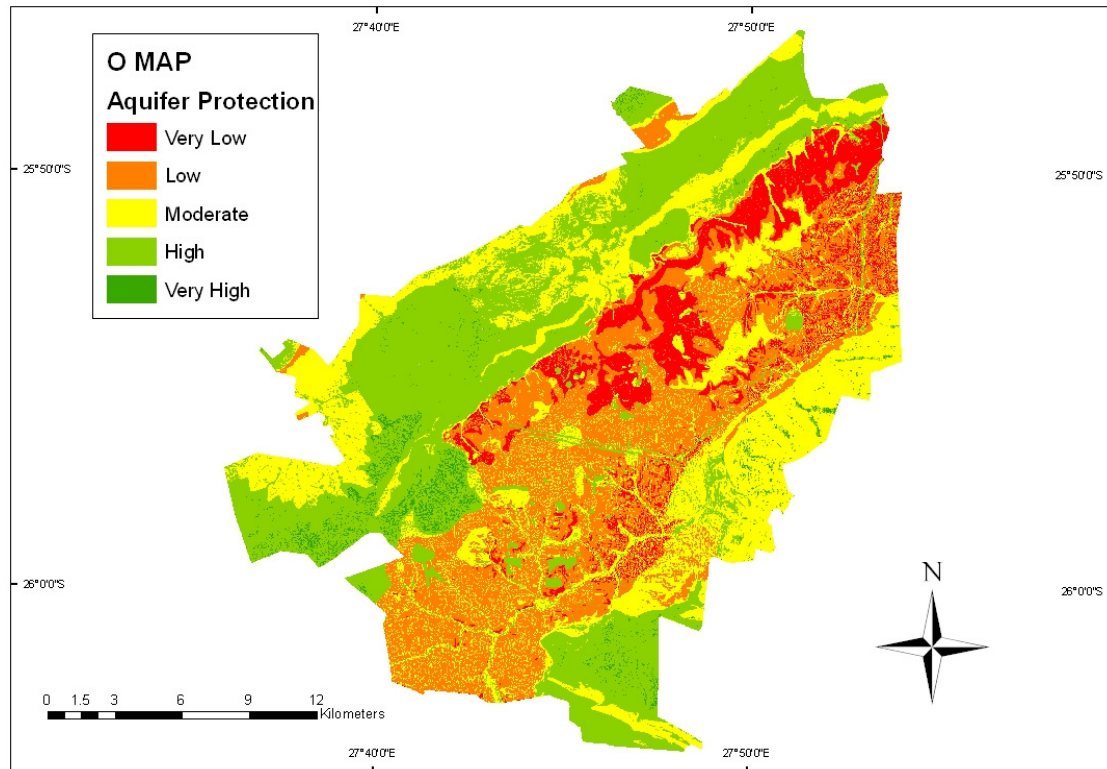


Figure 8. Example of an Overlying layer (O) factor map.

Rainfall data (including the co-ordinates of data recording points) for the mapping area and its surroundings must be collected. Available sources of data include the South African Weather Service, the Agricultural Research Council and the Department of Water Affairs and Forestry. The climatic data included in the Land Type Inventories of the Land Type Maps (Government Printer/Agricultural Research Council-Institute for Soil Climate and Water) is not sufficient for the determination of the P score as only average annual precipitation data are given. Thiessen polygons or a more advanced method can be used to decluster and regionalize the data and to determine which (weather stations) data points are influential on the mapping area. The data from the influential stations must then be analysed to determine the integrity thereof. This is required as many of the encountered data sets have long periods in which significant records are missing. If a single year of an influential station has more than 19 days' data missing during the rain season (Highveld / Escarpment: November – April) or more than 30 days' data missing during any other month of the year, that year's data is considered to be incomplete and unacceptable for further analysis. Stations that contain only incomplete and unacceptable

data or only limited acceptable data must be removed from the list of influential stations and the declustering redone for the remaining final list of influential stations.

Precipitation data of the final influential stations are then analysed to arrive at the annual rainfall and average annual rainfall for *wet years*. Pq sub-factors are then assigned to each sub area of equal rainfall based on the observed average annual rainfall for *wet years* (table XIII of Figure 5).

Since ground water vulnerability is commonly believed to increase with increasing recharge (as contaminant transport is more likely and transit time is reduced) a higher annual average rainfall for wet years is assigned a lower Pq sub-factor rating (i.e. higher reduction in aquifer protection). However recharge rates above a certain threshold will result in higher dilution of the contaminants. This is in accordance with the SINTACS method (Civita 1994 in Vías et al., 2006:5), which proposes, that a reduction in vulnerability occurs when recharge is higher than 300–400 mm/year. The average annual precipitation for the Cradle of Humankind World Heritage Site (COHWHS) is approximately 650 mm and Holland (2007) proposed an annual average recharge of 16 % or 114 mm. Based on the original COP method the recharge threshold of 300 mm/year would only be reached when the average annual precipitation is more than 1800 mm/year. This value seems highly exaggerated for the site and it is believed that dilution effects will become important at much lower recharge amounts. It was therefore decided to half the recharge threshold to 150mm/year. This means that when annual precipitation exceeds 900 mm, the dilution of potential contaminant is likely to be the dominant process and consequently the protection given by the O factor is less modified by the P factor. The Pq sub-factor rating therefore increases when the average annual rainfall for wet years exceeds 900mm/year.

7.3.2 Pi sub-factor

The rainfall data for each of the influential stations are analysed to arrive at the average annual number of rain days per *wet year*. The average annual rainfall for *wet years* is then divided by the average annual number of rain days per *wet year* to arrive at the temporal distribution of rainfall for each station, which is used to assign a Pi sub-factor to the corresponding sub area (table XIV of Figure 5). This is done to consider the

intensity with which rainfall events occur. Where rainfall generally occurs during intense storms that result in large amounts of Hortonian flow the aquifer vulnerability will be higher than in areas where an equal amount of rain falls over a few rain days and infiltration occurs more readily. Based on the above, areas with a higher average wet year rainfall and less rain days (i.e. larger mm/day values) are assigned lower P_i sub-factor ratings to reduce the protection by the overlying layers to a larger amount.

7.3.3 P score

The sum of the P_q and P_i sub-factor values yields the final P score for each of the sub areas and of the mapping area. P Scores range from 0.4 to 1 and table XV (Figure 5) is used to assign varying levels of aquifer protection reduction to the P scores. The illustration of the different P Scores within a mapping area (the P map) shows how the different precipitation regimes within a mapping area reduce the aquifer protection offered by the overlying layers (e.g. Figure 9).

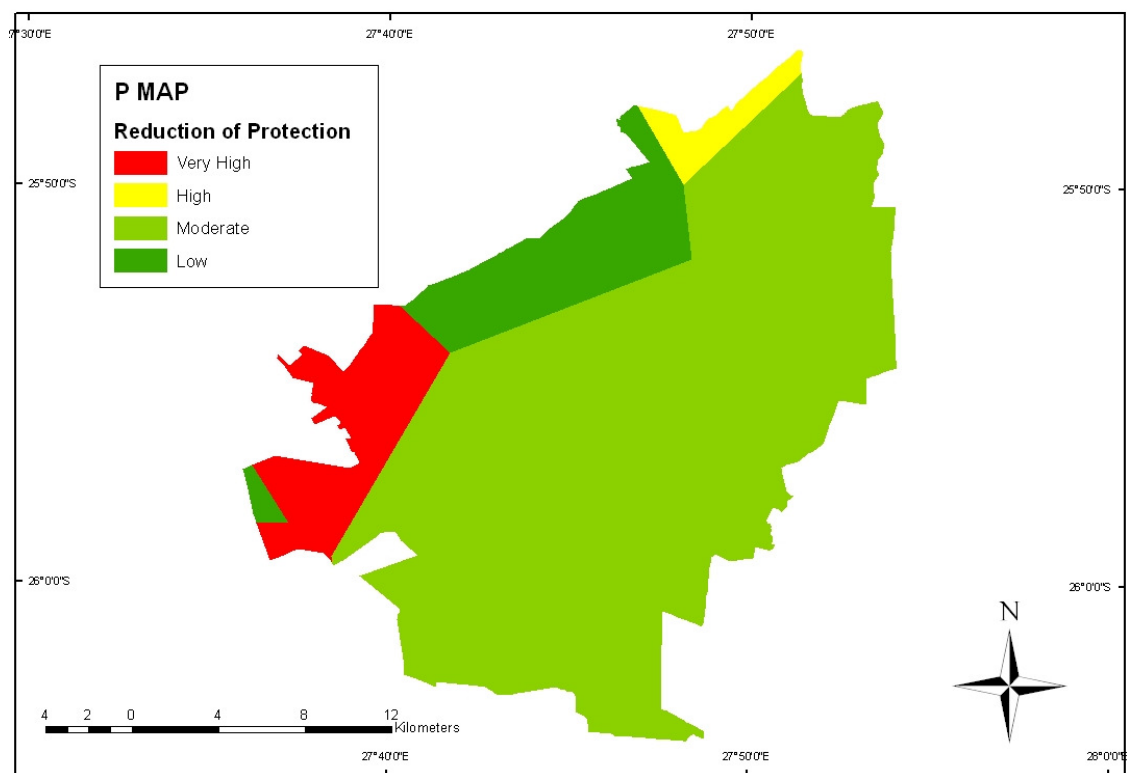


Figure 9: Example of a Precipitation (P) factor map.

Within small mapping areas that also have a very subdued topography no significant variations in precipitation regime should be present. In such cases the dominant observed P score should be assigned to the entire mapping area. However in large (regional) mapping areas or areas where significant topographical features result in different precipitation regimes multiple P Scores can be assigned to areas based on either the chosen declustering method or any other criteria (e.g. topographical features).

An investigation of P factors, using the proposed methodology, for different karst terrains in South Africa showed how the P factor varies significantly in areas with different regional precipitation regimes. In Figure 10 it can be seen that the reduction in aquifer protection is predominantly *low* in a karst terrain along the Mpumalanga Escarpment (Figure 10A), predominantly *moderate* in the Gauteng Highveld (Cradle of Humankind karst terrain) and exclusively *very high* in a karst terrain on the Ghaap Plateau.

The *very high* reduction in protection observed in the Ghaap Plateau is due to the average annual rainfall for wet years being high enough to cause significant recharge but not high enough to result in significant dilution of contaminants (i.e. Pq sub-factor = 0.2). This is similar to the Cradle of Humankind karst terrain where the Pq sub-factor ranges from 0.2-0.3. However in the majority of the Cradle of Humankind more rain days occur and subsequently the Pi sub-factor is equal to 0.4 (i.e. temporal rainfall distribution of 10-20mm/day) as opposed to the consistent Pi sub-factor of 0.2 in the Ghaap Plateau where a low number of rain days are present. The rainfall regime in the Ghaap Plateau is therefore more likely to result in the flushing of contaminants into the aquifer.

The dominance of a *low* reduction in aquifer protection in the escarpment karst terrain is due to the average annual rainfall in wet years exceeding 1200mm and as such resulting in significant dilution of contaminants. This high rainfall is distributed over a large amount of days and as such a temporal distribution of 10-20mm/day occurs for wet years in this area (i.e. Pi sub-factor = 0.4).

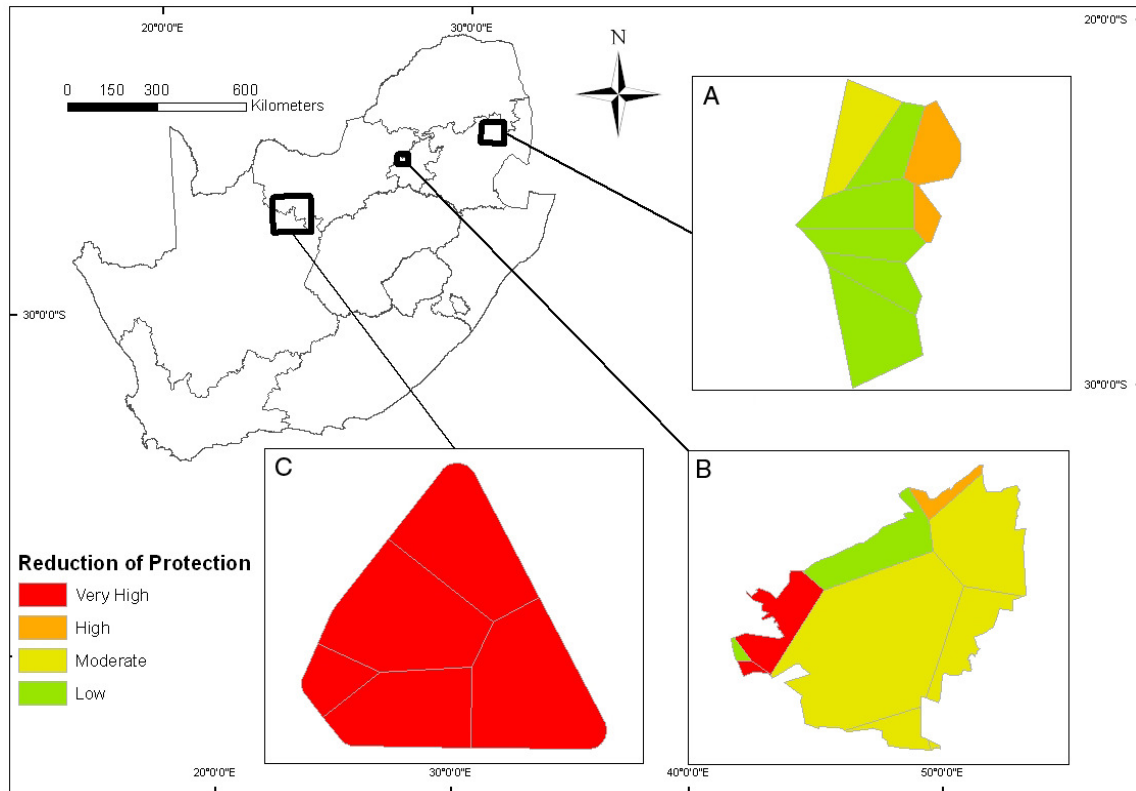


Figure 10. Precipitation (P) factor maps for various karst terrains in South Africa.

7.4 Concentration of flow map

The concentration of flow map is created for areas that fall into one of the following scenarios:

- **Scenario 1:** Swallow hole recharge areas: defined as any area within 2400m of a swallow hole and/or within 100m of a sinking stream.
- **Scenario 2:** Remaining karst areas: any area not within Scenario 1 and characterized by karstic rocks at surface.

Scenario 1 areas are essentially all areas in which the aquifer is recharged by swallow holes (i.e. localized or direct recharge), while Scenario 2 areas are more likely to be governed by diffuse recharge. A swallow hole is defined in this context as any locality in a karst region where surface water can disappear underground into an opening in the karstified bedrock. The definition therefore includes caves, sinkholes and swallets. A sinking stream is defined as a body of flowing water that flows (totally or partially) into a

swallow hole and disappears underground. As the location of all swallow holes is required to identify all Scenario 1 areas the steps followed in the determination of the *dh* sub-factor (section 7.4.1) should be followed before the mapping of Scenario 2 areas begins.

7.4.1 Scenario 1

Scenario 1 areas are assigned three sub-factors, namely; the *distance to swallow hole (dh)*, *slope/vegetation (sv)* and the *distance to sinking stream (ds)* sub-factors (tables VII to IX of Figure 5). The product of these three sub-factors is referred to as the C score and represents the degree to which the aquifer protection by the overlying layers is reduced due to the presence of karst phenomena that act as points of direct recharge.

dh sub-factor

The distance to swallow hole sub-factor is determined by the distance to the closest swallow hole (table VII of Figure 5). The *dh* rating increases with distance from a swallow hole as contaminants in distant areas are more likely to undergo natural attenuation before entering the swallow hole and less likely to be transported to the swallow hole than in areas in closer proximity. Although information on the exact location of all such features within a mapping area is not readily available, people living and/or working in the area may have useful knowledge of such features. Within conservation areas a database of caves and/or sinkholes may be kept by local conservation officials.

Aerial photograph interpretations yield valuable information on the location of such features. This is especially true in grass land areas where swallow holes are clearly visible as isolated occurrences of large trees (Figure 11A). However, features located in densely vegetated areas as well as more recent features will not be clearly visible on aerial photographs (Figure 11B & C). Extensive field mapping must therefore be performed to identify such features as well as to confirm the presence of features identified in aerial photographs.



Figure 11. Examples of swallow holes as seen in aerial photographs. A: Clearly visible feature. B: Feature hidden by dense vegetation, C: New feature not clearly visible on an aerial photograph.

Once a feature is identified its location must be recorded accurately and an assessment of the feature's "link" to the groundwater must be made. This refers to whether or not the identified feature will act as a point of direct recharge. Many karst depressions in South African karst terrains are not sinkholes but consolidation dolines that form when low density residual dolomite soils become consolidated over long periods of time. These features will not act as direct recharge points and as such will not reduce the aquifer protection. Figure 12 is an example of such a doline that was clearly visible on an aerial photograph (Figure 11A) but not a point of concentrated recharge.



Figure 12. A doline clearly visible in an aerial photograph which acts not as a concentrated recharge point.

Due to the age of the karstic rocks within South Africa multiple periods of karstification have occurred. This has resulted in features of different ages occurring within the same karst terrain. Younger karst features generally act as a direct link to the groundwater as no sediments have accumulated therein. However sediments may over time have accumulated in older features. An example of each of these cases is presented

in Figure 13 and a schematic diagram thereof is presented in Figure 14. If sediment is present the original karst conduit is likely to still exist below the sediment and therefore the feature will act as a point of direct recharge. However water transmission will be retarded to some extent within the sediment layer and therefore an increased dh sub-factor must be assigned to the areas surrounding such features.

A simple GIS buffer operation is used to assign dh sub-factors to the areas surrounding all swallow holes according to table VII (Figure 5). The buffering operation will also define all areas that fall under Scenario 1.

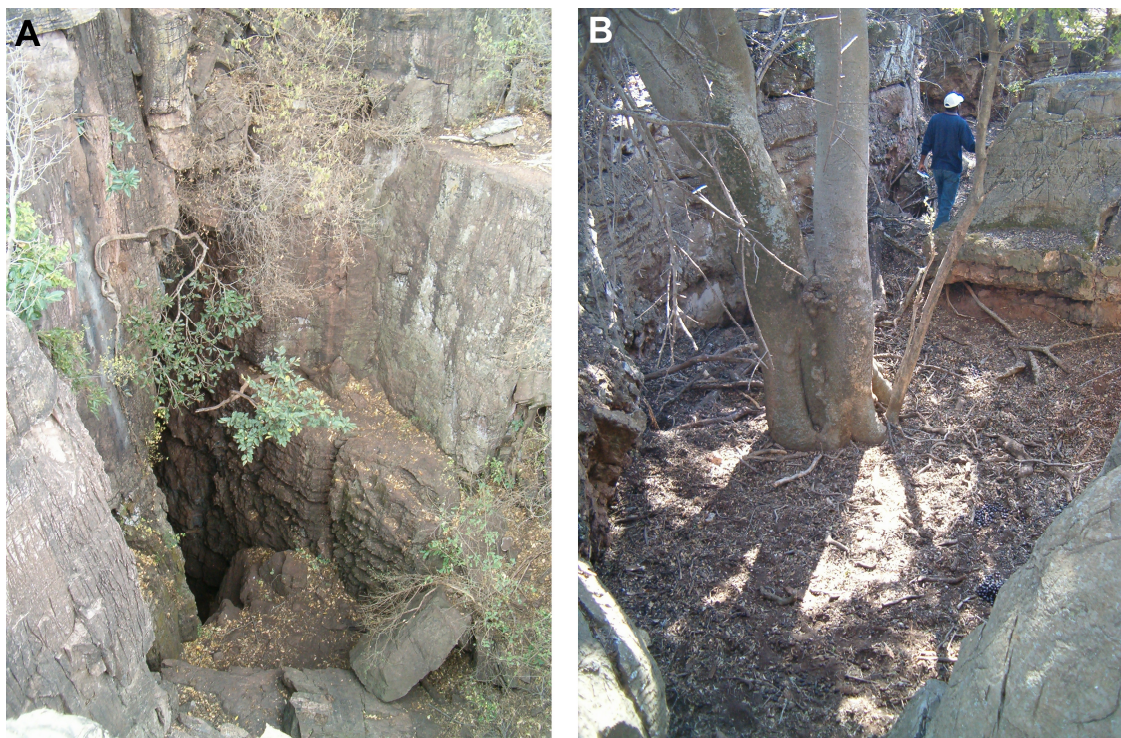


Figure 13. Examples of a swallow hole with (A) and without (B) sediment accumulation.

sv sub-factor

The slope/vegetation (sv) sub-factor is based on the slope gradient of an area and the vegetation cover present (table VIII of Figure 5). Using GIS analysis on a digital terrain model (DTM) the slope gradient within all Scenario 1 areas is determined. All areas with very low or very high gradients (i.e. $\leq 8\%$ or $\geq 76\%$) are assigned sv sub-factors irrespective of the vegetation cover present (table VIII of Figure 5). In areas with gradients of more than 8% and less than 76% an assessment of the vegetation cover is

required before *sv* sub-factors can be assigned. Aerial photographs are used to obtain data regarding vegetation cover, but once again a reasonable amount of ground truthing will be required. Areas are defined as having either *low* (grass land or no vegetation), *sparse* (grass land with minor shrubs, trees or bushes) or *high* (dense trees, shrubs or bushes) vegetation cover (Figure 15).

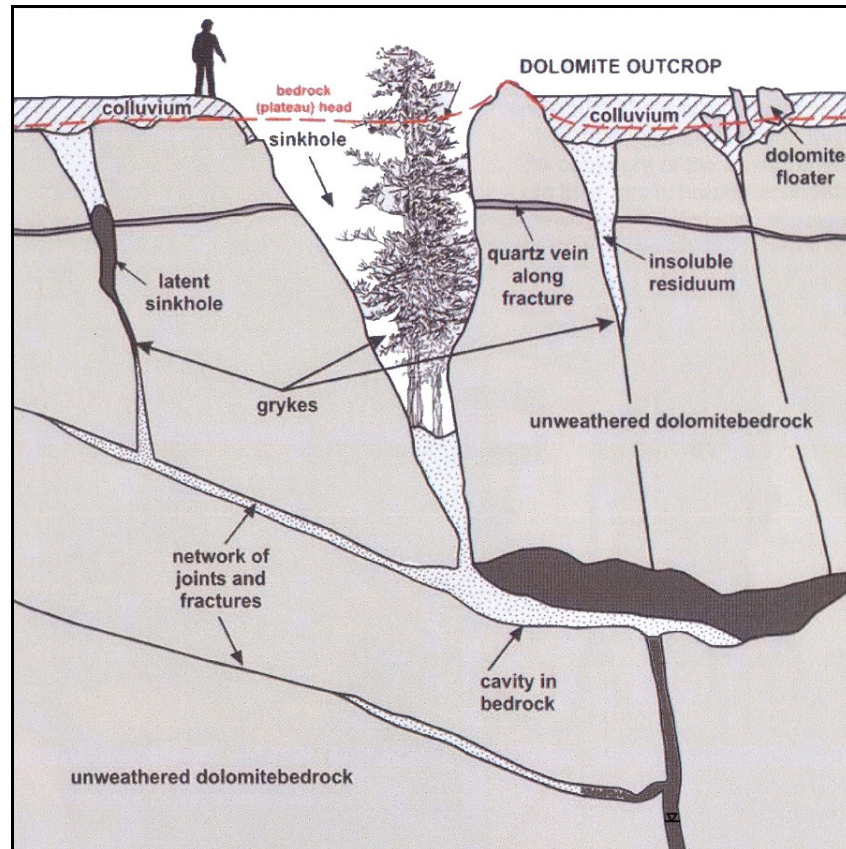


Figure 14. Schematic diagram of a typical karst setting where a swallow hole is blocked with sediment but still linked to the groundwater underneath the sediments (adapted from Trollip, 2006).

The slope steepness is positively correlated with the generation of surface runoff while the vegetation density is negatively correlated with the generation of runoff. In Scenario 1 areas increased surface runoff results in more localized recharge and therefore the values in table VIII (Figure 5) relate a steeper slope and a lower vegetation density to a higher reduction of aquifer protection. However, the effect of vegetation density on surface runoff generation is considered negligible in areas where the slope is less than 8% or more than 76%.

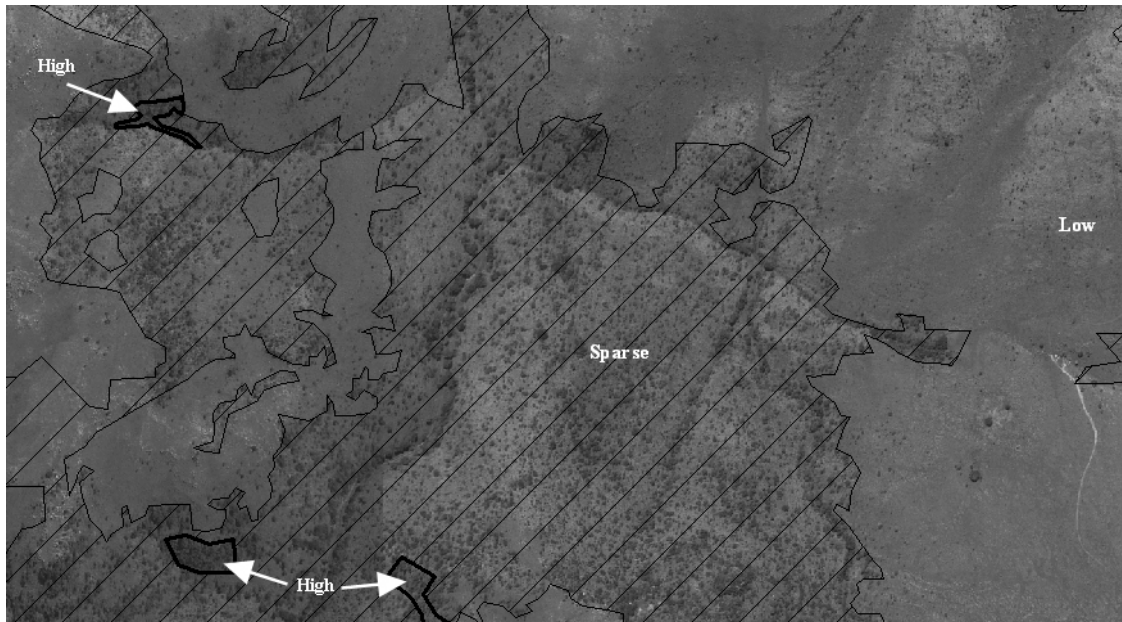


Figure 15. Vegetation cover density determined by aerial photograph interpretation.

By overlaying slope gradient and vegetation cover layers all Scenario 1 areas are then assigned a *sv* sub-factor according to table VIII (Figure 5).

ds sub-factor

The distance to sinking stream (*ds*) sub-factor value is assigned based on the distance from any stream or river that enters a karst conduit and continues flowing (entirely or partially) underground. The identification of such rivers or streams is done using aerial photographs, field mapping of river courses and the knowledge of local inhabitants and specialists. The actual point of “sinking” (i.e. where the river enters the underground karst system) will also be a swallow hole. A GIS buffer operation is used to delineate areas that are within 10m or 100m of such streams and *ds* sub-factors assigned to **all** Scenario 1 areas according to table IX (Figure 5). Within 10m of a sinking stream a very rapid transmission of contaminants into the stream (and subsequently directly into the aquifer via the swallow hole) is likely. Such areas are therefore assigned *ds* sub-factors of zero and hence the protection of the aquifer by the overlying layers reduced to zero. In areas between 10m and 100m from sinking streams the protection of the aquifer by the overlying layers is partially reduced ($dh = 0.5$), while in areas beyond 100m the protection remains unchanged.

Combination of layers

The distance to swallow hole (dh), slope/vegetation (sv) and distance to sinking streams (ds) layers are overlain in a GIS and the product of these three sub-factors yields the C score for all Scenario 1 areas.

7.4.2 Scenario 2

Scenario 2 areas are assigned two sub-factors, the *surface features* (sf) and *slope/vegetation* (sv) sub-factors (tables X and XI respectively of Figure 5). The product of these two sub-factors is referred to as the C score for all Scenario 2 areas and represents the degree to which the aquifer protection by the overlying layers is reduced due to the presence of karst phenomena that promote infiltration as opposed to runoff away from karstic rocks.

sf sub-factor

The surface features sub-factor is based on the geomorphological features of the karstic rocks and the nature of any layers (if present) above these materials. These variables determine the relative importance of surface runoff versus infiltration processes. Where karst is well developed, less surface runoff is generated and high infiltration rates will reduce the aquifer protection. Similarly, the absence of a layer above karstic rocks also promotes infiltration and as such reduces the aquifer protection. Table X (Figure 5) gives the ratios such reductions in protection (i.e. higher sf sub-factors).

The nature and presence of surface layers which cover karstic rocks should be deduced from the geological maps and soil maps used in the creation of the O factor map. However, the distribution of areas characterized by different karst development must be obtained using a combination of remote sensing and field mapping. Areas in which the rock is heavily karstified will appear different in aerial photographs when compared to areas in which surface layers are not karstified (Figure 16). Thus once areas have been visited and their karst development documented (Figure 17) the extent of such areas can be extrapolated to areas which appear similar on aerial photographs.

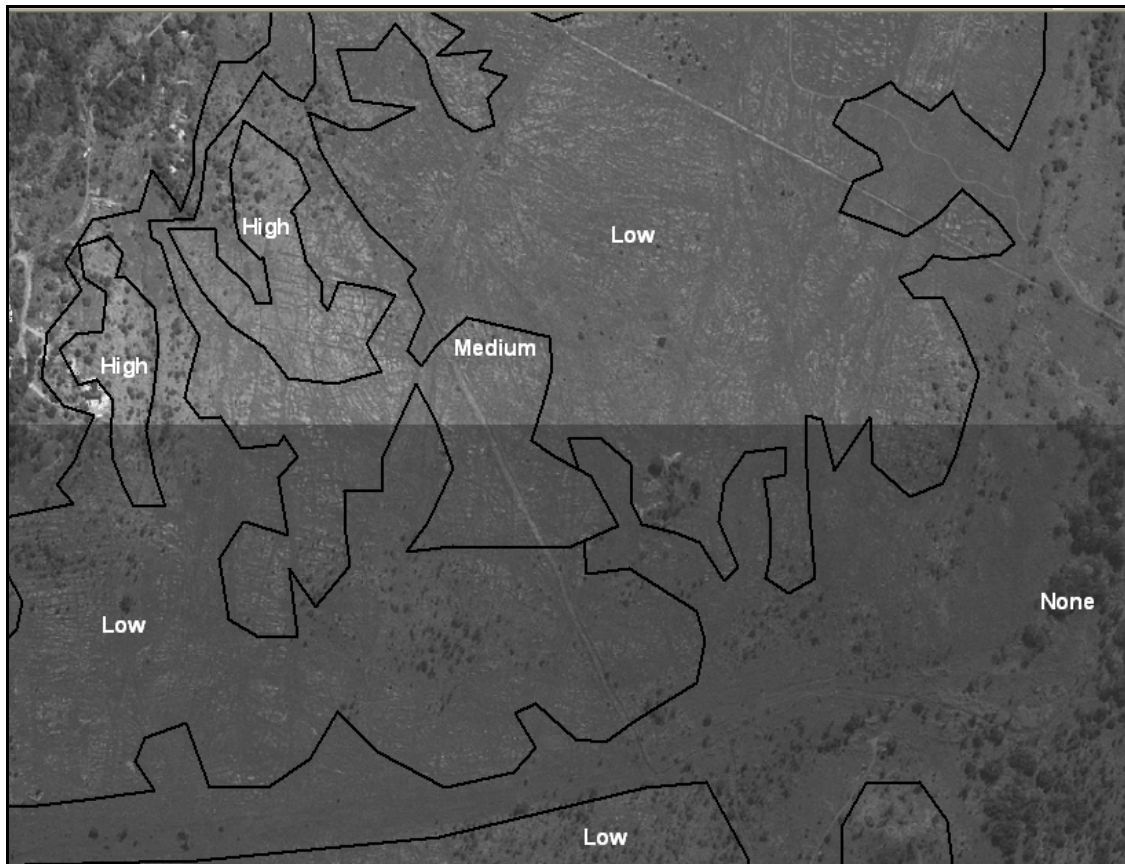


Figure 16. Extrapolation of surface karst development using aerial photograph interpretation.

sv sub-factor

In Scenario 2 areas the slope/vegetation (*sv*) sub-factor is determined as for Scenario 1 areas, i.e. based on the slope gradient of an area and the density of the vegetation cover present (table XI of Figure 5). Slope steepness is again positively correlated with the generation of surface runoff while vegetation density is negatively correlated with the generation of runoff. However, in Scenario 2 areas increased surface runoff results in less infiltration and therefore a lower recharge. The *sv* sub-factor values in table XI (Figure 5) therefore relate a steeper slope and a lower vegetation density with a lower reduction of aquifer protection. The effect of vegetation density on surface runoff generation is once again considered negligible in areas where the slope is less than 8% or more than 76%.

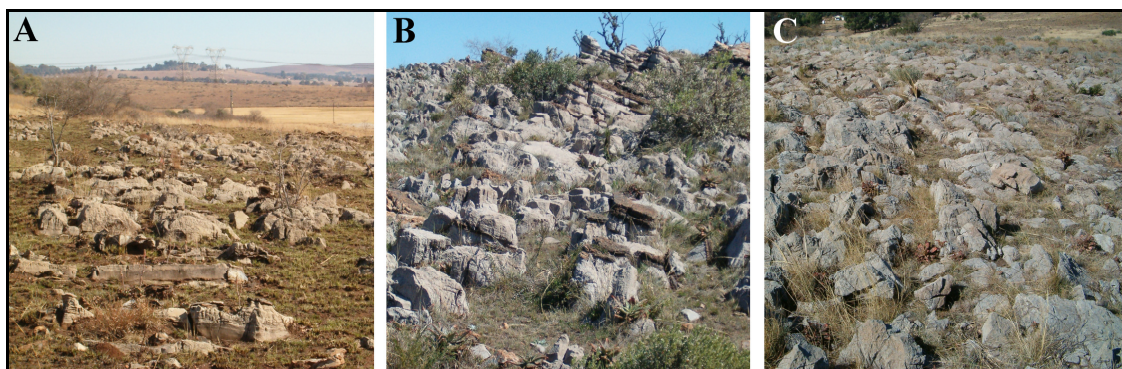


Figure 17. Karstic rock areas with different levels of the surface karst development: A: low (*fissured carbonate*), B: medium (*dissolution features*) or C: high (*developed*).

Using GIS analysis on a digital terrain model (DTM) the slope gradients of all Scenario 2 areas are determined. All areas with very low or very high gradients (i.e. $\leq 8\%$ or $\geq 76\%$) are then assigned *sv* sub-factors irrespective of the vegetation cover present according to table XI (Figure 5). In areas with slope gradients of more than 8% and less than 76% an assessment of the vegetation cover is required before *sv* sub-factors can be assigned. As before aerial photographs are used to obtain data regarding vegetation cover and a reasonable amount of ground truthing will be required. Areas are again defined as having either *low* (grass land or no vegetation), *sparse* (grass land with minor shrubs, trees or bushes) or *high* (dense trees, shrubs or bushes) vegetation cover (Figure 15).

By overlaying slope gradient and vegetation cover layers all Scenario 2 areas are then assigned a *sv* sub-factor according to table XI (Figure 5).

Combination of layers

The surface features (*sf*) and slope/vegetation (*sv*) layers are overlain in a GIS and the product of these two sub-factors yields the C score for all Scenario 2 areas.

7.4.3 C score

In Scenario 1 areas a C score of 0 is possible while in Scenario 2 areas the minimum C score is 0.1875 since no direct recharge is possible in Scenario 2 areas and therefore the protection of the aquifer by the overlying layers can not be reduced to zero. Table XII (Figure 5) is used to relate the C Scores to five levels of reduction in aquifer protection. The illustration of the different levels of reduction of aquifer protection across the mapped area is known as the *Concentration of flow or C map* (e.g. Figure 18).

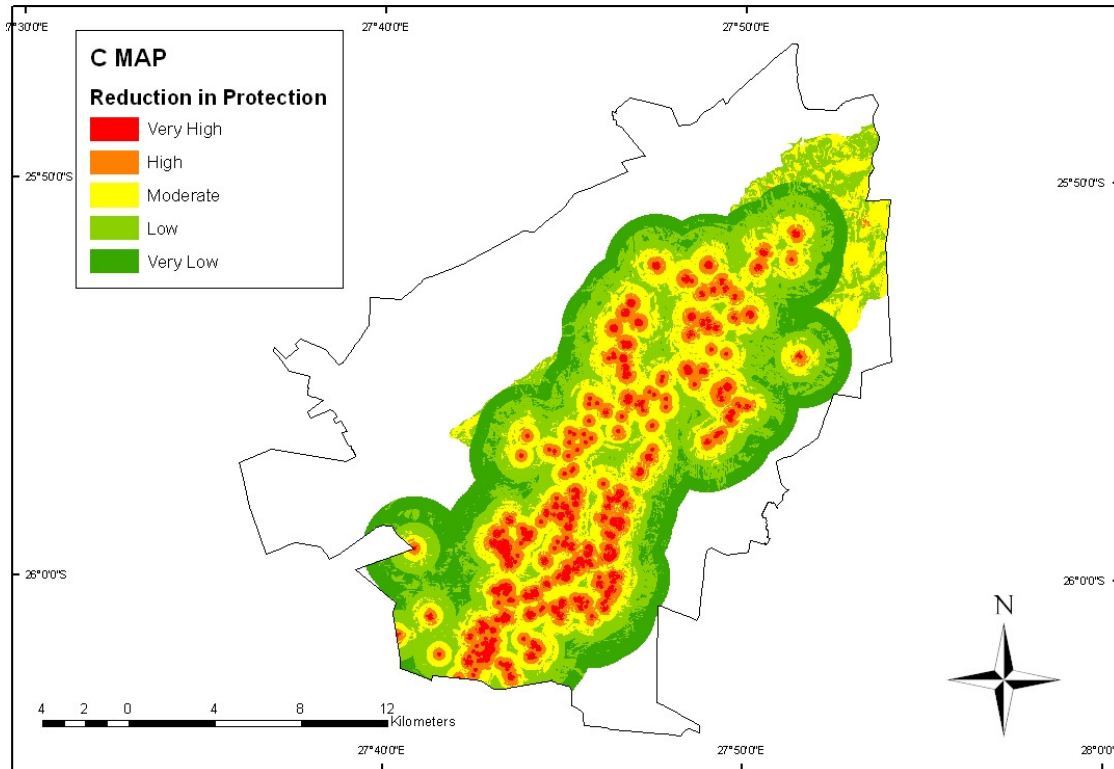


Figure 18: Example of a Concentration of flow (C) factor map.

7.5 Final vulnerability map

The three layers (O, P and C maps) are overlain to create the final aquifer vulnerability map. The final vulnerability or *VUKA* Index is calculated by the product of the three layer's scores (O, P and C SCORES). The *VUKA* Index is then used to classify areas into one of five aquifer vulnerability classes ranging from *very low* to *very high* (table XVI of Figure 5). The final aquifer vulnerability map is created by illustration of the different vulnerability classes of each sub area within the mapped area (Figure 19).

7.6 Modifications to original COP method

Several modifications of the original COP method were necessary to adopt it to South African karst terrains and are discussed below.

7.6.1 O factor

Table III in Figure 5 is a slightly modified version of the original COP *lithology and fracturation* sub-factor table. The modification was used purely to include common rock types found within South Africa and especially those found in South African karst

terrains. The *lithology and fracturation (ly)* sub-factor ratings were not modified. The modifications are as follows:

- “Silts” have been replaced by “Well graded sediments” to allow colluvial and alluvial sediments of mixed grading to be easily defined according to *ly* sub-factors.
- “Shales, mudstones and siltstones” have been added to the original “marly limestones” category.
- “Quartsites” have been added to the original “sandstones” category as many sandstone layers of the Transvaal Supergroup have been re-crystallized to quartsites.

The remainder of the O factor sub-score/sub-factor ratings are identical to those of the original COP method.

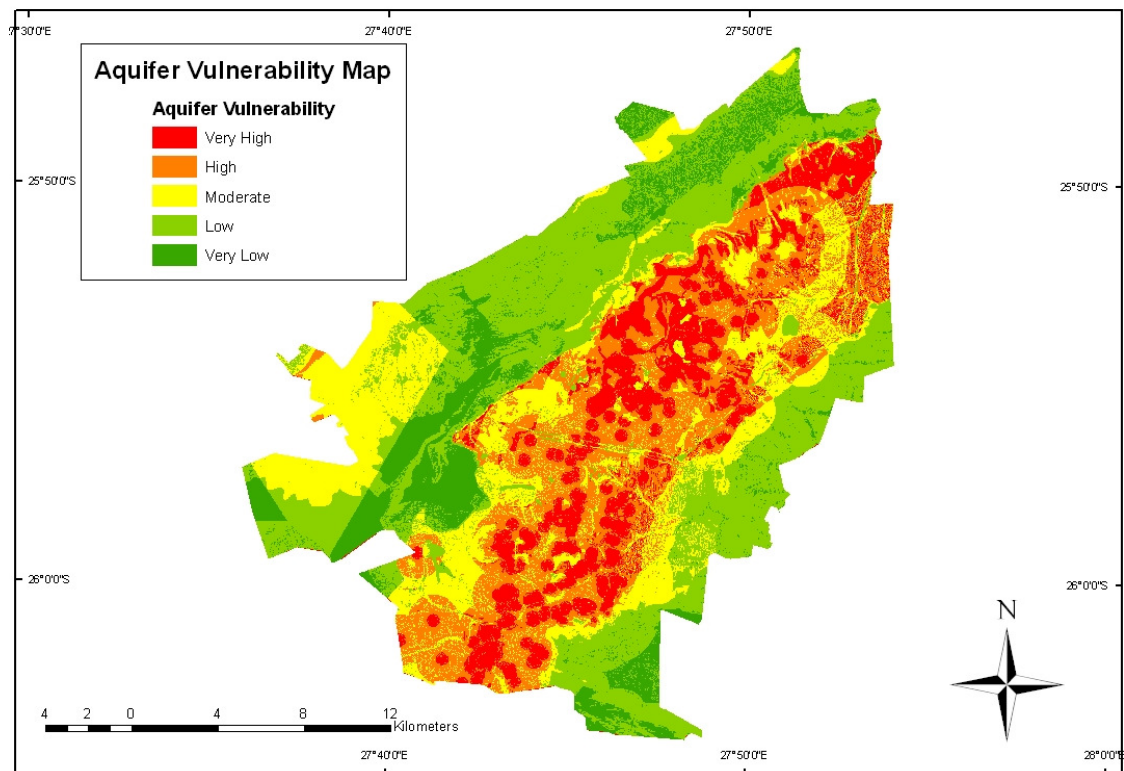


Figure 19: Example of an aquifer vulnerability map.

7.6.2 P factor

The definition of *wet years* in the original COP method (i.e. where annual precipitation exceeded the average annual precipitation by at least 15% (Vías et al., 2003)) was, for the sake of statistical consistency, modified to a year in which the annual precipitation exceeded or equaled *arithmetic mean plus 0.5 standard deviations*.

Similarly a revised parameter rating for the *Pq* sub-factor was created to more accurately incorporate the variability in the annual rainfall experienced in karst areas in South Africa and to increase the parameter sensitivity to suit South African conditions. The revision essentially consisted of dropping the threshold of the first class from 400mm/year to 300mm/year and reducing the class intervals from the original 400mm/year to 300mm/year. As discussed in section 7.3.1 this revision was focused on allowing the *Pq* sub-factor to accurately define the importance of dilution processes for high average annual rainfall. The revision is also more suited to South African conditions, where the average rainfall is lower than in Southwestern Europe (Spain), where the COP method was developed.

7.6.3 C factor

The distance to swallow hole (*dh*) sub-factor was modified significantly to fit South African conditions. Firstly the intervals of the buffer zones around the swallow holes was changed from the original 500m wide buffers to buffers that increase in width from 50m to 600m with increasing distance from the swallow hole. This is believed to better represent the non linear decrease in the probability of a contaminant entering a swallow hole with increasing distance from the swallow hole. The revised buffer zones also result in any area beyond 2400m from a swallow hole being considered as not part of the catchment of that swallow hole. The original buffering system only defined areas beyond 5000m as such to suit to the plateau type karst terrains found in Europe where a single swallow hole may have a catchment stretching up to 5000m on its upslope side. However the South African karst terrains do not have the same plateau nature and as such smaller catchments.

As mentioned in section 7.4.1 an additional, higher *dh* sub-factor rating option was added for swallow holes in which sediment has accumulated and a certain amount of

water transport retardation occurs before any infiltrating water can reach the karst conduit beneath the sediment. The exact physical retardation effect that the sediment has on infiltrating water was not quantified and in light of this a conservative approach was used. The *dh* sub-factor ratings for these swallow hole buffer zones are increased by 0.05 relative to the *dh* rating of a swallow hole in which no sediment is present. It is obvious from Figure 20B that, if the *dh* sub-factor ratings for sediment filled swallow hole buffer zones would be doubled in comparison to an open swallow hole, extensive large areas would have a lower reduction of protection; proving the sensitivity of the C map to the *dh* sub-factor.

An additional vegetation cover class of “*sparse*” was added, as large areas could not be placed into either of the two original “*high*” and “*low*” vegetation cover classes. The *sparse* vegetation cover areas were assigned *sv* sub-factors intermediate to those of the *high* and *low* vegetation cover areas. The original *sv* sub-factor ratings were therefore not edited, but an additional class added.

7.7 Utilization of aquifer vulnerability maps

Once an aquifer vulnerability map has been created using the described methodology, it can be used as a planning tool for urban planning as well as further groundwater investigations in the area. When development of any kind is planned, the map should be consulted in order to obtain information on areas that - due to their very high vulnerability - should not be developed and vice versa. Areas with moderate aquifer vulnerability require usually further investigations to arrive at **suitable** development types for the site that will not result in a high risk of aquifer contamination.

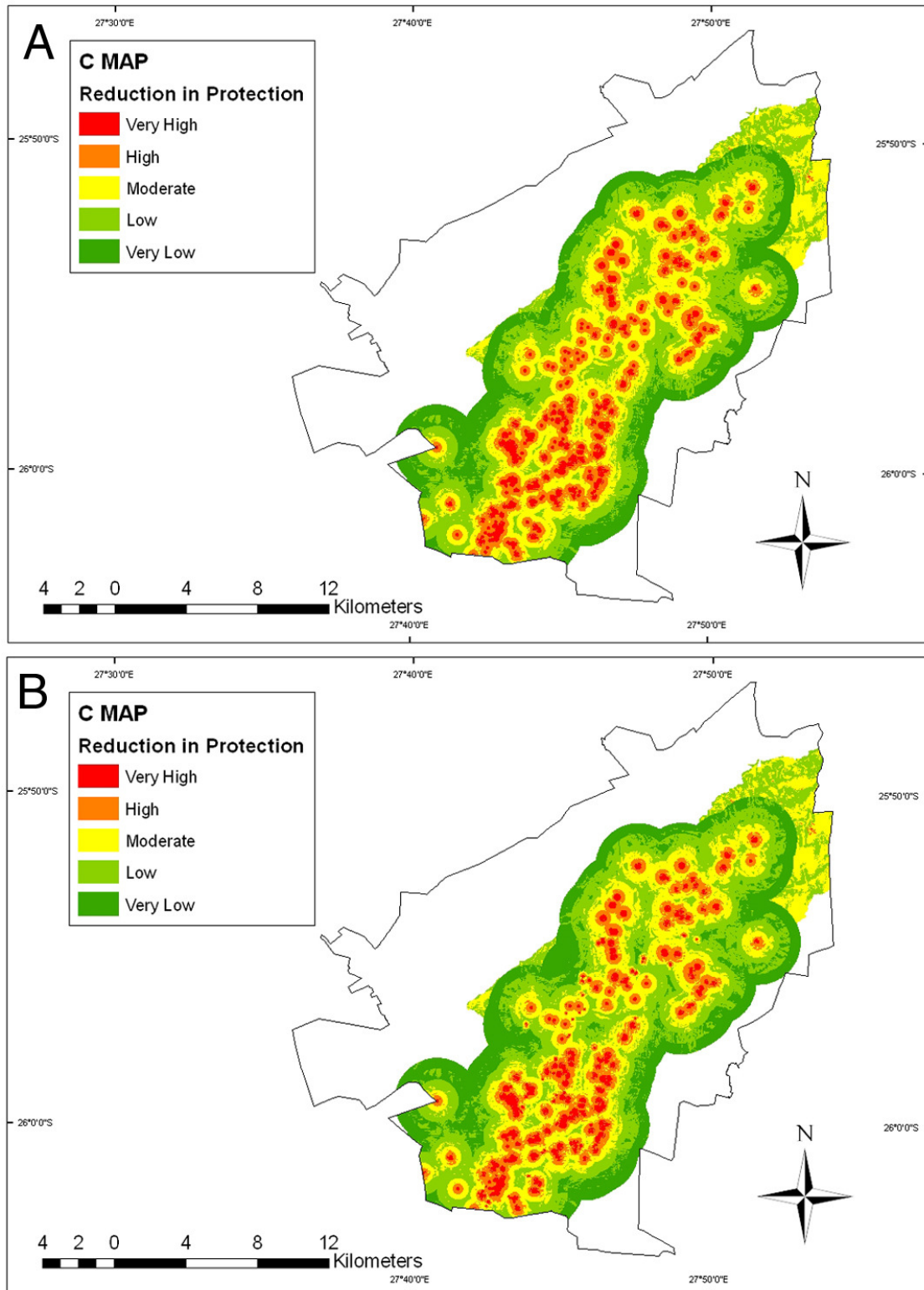


Figure 20: Example of A: a Concentration of flow (C) factor map created with conservative dh sub-factor ratings and B: a Concentration of flow (C) factor map created with excessive dh sub-factor ratings.

8 Aquifer Vulnerability map of the Cradle of Humankind

8.1 Physiography, climate and surface drainage

The Cradle of Humankind is a UNESCO world heritage site spreading between parts of both the Gauteng and North-West Provinces of South Africa. The area is situated between Krugersdorp in the south and Hartbeespoort Dam in the north (Figure 21). The terrain morphology is characterized by rolling hills with a maximum altitude of 1700m above sea level. The gradients of these hills are generally less than 20% but in places steep ridges with gradients of more than 75% are present. The area decreases in altitude from the southwest to the northeast with the lowest parts being at approximately 1200m above sea level.

The area receives an average annual precipitation of approximately 650mm and a mean annual evaporation of about 1 700 mm (DWAf, 1992). The mean daily maximum temperature across the study area ranges from 22 °C to 25°C while the mean daily minimum temperature ranges from 10 °C to 12 °C.

The Cradle of Humankind is drained by two main rivers and their tributaries, the Blaauwbankspruit and the Skeerpoort River. The larger Blaauwbankspruit, drains the southern parts of the area before entering the Crocodile River. The north-western parts of the Cradle of Humankind are drained by the Skeerpoort River, which enters the Magalies River. Smaller areas that do not form part of these two river catchments are drained by smaller, non-perennial streams. Ultimately all surface drainage from the Cradle of Humankind enters into the Hartbeespoort Dam.

The described drainage network is covered by parts of then the A21D, A21E, A21F, A21G and A21H quaternary drainage basins of the A21 tertiary drainage basin. The A21 tertiary drainage basin is part of the Limpopo river basin. The catchment management agencies relevant to the COHWHS are the Crocodile (West) and Marico Water Management Agencies.

The karstic areas of the COHWHS have well developed karst features. Several perennial springs are present across the area and these include both contact and barrier type springs. Numerous dolines, sinkholes and caves have been formed during the long

history of the carbonate rocks and are still being formed under present conditions. The two most well-known caves in the study area are the Sterkfontein and Wonder caves.

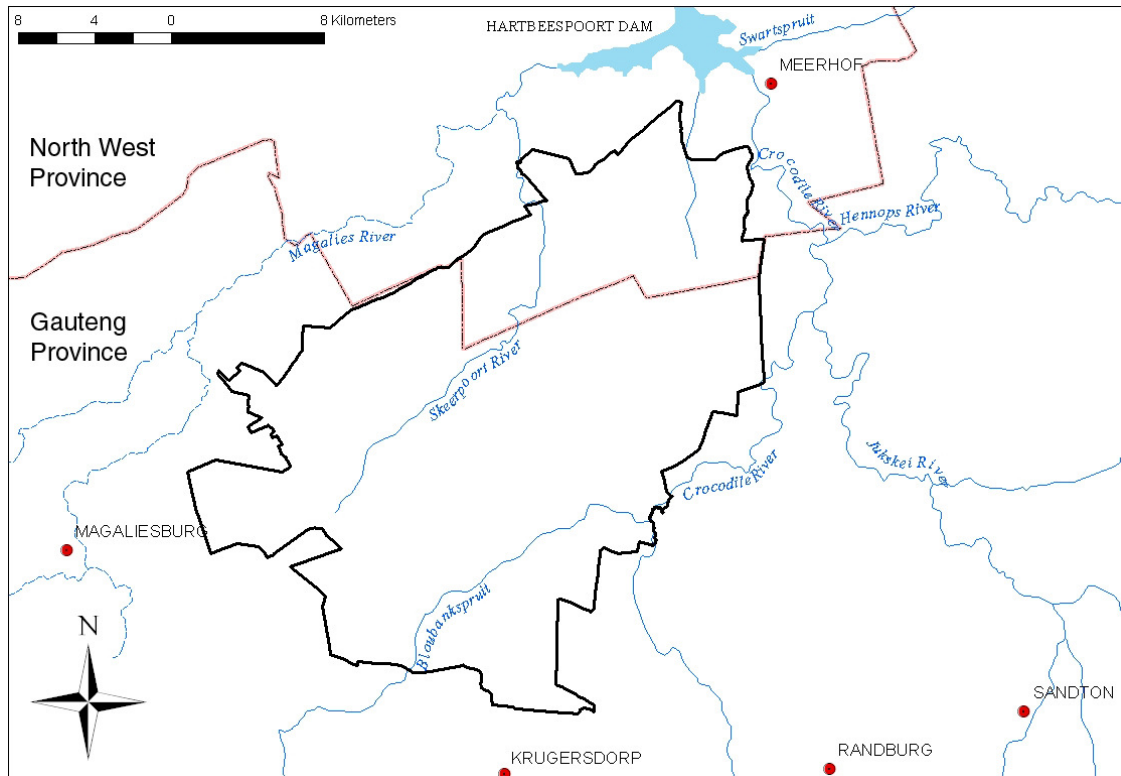


Figure 21: Location of the Cradle of Humankind World Heritage Site.

8.2 Geological setting

8.2.1 General geology

The mapping area covers an area of approximately 515 km² on the 1:250 000 scale geological map sheets 2626 West Rand and 2526 Rustenburg. It is predominantly underlain by strata of the Chuniespoort and Pretoria Groups of the Transvaal Supergroup with minor sections underlain by rocks of the Halfway House Granites, Ventersdorp Supergroup and Witwatersrand Supergroup (Figure 22).

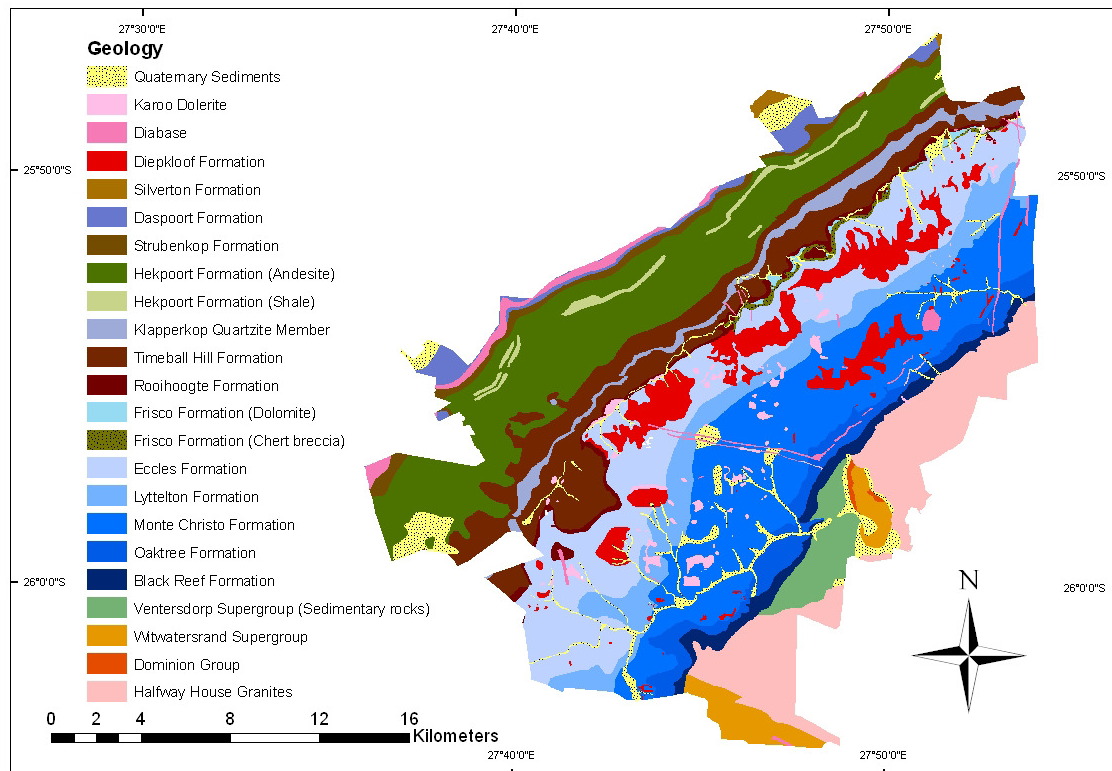


Figure 22: Geological map of COHWHS (Obbes, 2000 & own mapping).

The Halfway House Granites are Swazian age intrusives that are exposed as a domical “window” of granitic basement rocks (SACS, 1980). They consist of tonalitic gneisses, migmatites, gneisses and porphyritic granodiorites, dated at 3203 ± 65 Ma (Allsopp, 1961 in SACS, 1980:87). According to Anhaeusser (1973 in Robb et al, 2006:81) multiple magmatic events were responsible for the formation of these rocks. The early events emplaced mafic and ultramafic rocks (greenstones), which were later intruded by a suite of tonalite-trondhjemite-granodiorite granitoid rocks. The different intrusion stages resulted in the metamorphism of many of the rock units (Robb et al, 2006).

The Witwatersrand Supergroup is Archaean in age (3074 to 2714 Ma) and is preserved within the Witwatersrand basin. It consists of a lower West Rand Group (maximum thickness 5150m) and an upper Central Rand Group (maximum thickness 2880m) (Robb & Robb, 1998). Sandstone and shale dominate within the West Rand Group, which consists of three Subgroups (Hospital Hill, Government and Jeppestown

Subgroups) with different sandstone/shale ratios that are separated by basin wide unconformities (Robb & Robb, 1998). The Central Rand Group consists predominantly of sandstone and conglomerate with only minor shale (sandstone/shale ratio in order of 1:12). Within the two Subgroups of the Central Rand Group (Johannesburg and Turfontein Subgroups) at least 10 basin wide unconformities occur and these are used to divide the Subgroups into Formations (Robb & Robb, 1998). The Witwatersrand Basin sedimentation took place along the interface between a system of large rivers and a major body of still-standing water or an inland sea. At least four periods of deformation have significantly affected the Witwatersrand Basin development: Dominion related rifting (thermal relaxation after extrusion of Dominion lavas created an area of negative relief), Syn-Witwatersrand compression, Mid-Ventersdorp extension (major grabens formed) and Vredefort-related deformation (Robb & Robb, 1998).

The 2714-2709 Ga Ventersdorp Supergroup is made up of a lower Klipriviersberg Group, middle Platberg Group and the upper Bothaville (sedimentary) and Allanridge (volcanic) Formations. All four of the above mentioned stratigraphic units are unconformable and their thicknesses vary significantly (maximum total thickness is 8000m) (Brink, 1979). The Ventersdorp Supergroup is an accumulation of andesitic to basaltic lavas with related pyroclastic rocks (agglomerates and tuffs) and a number of sedimentary intercalations (Brink, 1979).

The Transvaal Supergroup is preserved in three separate structural basins, the Kanye (Botswana), Griqualand West and Transvaal basins. The Neoarchaeo-Palaeoproterozoic Transvaal Supergroup comprises five major litho-stratigraphical subdivisions: the so-called protobasinal rocks (purely a descriptive and not a genetic connotation), the Black Reef Sandstone Formation, the Chuniespoort Group carbonate-BIF platform succession, the volcano-sedimentary Pretoria Group and the uppermost Bushveld-related Rooiberg Felsite Group (Figure 23) (Eriksson & Reczko, 1995).

The study area is situated within the Transvaal basin, which is situated in the center of the Kaapvaal Craton. The Transvaal basin contains one of the thickest (c.15 km (Button, 1986 in Eriksson et al., 2001:209)) and most complete sequences of the distinct Neoarchaeo-Palaeoproterozoic volcano-sedimentary successions that are preserved

globally (Eriksson et al., 2001). This basin forms the floor rocks to, and outcrops in a limited band around, the c. 2.05 Ga Bushveld Complex intrusion (Eriksson & Reczko, 1995). Minor fragments of these floor rocks also occur as inliers in the central parts of the Bushveld Complex (Figure 23) (Hartzer, 1995 in Eriksson et al., 2001:209).

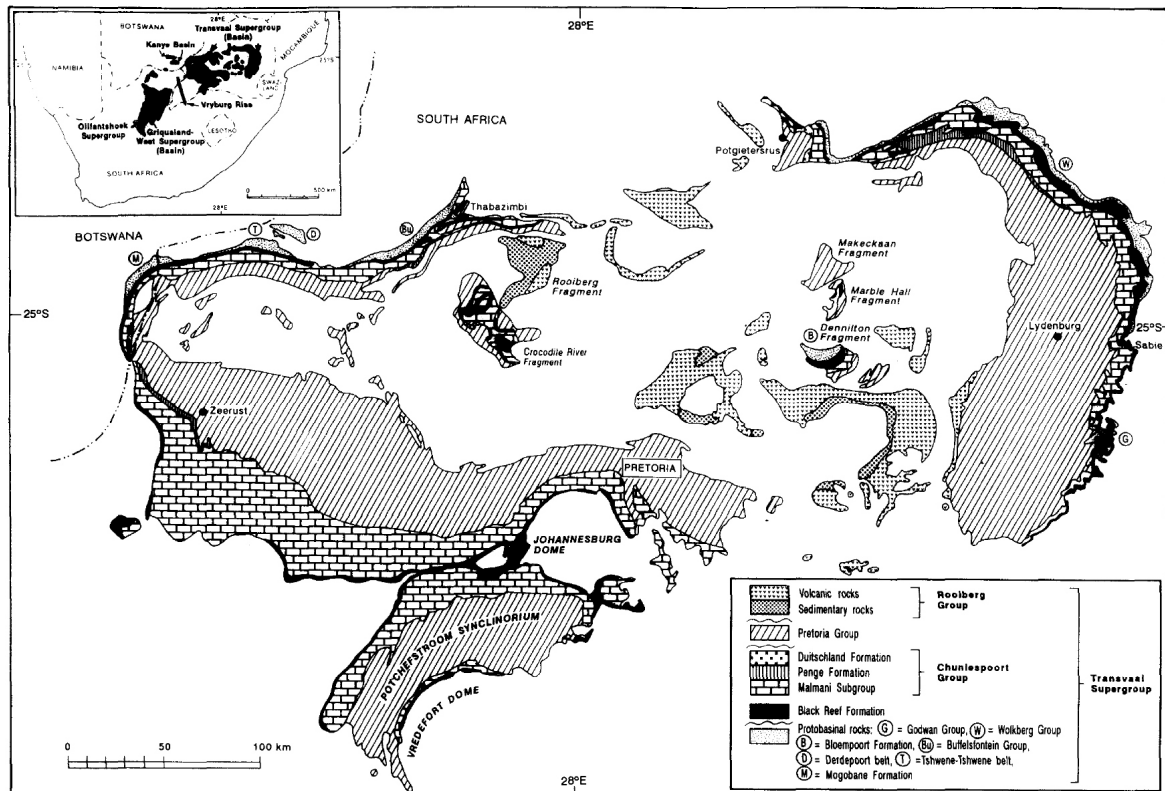


Figure 23: Geological map illustrating the distribution of the Transvaal Supergroup (Eriksson & Reczko, 1995).

The protobasinal successions of the Transvaal basin are preserved in discrete units around the margins of the preserved basin and in two of the fragments of Transvaal Supergroup rocks located within the Bushveld Complex. These successions are not present within the study area.

The onset of the Transvaal Supergroup sedimentation in the Transvaal basin is marked by the Black Reef Formation, which succeeds the protobasinal successions unconformably across the preserved basin (Eriksson & Reczko, 1995). The Black Reef Formation is in turn conformably overlain by the Chuniespoort Group which consists of the lower Malmani Subgroup (stromatolitic dolomite with chert interbeds) and the upper

Penge (banded iron formations) and Duitschland (mixed clastic and carbonate rocks) Formations. The later two units are absent from the study area. The Malmani Subgroup is subdivided into the Oaktree, Monte Christo, Lyttelton, Eccles and Frisco Formations (SACS, 1980).

The Pretoria Group overlies the Chuniespoort Group unconformably and buries a palaeokarst landscape developed on exposed dolomites during a depositional hiatus of at least 80 Ma due to uplift, weathering and erosion (Eriksson & Reczko, 1995). The Pretoria Group comprises a predominantly alternating sequence of mudrock and sandstone formations with subordinate conglomerates, diamictites and carbonate rocks and significant interbedded basaltic-andesitic lavas (Eriksson & Reczko, 1995). The basaltic-andesitic lavas belong to the Hekpoort Formation which also contains small lacustrine shale deposits. These deposits represent intermittent hiatuses in the volcanism (Eriksson et al, 2006). Many of the sandstones present in this group have been recrystallized to quartzites and the mudrocks of numerous formations (e.g. Timeball Hill, Silverton and Houtenbek Formations) contain common, thin, tuffaceous interbeds (Eriksson et al., 1993 in Eriksson & Reczko, 1995:499).

Age estimates based on various evidence from all three of the preserved basins indicate the entire Transvaal Supergroup to have originated between 2658 ± 1 Ma and 2224 ± 21 Ma (Eriksson et al., 2001) with the carbonate sequence being deposited over a period of at least 120 m.y. between 2643 and 2520 Ma (Obbes, 2000). Deformation of the Transvaal Basin sedimentary strata is limited to open interference folding, faulting and syn-Bushveld dykes and sills (Eriksson et al., 2001) and according to Eriksson et al. (1995) the Transvaal strata dip at angles up to 20° toward the centrally located Bushveld intrusives.

The various igneous intrusions (specifically sub-vertical dykes) that have intruded the dolomites of the Malmani Subgroup divide the dolomite into a number of groundwater compartments in which caverns, faults and joints widened by solution weathering contain significant quantities of groundwater (Brink, 1979).

8.2.2 Detailed geological description of Chuniespoort Group

The advance of the Chuniespoort Group Epeiric Sea is represented by a transgressive black shale that overlies the Black Reef rocks (Clendenin, 1989 in Eriksson & Reczko, 1995:494). The rocks of the Chuniespoort Group represent portions of one widespread carbonate-BIF platform sequence that covered much of the Kaapvaal Craton in the late Archaean (Eriksson et al., 1995). The Chuniespoort Group covers large areas in the preserved marginal portions of the Transvaal basin and restricted outcrops occur in the Marble Hall, Dennilton and Crocodile River fragments (Eriksson & Reczko, 1995). The basal Malmani Subgroup comprises five formations (basal Oaktree, Monte Christo, Lyttelton, Eccles and uppermost Frisco Formations) of dolomite and is characterized by a sheet-like geometry (Eriksson & Reczko, 1995). The maximum thickness this subgroup attains is about 2100 m and little variation in the thickness of the individual sheet-like formations exists.

The interbedded mudrocks and sandstones, as well as chert-in-shale breccias in the Malmani succession, are believed to represent insignificant unconformities (Clendenin, 1989 in Eriksson & Reczko, 1995:495). Most workers agree on a carbonate ramp depositional model for the Malmani dolomites with supratidal, intertidal and subtidal to shallow basinal facies (Eriksson et al., 1975; Beukes, 1986; Clendenin, 1989 in Eriksson & Reczko, 1995:495).

The subdivision of the Malmani Subgroup into its constituent formations is based on the interbedded chert and shales, the variety of stromatolite structures present and the low-angle unconformities within the subgroup (Button, 1973; Clendenin, 1989 in Eriksson et al., 2001:214; SACS, 1980). Stromatolite types include giant domes, laminated mats, columnar stromatolites, fenestral microbial laminites and local oolitic beds (Altermann & Siegfried, 1997 in Eriksson et al., 2001:215). The dolomites of the Malmani Subgroup grade up into the Penge Formation banded iron formation (BIF) which consists of micro- and macro banded lithologies and subordinate interbeds of mudrock and intraclastic breccias (Beukes, 1978; Hälbich et al., 1993 in Eriksson et al., 2001:215) that appear to have a sheet like geometry (Eriksson & Reczko, 1995).

In the study area (Figure 22) the Oaktree Formation consists of dark-grey, chert-free dolomite that contains large stromatolite domes, shale marker beds, the Convolute Chert Marker (Eriksson & Truswell, 1974 in Obbes, 2000:3) and a tuffite unit (Obbes, 2000). According to Obbes (2000) the Oaktree Formation has no distinctive geomorphic expression, a low relief and a uniform dark colour. During mapping Obbes (2000) used the change in colour from dark-brown to light-grey dolomite and the corresponding increase in chert content as the contact of the gradational transition from the Oaktree Formation and the Monte Christo Formation.

The Monte Christo Formation is subdivided by Obbes (2000) into the following four members based on the subdivision by Eriksson & Truswell (1974). It must however be noted that this subdivision is not formally accepted by the South African Committee for Stratigraphy (SACS).

- Rietfontein Member: Dark grey dolomite characterised by wave and current ripples, and numerous chertified and dolomitized oolite beds. Streaky appearance moderate relief, coarse texture and well defined bedding traces on aerial and orthophotographs. Upper contact is below laterally continuous, chert-in-shale breccia.
- Mooiplaats Member: Dark grey dolomite with more chert than underlying layer. Characterised by chertified stromatolites, ripple marks and oolite beds. Streaky appearance, prominent relief, light tone and fairly well defined bedding traces on aerial photographs. Upper contact is base of a laterally continuous silicified chert breccia.
- Rietspruit Member: Consists of three chert-poor, colour banded dolomite units and three chert-in-shale breccias. Dark tone, low relief, smooth texture and poor bedding traces on aerial photographs. Upper contact is base of a chert breccia.
- Crocodile River Member: Consists of certified stromatolites, oolitic and wave-rippled dark-grey dolomite units. Well-defined bedding traces and prominent topographic expression on aerial photographs. Upper contact is below prominent, laterally continuous chert-in-shale breccia.

The Lyttelton Formation consists of dark-grey dolomite with more chert in its lower parts than in the central portions and the dolomite in this formation weathers to a chocolate-brown colour. Megadomal stromatolites are common and chertified columnar stromatolites and cross-bedded dolarenite beds also occur. In aerial photographs the Lyttelton Formation is characterised by a dark tone, a relatively subdued topography and poor bedding traces. The contact between the Lyttelton and Eccles Formations is gradational and Obbes (2000) used the change in colour from dark brown to grey and the increased chert content to define this contact.

The Eccles Formation exists as the prominent Schurweberge and consists of light-grey interbedded chert and dolomite that weathers to what is referred to as a “bread and butter” appearance. On aerial photographs excellent bedding traces are visible in areas of Eccles Formation. Near the top of the Eccles Formation a chert-in-shale breccia occurs and this is overlain by a dark-brown, chert-poor dolomite (Obbes, 2000). The upper part of the Eccles Formation consists of a silicified chert breccia known as the Leeuwenkloof Member (name not yet accepted by SACS) (Obbes, 2000).

The Frisco Formation is a chert-poor, dark-grey dolomite lithology that weathers to a dark brown colour. It contains stromatolites, gas escape structures and horizontally laminated dolarenite (Obbes, 2000). In the lower part of the unit tuffite and shale beds occur and the upper contact of this formation is the erosional unconformity with the overlying Rooihogte Formation. The Frisco Formation is characterised by a subdued topography and ill-defined bedding traces on aerial photographs (Obbes, 2000). In the study area Obbes (2000) considered the basal contact of the Rooihogte Formation, Pretoria Group, Transvaal Supergroup to be at the contact between the Malmani Subgroup dolomites and any of the units that make up the Rooihogte Formation.

The Diepkloof Formation (name not yet accepted by SACS) (Obbes, 2000) consists of a variable thickness of residual, chert clasts in siliceous-ferruginous matrix, breccia and occurs as a prominent capping on some topographically high-lying areas. Obbes (2000) proposes that this unit (previously incorrectly mapped as part of the Rooihogte Formation) is the weathered product of the underlying carbonate rocks.

8.3 Overlying layers map

The overlying layer map was created by assigning *soil* O_S and the *lithology* O_L sub-factors (tables I to IV in Figure 5) according to the proposed mapping guidelines.

8.3.1 Soil sub-score (O_S) map

The soil data for the COHWHS were derived from the South African Land Type Maps (Government Printer/Agricultural Research Council-Institute for Soil Climate and Water). The land-type data were regionalized to arrive at a distribution of land-types. The Land Type Inventories for all *Land Types* present in the COHWHS are included in Appendix A. The distribution of topographic units (e.g. convex/concave hills, ridges, peaks, saddles etc.) was obtained using the TOPOSHAPE function in IDRISI 32[®], while the slope gradients were obtained using the TIN SLOPE function in ARC GIS[®].

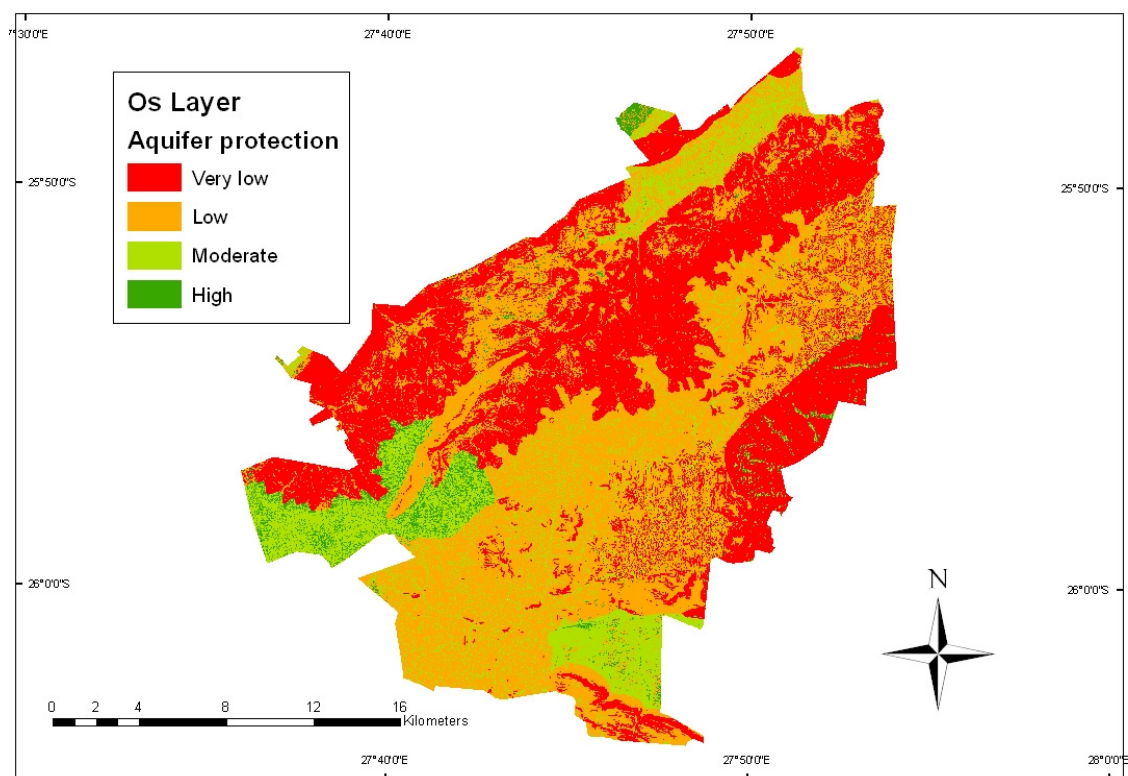


Figure 24. Soil (O_S) sub-score map for the COHWHS.

The soil (O_S sub-score) map shows how the vast majority of the soils cover in the COHWHS offers *very low* or *low* aquifer protection.

In the *Land Types* underlain by the dolomitic rocks (essentially Scenario 1 areas) of the Malmani Subgroup (*Land Types* Fa12, Fa18 and Ib6) all soils are generally loamy and the hill crests and steep upper slopes are generally not covered by any soil or by very thin soils (*very low* aquifer protection by soils). The intermediate gradient mid-slopes in these *Land Types* are generally covered by soils that are less than 0.5m thick (*low* aquifer protection by soils). The low gradient lower slopes are covered by loam soils that range in thickness from >0.5m thick (*Land Type* Ib6) to 0.5-1m thick (*Land Types* Fa12 and Fa18) and therefore offer *low* to *moderate* aquifer protection. Finally, the drainage lines within these *Land Types* have soils of 0.5->1m in thickness which also provide *moderate* aquifer protection. Overall *Land Type* Ib6 is characterized by a steeper gradient and consequently has a high surface flow towards points of concentrated recharge (hence a *very low* aquifer protection). The other two *Land Types* underlain by dolomitic rocks have a more subdued topography and the aquifer protection by soils ranges from *very low* to *low* with small areas with *moderate* aquifer protection by soils in lower gradient areas.

Within the areas underlain by the granodiorites of the Halfway House Granite Inlier (*Land Type* Bb2) a generally *very low* aquifer protection by soils exists due to predominant slopes on which sandy soils less than 0.5m in thickness are present. Minor areas of *moderate* aquifer protection by soils can be seen, which are located on the crests of hills where slightly deeper (0.5-1m) loamy soils occur.

The two main areas with a generally *moderate* level of aquifer protection by the soil is present are the low gradient area underlain by of the mudrocks of the Timeball Hill Formation and andesites of the Hekpoort Formation (*Land Type* Ba44) and the area underlain by undifferentiated mafic and ultramafic rocks of the Halfway House Granite Inlier (*Land Type* Ab12). In *Land Type* Ba44 areas soils are generally 0.75m thick and loamy (*moderate* aquifer protection). However the mid slope areas contain soils with a clayey nature and the drainage lines have soils with high clay contents that range in thickness from 0.5m to >1m and as such some parts of this area provide a *high* aquifer protection.

The generally *moderate* aquifer protection area underlain by the undifferentiated mafic and ultramafic rocks of the Halfway House Granite Inlier (*Land Type* Ab12) soils

are generally loamy and range in thickness from <0.5m on the hill crests (minor areas of *low* aquifer protection by soils) to 0.5-1m on the slopes and low lying areas (*moderate* aquifer protection by soils). In this *Land Type* minor low lying areas with very low gradients are present and the soils are predominantly clayey in nature and thicker than 1m, providing *high* aquifer protection.

Land Type Ib4 is underlain by similar lithologies as Ba44 but is characterized by a steeper topography. Here the soil cover on the majority of the slope areas is very shallow or absent (*very low* aquifer protection by soils) and the hill crests and lower slopes have less than 0.5m of loamy soils (*low* aquifer protection by soils).

Two *Land Types* underlain predominantly by rocks of the Witwatersrand Supergroup (Ib41 and Ib42) are present in the southern parts of the COHWHS and are characterized by a *low* to *very low* aquifer protection by soils. This is because the majority of these *Land Types* consists of land classes that have loamy soils less than 0.5m thick (*low* protection) or rock out crop (*very low* protection). Only very small valley sections with very low gradients (0-2%) are characterized by soils that are thicker than 1m and offer *moderate* to *high* aquifer protection.

The *Land Types* dominated by quartzite lithologies of the Pretoria Group and lesser amounts of shale and slate (Fb14 and Ib3) are elongated and stretch from northeast to southwest in the northwestern parts of the COHWHS. In these *Land Types* the steep upper slopes generally have no soil cover and therefore offer *very low* aquifer protection. The hill crests and mid-slopes are characterized by thin (<0.5m) loamy soils (*Land Type* Fb14) or rock outcrops (*Land Type* Ib3) and as such offer *low* to *very low* aquifer protection. Lower slopes are characterized by loamy soils that range in thickness from <0.5m to 0.5-1m in thickness and therefore offer *low* to *moderate* aquifer protection. As in many other *Land Types*, the only areas characterized by *high* aquifer protection by soils are the very low gradient areas where clayey soils are present with a thickness of 0.5-1m. The generally steep gradients of these *Land Types* in the COHWHS results in a generally *very low* to *low* aquifer protection by soils.

Within the northwestern extremities of the COHWHS three small areas are predominantly underlain by Pretoria Group shale and slate units. These *Land Types*

(Ba23, Ea30, Ea72) are characterized by a generally *high* or *moderate* aquifer protection by soils because the majority of the soils in these low gradient *Land Types* are loamy or clayey and at least 0.5m thick. Only the low gradient crests of very small hills have a *low* aquifer protection due to the soils there being less than 0.5m thick.

Land Type Ba7 is underlain by shale, quartzite and siltstones of the Daspoort and Timeball Hill Formations as well as rocks of the Hekpoort Formation. Here the hill crests and upper slopes offer *low* aquifer protection (loamy soils less than 0.5m thick) while the lower slopes offer *moderate* aquifer protection (loamy soils more than 1m thick).

During the derivation of the distribution of the different topographic units small areas could have been assigned to the incorrect topographical unit due to the resolution of the digital elevation model used (20m). However at the scale used it can be seen that these local variations are insignificant in that only the broader distribution of soil types is visible. Should a detailed, site-specific aquifer vulnerability map be needed a detailed field investigation of soil cover would be required.

The assigning of soil properties to each of the terrain units within each *Land Type* based on predominant soil type present within that terrain unit has also led to local generalisations and over/underestimations of the aquifer protection by soils. However this is once again believed to be acceptable for the scale of the map produced.

8.3.2 Lithology sub-score (O_L) map

The lithology sub-score for the COHWHS was principally derived from a composite geological map created from the (a) 1:250 000 geological maps covering the COHWHS (2626 West-Rand and 2526 Rustenburg), (b) a map subdividing the Malmani dolomites for the major part of the COHWHS published by the Council for Geoscience (Obbes, 2000) and (c) an unpublished map subdividing the Malmani dolomites in the southern part of the COHWHS (south of 26° S), created by two German exchange students as part of this project. A *depth-to-water-table map* was created by interpolating water depth point data obtained from field measurements and NGDB/DWAF data (inverse distance weighting method). The water depth point data is included in Appendix B. Groundwater compartments were not interpolated separately, as no strong evidence of

continuous compartment boundaries could be identified and the karst network is believed to be continuous across these barriers.

A simplified calculation was used to account for the varying lithology on the down dip side of all plunging geological contacts. Between the surface contact of the geological units and where the underlying lithology entered the water table half of the thickness (“ m_1 ”) was assigned the l_{y1} sub-factor of the surface lithology, while the other half of the thickness (“ m_2 ”) was assigned the l_{y2} sub-factor of the underlying lithology.

In view of data scarcity and applying a precautionary approach all aquifers were considered to be unconfined.

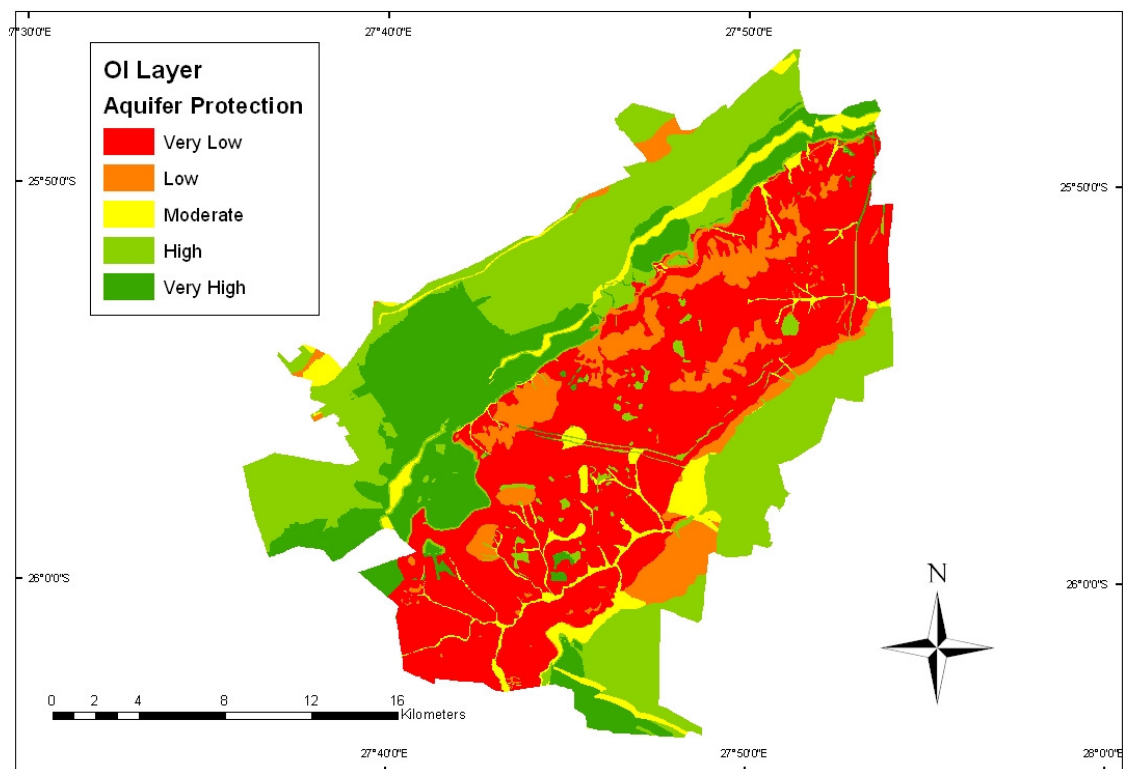


Figure 25. Lithology (O_L) sub-score map for the COHWHS.

The lithology sub-score map (Figure 25) clearly shows the inferior aquifer protection area that runs across the entire COHWHS from northwest to southeast where the Malmani Subgroup dolomite units are present. Where the dolomite is present as the surface lithology, the aquifer protection is *very low*. Where chert breccia of the Diepkloof Formation overlies the dolomites, a *low* aquifer protection is visible. Alluvial layers along

some drainage channels within the dolomite areas increase the aquifer protection to *moderate* while igneous dykes offer *high* to *very high* protection.

On the south-eastern side of the dolomite areas the following areas occur:

- *Low* aquifer protection areas: Ventersdorp Supergroup and Black Reef Formation with shallow water table.
- *Moderate* aquifer protection areas: Ventersdorp Supergroup, Black Reef Formation and quartzite lithologies of the Witwatersrand Supergroup with intermediate water table depth.
- *High* aquifer protection areas: Halfway House Granites, Dominion Group, Witwatersrand Supergroup and Quaternary sediments with shallow to intermediate water table.
- *Very high* aquifer protection areas: Halfway House Granites and shale units within Witwatersrand Supergroup with intermediate water table depth.

Depending on the water table depth, the shale, slate, siltstone, mudrock and andesitic lava units of the Pretoria Group provide *high* or *very high* aquifer protection in the areas to the northwest of the dolomite areas. The Quartzite ridges of the Daspoort Formation and the Klapperkop Quartzite Member can be seen as elongated areas of *moderate* aquifer protection (or *low* protection where water table is very shallow) within this area.

The depth of water at known springs (i.e. 0m) was not used during the interpolation of the water depth across the study area. This is due to the fact that the water depths decrease with different trends from all springs depending on the type of spring (e.g. barrier, karst or contact). The aquifer protection will therefore have been underestimated at some spring locations where the water table is closer to the surface than the used interpolation prescribes. The actual size of such areas is however believed to be negligible at the scale of the map.

The distribution of different groundwater compartments within the study area is not clearly defined and the continuity of the features responsible for the compartmentalization (predominantly dikes) has not been confirmed. The integrity of such dikes is believed to have been compromised by two processes. Firstly weathering of

the rocks is believed to have resulted in a significant increase in the permeability of the upper portions of the dikes. Secondly due to the presence of fractures or faults within the unweathered parts water from a karst conduit will migrate through such discontinuities and ultimately result in the erosion of the barrier. The final product of this process is a karst conduit that extends through the barrier.

It therefore can be concluded that although the barriers may once have compartmentalized the aquifer, at present these barriers may only temporarily prevent groundwater from moving from one “compartment” to the other. Groundwater water will inevitably migrate along any intact barrier sections until reaching an area where the barrier has been compromised. The water depth within the “compartments” will therefore equalize over a relatively short period of time. Based on the above assumptions the ground water “compartments” were not considered during the ground water depth interpolation.

The accuracy of the utilized geological map is believed to be acceptable for the scale of the map produced. However field investigations did show the geological map to contain minor spatial inaccuracies that would be significant should smaller scale maps be produced.

8.3.3 Overlying layers (O) map

The overlying layer (O factor) map (Figure 26) clearly shows how the combined effect of the soil and lithology sub-scores result in an aquifer protection distribution that differs clearly from its sub layers.

As expected the dolomitic lithologies offer only inferior protection of the aquifer, considering that both the lithology and soil protection associated with these lithologies was *low* or *very low*. The dolomitic areas are mostly classified as areas of *very low or low aquifer protection* zones except where thick sediment cover or chert breccias with soil cover occur, in which case a *moderate* aquifer protection is assigned.

To the southeast of the dolomite lithologies the aquifer protection remains *low to moderate* in areas underlain by the Ventersdorp Supergroup, Black Reef Formation and quartzite lithologies of the Witwatersrand Supergroup. In areas that have a *high* aquifer protection provided by the Dominion Group, Witwatersrand Supergroup and Quaternary

sediments the overall aquifer protection is generally *moderate*, due to the *very low* or *low* aquifer protection provided by the soils in the same area. The mafic and ultramafic parts of the Halfway House Granites Inlier have a *high* aquifer protection while the granitic parts of the inlier have a generally *moderate* aquifer protection. The reason for this is that although the aquifer protection by both lithologies is generally *high*, the soils in the mafic and ultramafic parts offer a *moderate* aquifer protection as opposed to the generally *very low* aquifer protection provided by the soils in the granitic sections.

The shale units within Witwatersrand Supergroup, which offered a *very high* aquifer protection, are covered by soils that offer only a *very low* to *low* aquifer protection and as such the overall aquifer protection in these areas is *high*.

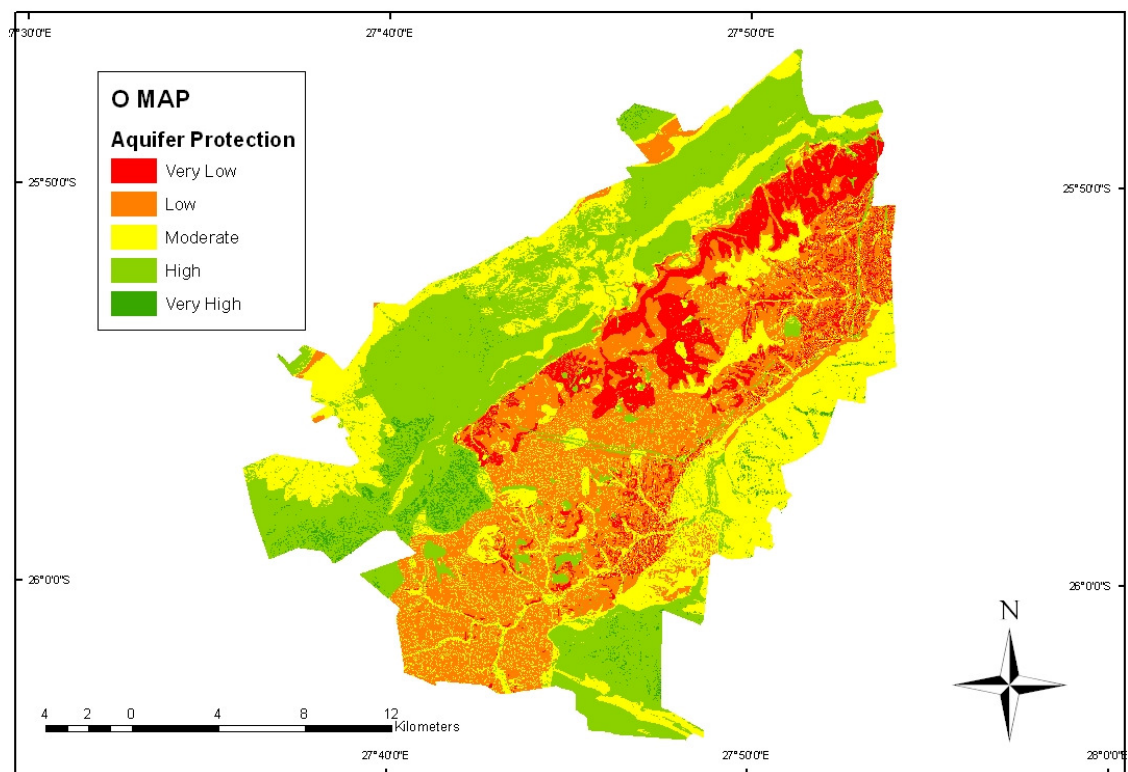


Figure 26: Overlying layer (O) factor map for the COHWHS.

The aquifer protection within the areas to the northwest of the dolomite lithologies is *moderate* to *high* except for one small area of *low* aquifer protection. This is different to the aquifer protection by lithologies, which was generally *high* to *very high* with elongated areas of *moderate* to *low* aquifer protection where the quartzite ridges. The reason for this generally lower overall aquifer protection is the fact that the soils in

this area offer *very low* to *low* aquifer protection. One area (*Land Type* and Ba44) does however retain some of its *very high* aquifer protection as this area is overlain by soils that provide *high* to *very high* aquifer protection.

8.4 Precipitation (P) map

Rainfall data for weather stations in the greater COHWHS area were retrieved from the South African Weather Service and the Agricultural Research Council. The data were analyzed according to the proposed mapping guidelines to arrive at the P map (Figure 29) and its two sub-factor maps. A summary of the precipitation data from each of the relevant weather stations is included in Appendix C.

8.4.1 Rainfall (Pq) map.

The Pq sub-factor map (Figure 27) shows how the majority of the study area has a *moderate* reduction in aquifer protection ($Pq=0.3$) due to the average rainfall for wet years (300-600 mm/year). The areas situated along the north-western border of the study site show a *high* reduction in protection ($Pq=0.2$) due to the ridges that extend from northeast to southwest affecting the average rainfall for wet years to 600-900 mm/year.

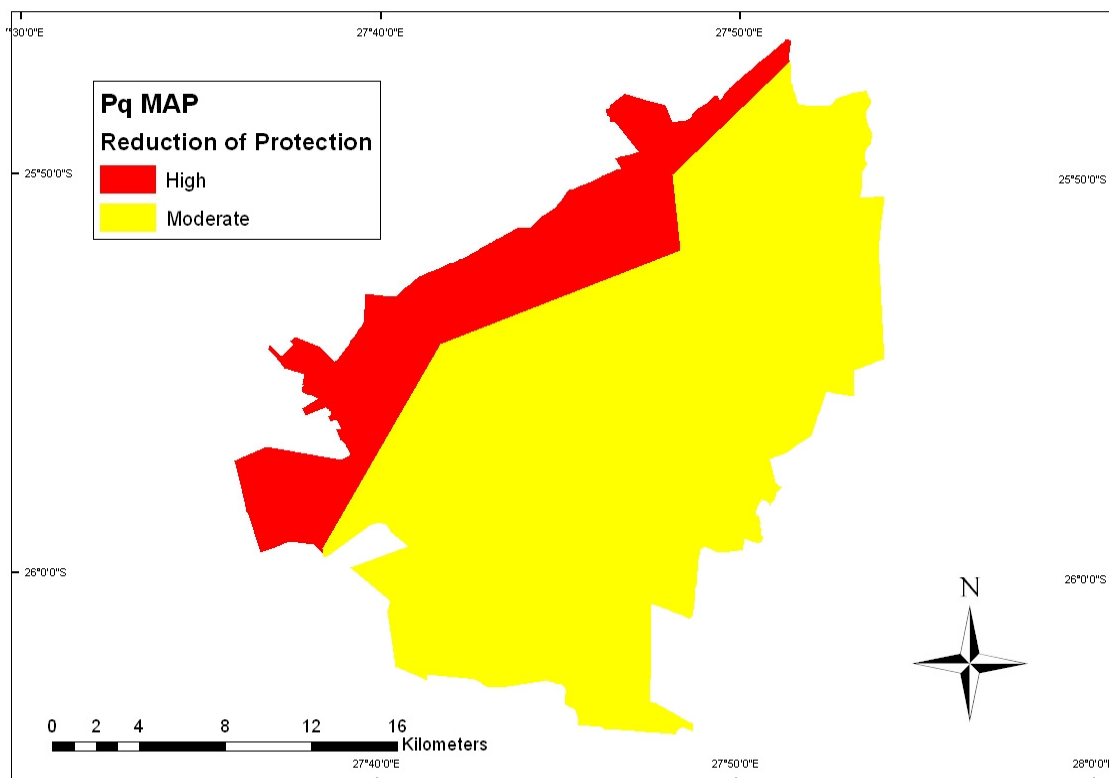


Figure 27. Rainfall (Pq) sub-factor map for the COHWHS.

8.4.2 Temporal distribution (P_i) map.

The P_i sub-factor map (Figure 28) shows, similarly to the P_q map, how the majority of the study area has a *moderate* reduction in aquifer protection ($P_i=0.4$) based on the temporal distribution of the rainfall in wet years (10-20 mm/day). The areas situated along the north-western border of the study site again show a different reduction in protection due to the ridges affecting the rainfall in these areas. These areas however do not show a uniform variation in the reduction in aquifer protection. This is due to the data for the two polygons with a *low* reduction in aquifer protection being very limited (15 and 5 year record respectively) and therefore not a true reflection of the precipitation regime. Those polygons with a *high* reduction in aquifer protection have more complete precipitation records (minimum 22 years) and are most probably a better indication of the true conditions along the northwestern edge of the COHWHS.

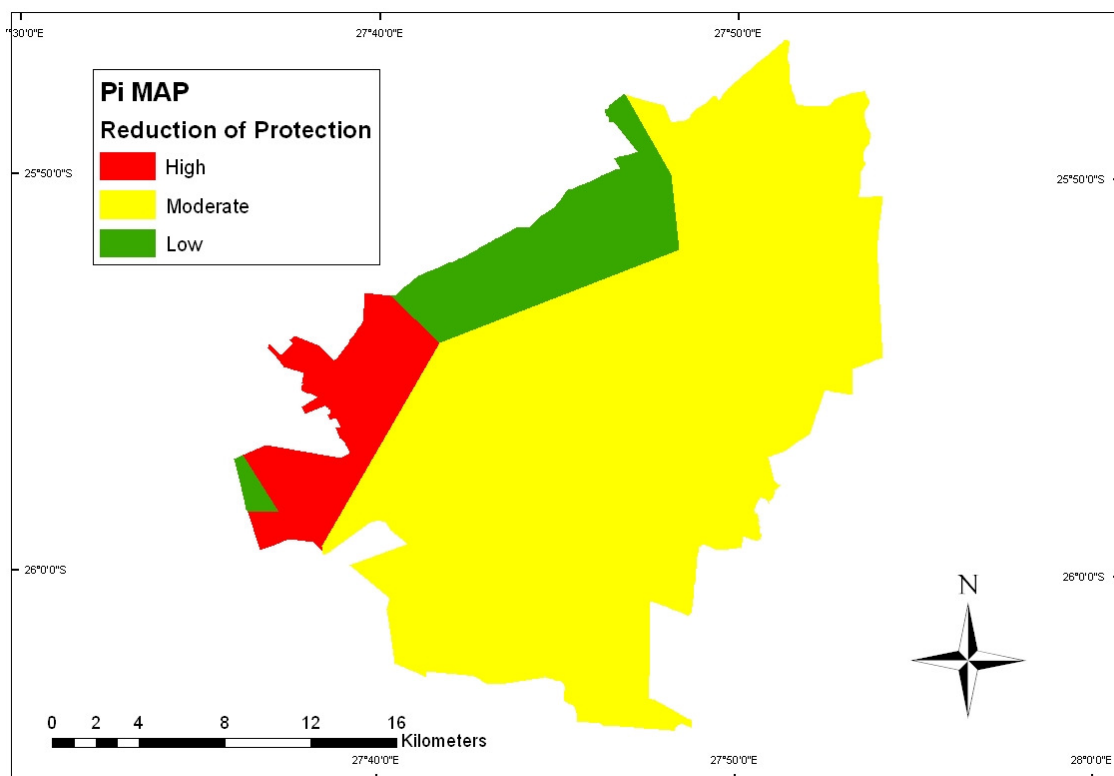


Figure 28. Temporal distribution (P_i) sub-factor map for the COHWHS

8.4.3 Precipitation (P) map

The P map illustrates the relative reduction of the protective function of the layers overlying the groundwater resource due to the differences in the precipitation regime across the study area. It can be seen that the map is simple and does not show large variations in the reducing influence of precipitation on aquifer protection. The majority of the study area is defined as having a *moderate* reduction in protection P factor. However, variations are seen in the northwestern parts of the area where *low* reduction in protection and *very high* reduction in protection areas are seen. This is due to the ridges that extend from northeast to southwest in these parts of the study area and effect the distribution of rainfall.

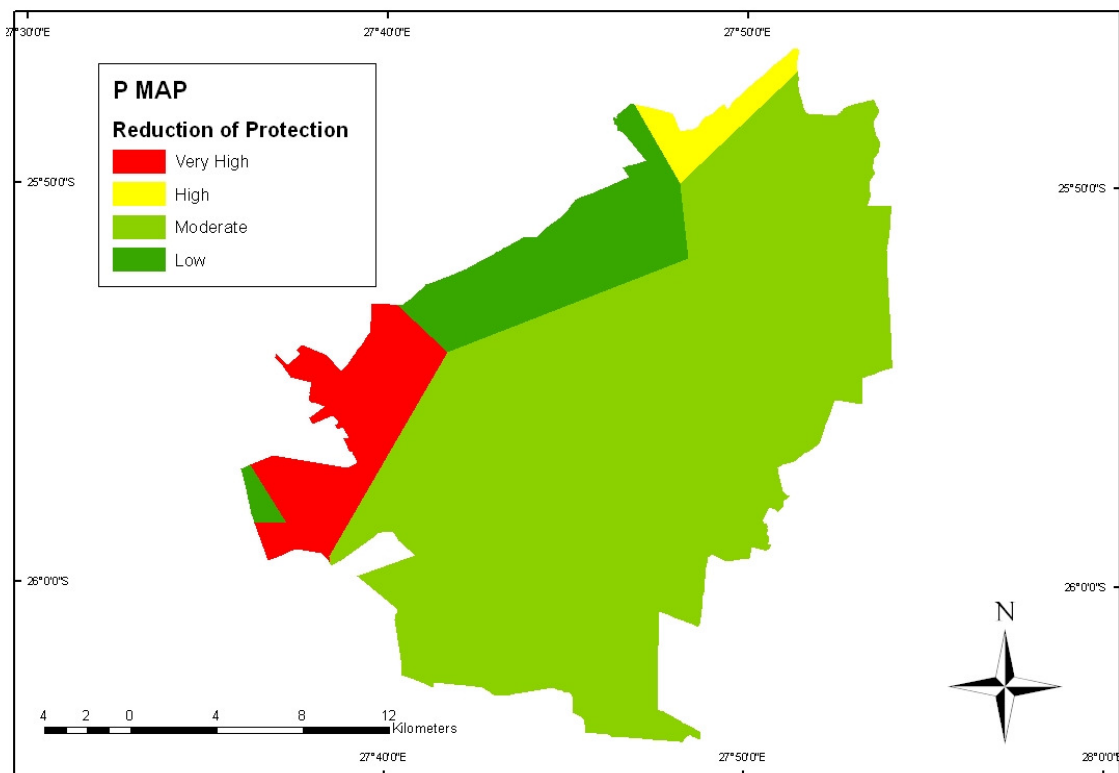


Figure 29. Precipitation (P) factor map for the COHWHS.

As mentioned in section 8.4.2 it is assumed that the limited data available for some weather stations resulted in inaccurate P_i sub-factors for some areas along the north-western border of the mapping area. The areas with a *high* or *very high* reduction in aquifer protection are believed to be a more accurate representation of the conditions along the entire north-western border of the COHWHS.

The observed variations in the P map are not a perfect representation of the P factor as the precipitation regime is unlikely to alter the aquifer protection along lines not directly related to topography or predominant wind direction. It is more likely that the entire northwestern border of the COHWHS has a *high* to *very high* reduction in aquifer protection while the remaining area has a *moderate* reduction of protection. However, the map was used for the remainder of the mapping process as precipitation data scarcity within the study area prevented the identification of more realistic precipitation trends within the mapped area.

8.5 Concentration of flow map

The concentration of flow map was created using the proposed mapping methodology of assigning different sub-factors to Scenario 1 and Scenario 2 areas.

8.5.1 Distance to swallow hole (*dh*) map (Scenario 1 areas only)

During extensive “karst feature” mapping within the study area, the location of numerous sinkholes, caves and dolines that act as “concentrated recharge points” were mapped and used to define Scenario 1 areas. The remaining parts of the study area that are characterized by karstic rocks on surface were defined as Scenario 2 areas. The coordinates and sediment fill status of all identified swallow holes is included in Appendix D.

The *dh* sub-factor map (Figure 30) reveals that the southern, lower lying parts of the karstic region within the COHWHS have more swallow holes and consequently larger areas within close proximity to a swallow hole (red areas). The spatial extent of Scenario 1 areas is much larger than Scenario 2 areas due to the large number and wide distribution of swallow holes within the mapped area. This is a common situation in South African karst terrains due to the long history of the karst system which has included numerous periods of karstification. Despite the extensive field investigations performed it is possible that some swallow holes within the mapped area were not identified.

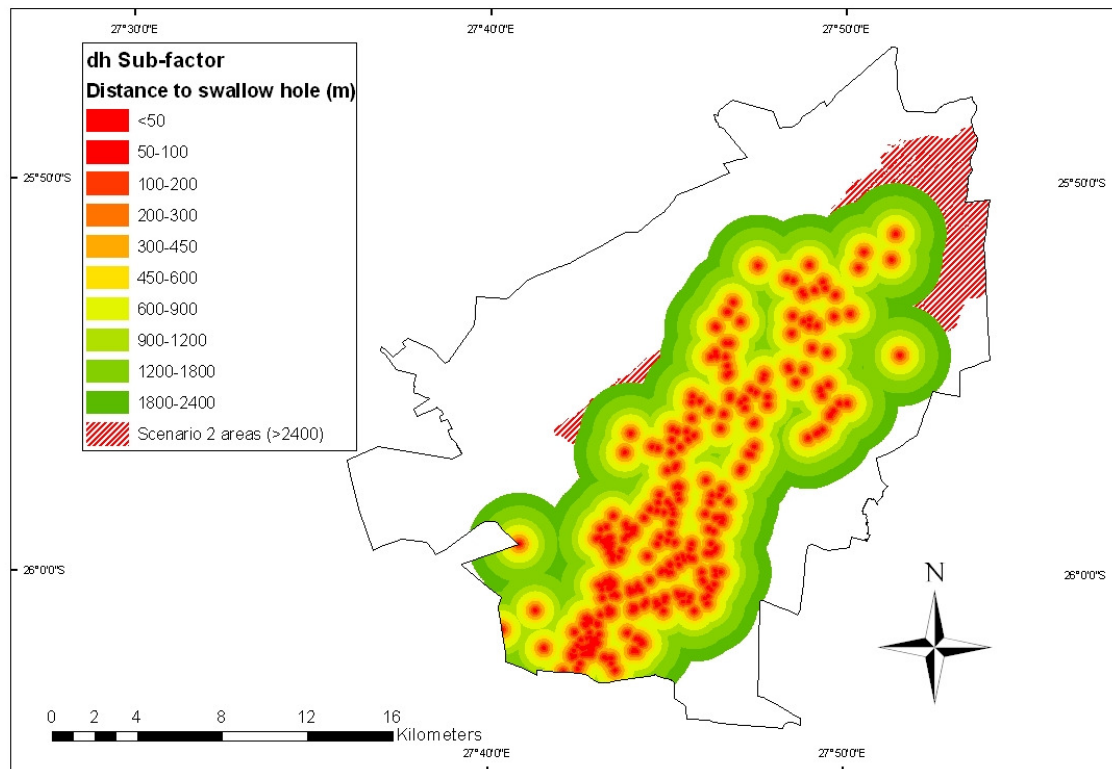


Figure 30: Distance to swallow hole (*dh*) sub-factor map for the COHWHS.

Where a buffer around swallow hole extends into a catchment area not relevant to the swallow hole, an overestimate of the *dh* sub-factor will exist. However in order to limit buffers to swallow hole catchment areas would require a significant amount of time and render the vulnerability mapping process impractical. The precautionary buffering utilised is therefore justified. Detailed site-specific investigations should however consider the actual catchment of any swallow holes during the determination of the *dh* sub-factor.

8.5.2 Slope and vegetation (*sv*) map (Scenario 1 and Scenario 2 areas)

The vegetation cover within both Scenario 1 and 2 areas was defined based on aerial photograph interpretation and ground truthing. The vegetation cover illustrated in the aerial photographs used was, by means of numerous field checks, adjudged to represent the present vegetation cover within the mapping area to an acceptable degree. The slopes within all Scenario 1 and 2 areas were determined based on the digital elevation model using ARC GIS[®].

As seen in Figure 31 the southern and southeastern parts of the Scenario 1 and 2 areas are dominated by slope gradients of less than 31%. The areas with gradients of 8-31% have generally *low* or *sparse* vegetation cover. Only minor elongated areas located along drainage courses have dense vegetation cover. In the northern and northwestern parts of the Scenario 1 and 2 areas the topography changes, slopes reach 31-76% in parts and much smaller areas have <8% gradients. The vegetation cover in these parts is also more commonly *sparse* with lesser *low* vegetation cover areas. As in other areas the *high* vegetation cover areas are confined to drainage courses.

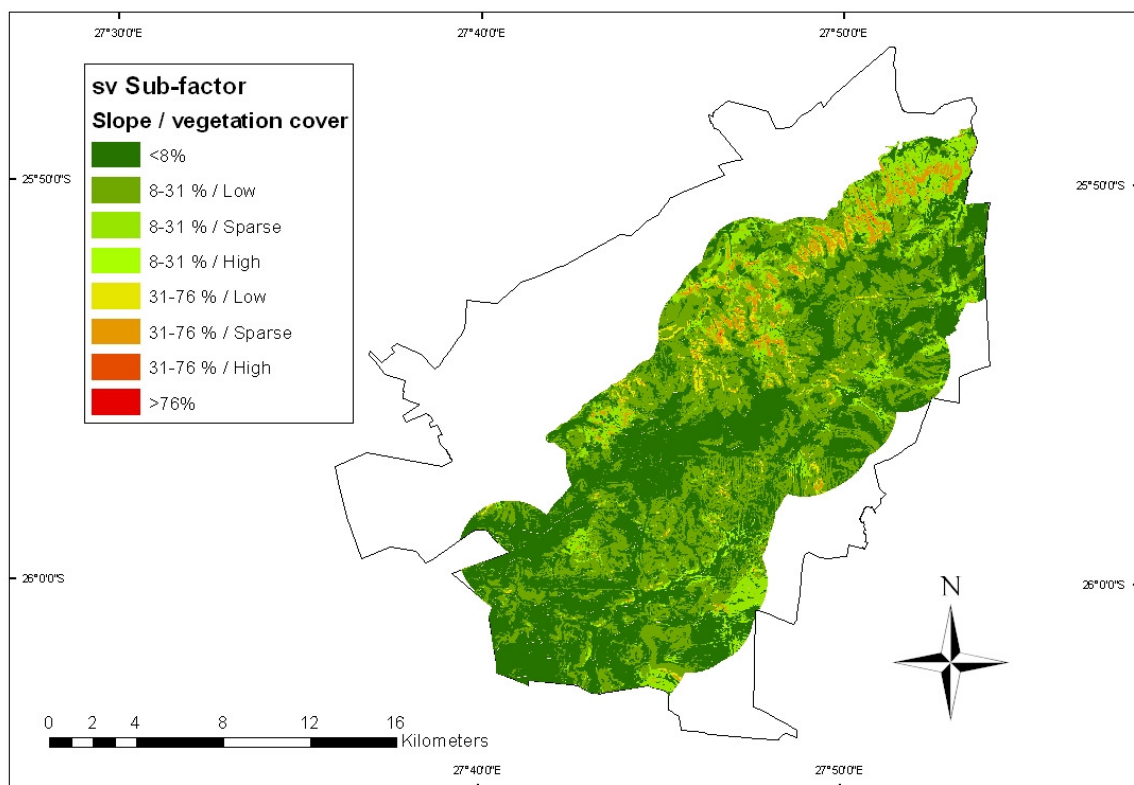


Figure 31: Slope and vegetation (*sv*) sub-factor map for the COHWHS.

8.5.3 Distance to sinking stream (*ds*) map (Scenario 1 areas only)

No sinking stream is present within the study area and as such all Scenario 1 areas were assigned a *ds* sub-factor value of 1.

8.5.4 Karst development/surface layers (*sf*) map (Scenario 2 areas only)

The surface karst development within Scenario 2 areas was defined based on aerial photograph interpretation and ground truthing. The presence or absence of a

surface layer was determined based on the geological maps and soil maps and on ground truthing.

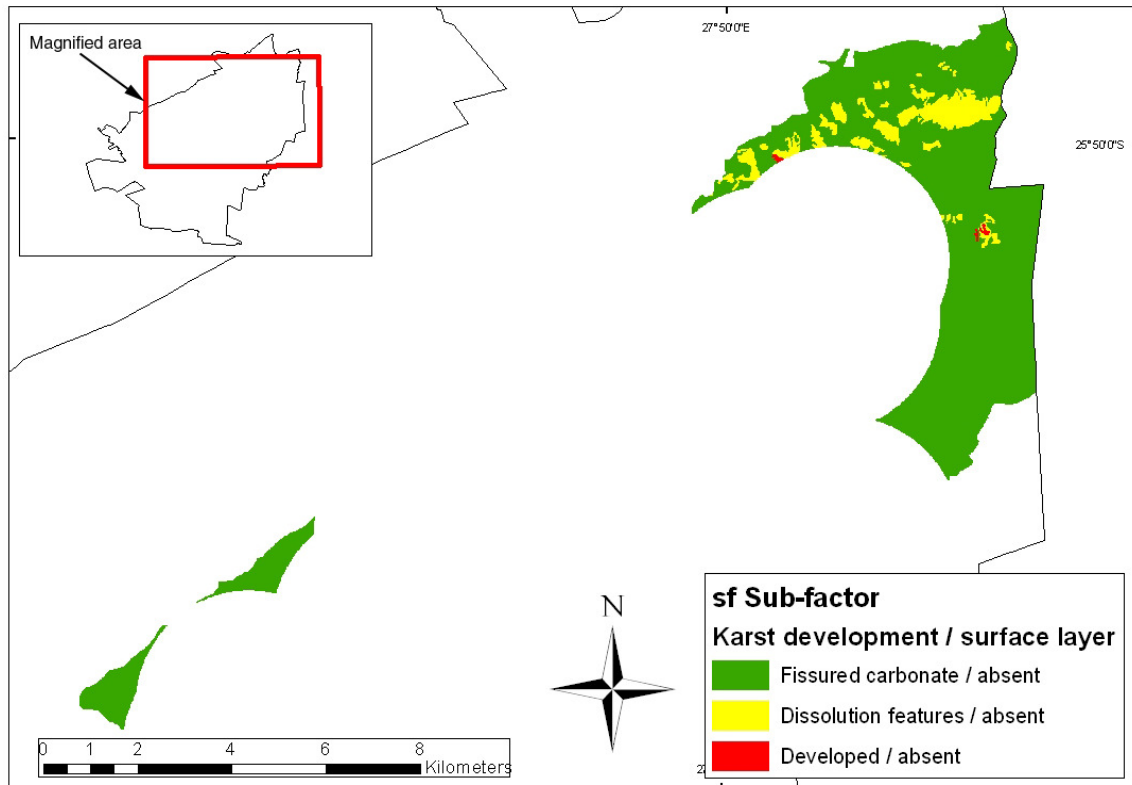


Figure 32: Karst development / surface layers (*sf*) sub-factor map for the COHWHS.

The Scenario 2 areas are generally characterized by fissured carbonate rocks in which no significant karst development has occurred (Figure 32). However, some northern Scenario 2 areas show dissolution features at surface and some very small areas have well developed karstic features on surface.

It is possible that during the aerial photograph interpretation vegetation cover concealed the true nature of surface karst development in places. It is however believed that the karst development / surface layers sub-factor map represent the actual presence of surface karst in Scenario 2 areas accurately for the scale of the proposed map.

8.5.5 Concentration of flow (C) map

The concentration of flow (C factor) map (Figure 33) clearly shows the influence of the numerous swallow holes in the COHWHS on the reduction of aquifer protection in the already lower protected karstic areas. The reduction in aquifer protection decreases

with distance from these features, though the modification based on the slope and vegetation cover is visible on a small scale as either an increase or decrease in protection reduction of the zones around the swallow holes. The full range of reduction in aquifer protection (*very high to very low*) occurs within Scenario 1 areas.

Scenario 2 areas show a sudden change in C factor (most significantly in the northern parts of the Malmani dolomites) due to the additional consideration of karst development and vegetation in Scenario 2 areas. The variation in slope and vegetation cover in Scenario 2 areas results in the large areas originally defined by a single *sf* sub-factor having varying degrees of reduction in aquifer protection. As expected the reduction in protection within Scenario 2 areas does not cover the full range but rather only ranges from *low to high*.

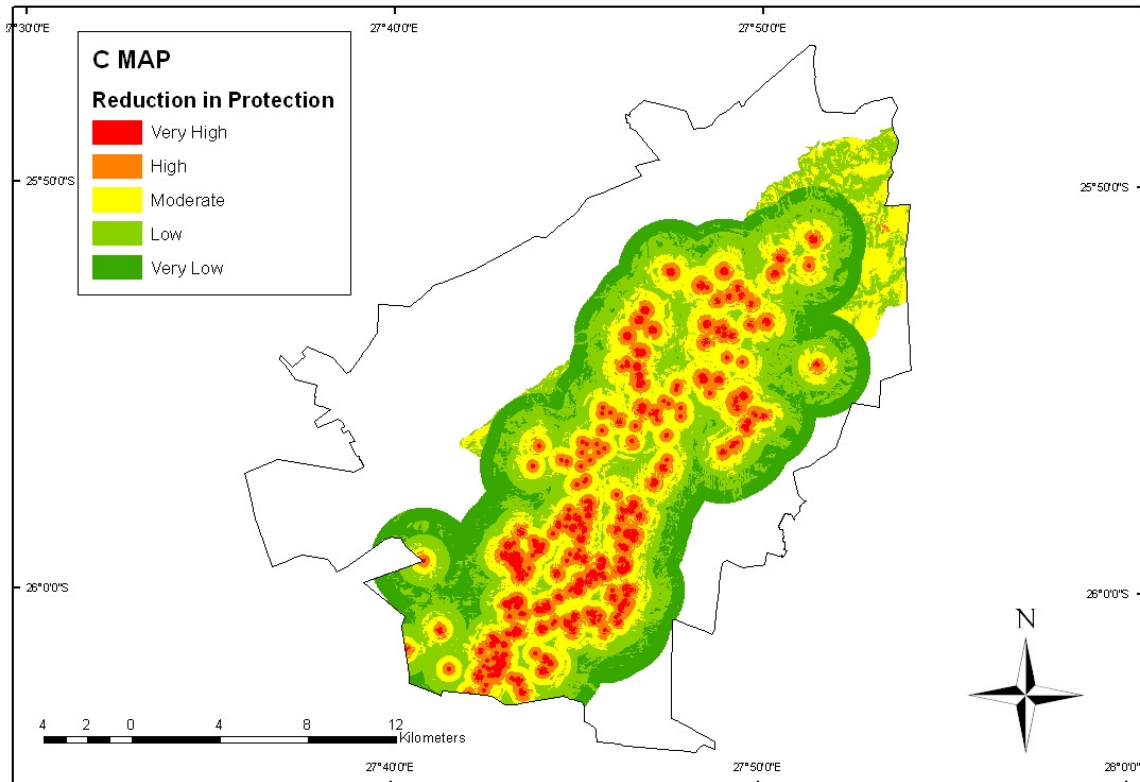


Figure 33: Concentration of flow (C) factor map for the COHWHS.

8.6 Final vulnerability map

The final vulnerability (modified COP or VUKA) index, the product of the three sub-factors, is categorized in five vulnerability classes ranging from *very low* to *very high* (Table 2).

Table 2: Final aquifer vulnerability classes.

| Vulnerability index | Vulnerability classes |
|---------------------|-----------------------|
| 0 – 0.5 | Very high |
| 0.5 – 1 | High |
| 1 – 2 | Moderate |
| 2 – 4 | Low |
| 4 – 15 | Very low |

Within karstic areas a larger variation in vulnerability is seen due to the additional consideration of the C factor. It is obvious from Figure 34 that the vulnerability of the COHWHS is clearly dominated by the lithology and the occurrence of swallow holes. The areas underlain by the Malmani dolomites in the central part of the COHWHS are the most vulnerable areas with the vulnerability ranging from *very high* (close to swallow holes) to *moderate* (at distance from swallow holes). The original *very low* to *low* protection by the overlying layers (*high* to *very high* vulnerability) has therefore been increased to *moderate* in some areas (due to the *very low* reduction in protection provided by the C factor) while other areas (*very high* reduction in protection by C factor) have retained the it original poor protection (*high* to *very high* vulnerability). Scenario 2 areas have retained the original *very low* to *low* aquifer protection (*very high* to *high* vulnerability) defined by the O factor. This is because the C factor in these areas generally ranged from *low* to *moderate* and therefore was insufficient to lower the vulnerability of these areas. The P factor across the karstic area was *moderate* and as such did not reduce the vulnerability of this area or result in any variation of aquifer vulnerability.

The areas to the southeast of the karstic rocks have an aquifer vulnerability of *moderate* to *very low*. The aquifer vulnerability in this area is generally lower than the original vulnerability defined by the O factor (*low* to *high*) as a result of the reduction in

protection by the precipitation regime in this entire area was only *moderate* and therefore not high enough to retain the *low* protection classes.

In the western parts of the areas to the northwest of the dolomite lithologies the effects of the reduction in protection by the precipitation regime (P factor) are clearly visible as a slight increase in aquifer vulnerability where the P factor changes from *low* to *very high*. As mentioned in section 8.4 the P factor map was not ideal but used due to data scarcity. The areas with *low* to *very low* aquifer vulnerability therefore show an increase from the generally *moderate* to *high* protection (*moderate* to *low* vulnerability) seen in the O factor map for these areas. As in the southeastern parts of the COHWHS this is due to the reduction in protection by the precipitation regime (P factor) in these areas not being high enough (*moderate* to *low*) to retain the lower protection classes. In the areas with the slightly higher vulnerability the P factor was *very high* and this resulted in the original *moderate* to *high* protection (*moderate* to *low* vulnerability) being retained.

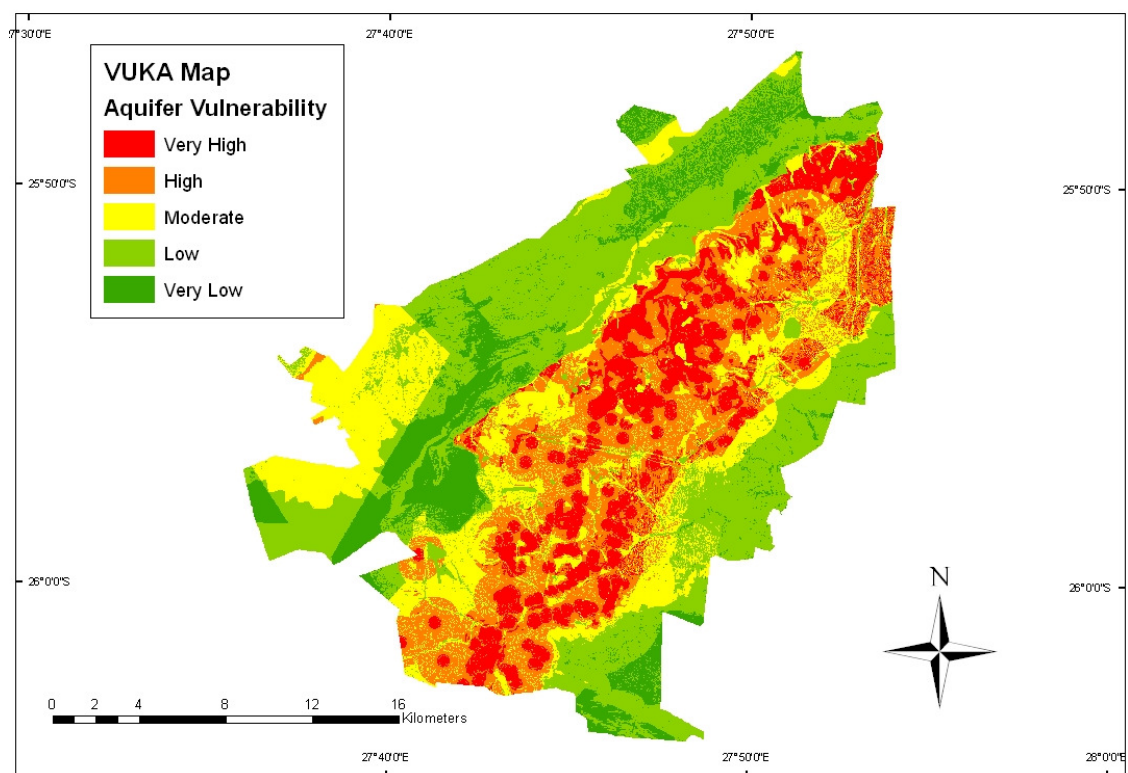


Figure 34: Aquifer vulnerability map for the COHWHS.

The map is believed to accurately show the variations in the intrinsic, resource aquifer vulnerability within the Cradle of Humankind World Heritage Site. Despite the identification of sources of error within the source data and interpretation methods used during the creation of the map, the scale of the map is such that these errors are negligible. It must however be stressed that this map illustrates the regional intrinsic, resource aquifer vulnerability. Should a highly accurate aquifer vulnerability map of a small area within the COHWHS be required for any reason a detailed investigation thereof would be required.

9 Recommendations for future research

9.1 Integration with dolomite risk mapping methodologies

Currently development of dolomite requires that a dolomite stability investigation be performed to determine the stability of the proposed development area with respect to risk of sinkholes and or dolines occurring. It is proposed that all dolomite land should be investigated with respect to aquifer vulnerability before dolomite stabilities are performed and that areas that show a *very high* or *high* vulnerability should preferably not be developed in any way that a hazard is created.

9.2 Validation of maps

The aquifer vulnerability maps created during this research have not been validated in any way yet. One possible method to validate or rather confirm the maps is to use a different method (e.g. PI method) and to compare the resultant maps (see for example section 5.9.4). The PI method will most probably show results very different to the ones presented here as this method was, like the original COP method, developed for European conditions and similar modification to the PI method would be required.

The analysis of observations (hydrographs, chemo-graphs, isotopes or tracer experiments) may however be used to validate specific parts of the conceptual model used in the modification of the original COP method for the COHWHS. For example, tracer tests performed at numerous swallow holes, both with and without sediment accumulation, will confirm if the sediment layers act as a significant water transmission barrier and therefore validate or invalidate the addition of a second set of *dh* sub-factors

(section 7.4.1). By performing the tracer tests under different seasonal recharge regimes (either during periods of high and low natural infiltration or by the artificial addition of an increased water amount), the effect of dilution on Pq sub-factor (section 7.3.1) could be investigated.

Finally a detailed record of the precipitation regime within the COHWHS can be collected by means of automatic weather stations that record the hourly precipitation. The data can then be analysed to determine the intensity of the rainfall events and therefore the actual likelihood of the occurrence of Hortonian flow. The Pi sub-factor can then be modified accordingly. GPACE are currently recording such data at two stations within the COHWHS. It is however suggested that further stations are installed to determine precipitation trends across the study area. This would enable the creation of a more detailed and realistic P score map for the study area.

9.3 Hazard and risk mapping

The assessment (mapping and evaluation) of ground water pollution hazards within the study area would provide the data required to create a hazard map. Once such a map is completed it may be used in conjunction with the aquifer vulnerability map to arrive at a map depicting the risk of groundwater pollution within the COHWHS, an invaluable information source for concerned authorities as well as urban planners.

10 References

- Aller, J.R., Bennet, T., Feheer, J.H., Petty, R.J., Hackett, G., 1987. DRASTIC: a standardised system for evaluating groundwater pollution potential using hydrogeological settings. EPA, Ada, OK, EPA/600/2-87-035.
- Allsopp, H.L., 1961. Rb-Sr age measurements on total rock and separated-mineral fractions from the old granite of the central Transvaal. *J Geophys. Res.*, 66 (5) p. 1499-1508.
- Altermann, W. and Siegfried, H.P., 1997. Sedimentology, facies development and type-section of an Archaean shelf-carbonate platform transition, Kaapvaal Craton, as deduced from deep borehole core at Kathu, South Africa. *Journal of African Earth Sciences*, 24, 391-410.
- Andreo, B., Goldscheider, N., Vadillo, I., Vías, J.M., Neukum, C., Brechenmacher, J., Carrasco, F., Hötzl, H., Jiménez, P., Perles, M.J. and Sinreich, M., 2003. Sierra de Líbar, Southern Spain. In Zwahlen, F. (ed), 2003. Vulnerability and risk mapping for the protection of carbonate (karst) aquifers, final report (COST action 620). European Commission, Brussels. pp 183-199.
- Andrieux, C., 1976. Le système karstique du Baget. 2. Géothermie des eaux à l'exutoire principal selon les cycles hydrologiques 1974 et 1975. (The Baget karst system. 2. Groundwater geothermics at the main spring during 1974 and 1975 hydrological years). *Annales scientifiques de l'Université de Besançon*, 3, 25:1-26.
- Anhaeusser, C.R., 1973. The Geology and Geochemistry of the Archaean Granites and Gneisses of the Johannesburg-Pretoria Dome. In Lister, L.A. (ed), 1973. *Symposium on Granites, Gneisses and Related Rocks*. Spec. Publ. Geol. Soc. S. Afr., 3, 361-385.
- ASTM (American Society for Testing and Materials), 1995: Standard Guide for Risk-Based Corrective Action Applied at Petroleum Release Sites. E1739-95e1, ASTM International.

- Atkinson, T.C., Harmon, R.S., Smart, P.L. and Waltham, A.C., 1978. Palaeoclimatic and geomorphic implications of $^{230}\text{Th}/^{234}\text{U}$ dates on speleothems from Britain. *Nature* 272: 24–28.
- Bakalowicz, M., 1975. Géochimie des eaux karstiques et karstification. (Karst groundwater geochemistry and karstification). *Annales de Spéléologie* 30(4): 581–589.
- Bakalowicz, M., 1979. Contribution de la géochimie des eaux à la connaissance de l'aquifère karstique et de la karstification. (Contribution of water geochemistry to the knowledge of karst aquifer and karst processes). Doctorat és Sciences naturelles Thesis, P. et M. Curie Paris-6, Paris, 269 pp.
- Bakalowicz, M., 2005. Karst groundwater: a challenge for new resources. *Hydrogeology Journal*, 13: 148–160.
- Bakalowicz, M., Blavoux, B. and Mangin, A., 1974. Apports du traçage isotopique naturel à la connaissance du fonctionnement d'un système karstique—teneurs en oxygène 18 de trois systèmes des Pyrénées, France. (Natural isotope tracing as an informer of karst system functioning. Oxygen-18 content of three karst systems in the Pyrenees, France.). *J Hydrol* 23: 141–158.
- Barber, C., Bates, L.E., Barron, R. and Allison, H., 1993. Assessment of the relative vulnerability of groundwater to pollution: a review and background paper for the conference workshop on vulnerability assessment, AGSO 14(2/3), pp 147-154.
- Barnard, H., 1997. Geohydrological investigation of the catchment of Maloney's eye. Unpublished M Sc Thesis. University of the Free State, Bloemfontein, RSA.
- Barnard, H.C., 2000. An Explanation of the 1:500 000 General Hydrogeological Map. Department of Water Affairs and Forestry, Pretoria, RSA.
- Bekesi, G. and McConchie, L., 2002. The use of aquifer-media characteristics to model vulnerability to contamination, Manawatu region, New Zealand. *Hydrogeology Journal*, 10: 322–331
- Berg, R.C. and Kempton, J.P., 1988. Stack-unit mapping of geologic materials in Illinois to a depth of 15 metres. Illinois State Geol Surv Circ 542, 23 pp.

- Beukes, N. J. 1986. The Transvaal Sequence in Griqualand West. In: *Mineral Deposits of Southern Africa* (Edited by Anhaeusser, C. R. and Maske, S.) pp819- 828. Geological Society South Africa, Johannesburg.
- Boormand D.B., Hollis J.M. and Lilly A., 1995. Report no.126, Hydrology of soil types: a hydrologically-based classification of the soils of the United Kingdom. Published by the Institute of Hydrology.
- Brechenmacher, J., 2002. Application of the PI method for Groundwater vulnerability mapping in the karst aquifer of Sierra de Líbar (Andalusia / Spain) Processing and analysis with GIS. Diplom. Thesis in Geoecology. Univ. of Karlsruhe. Unpublished. 109 p.
- Bredenkamp, D.B., 1995. *Dolomitic Groundwater Resources of the Republic of South Africa*. Technical Report Gh3857. Directorate Geohydrology. Department of Water Affairs and Forestry, Pretoria, RSA.
- Bredenkamp, D.B., van der Westhuizen, C., Wiegmanns, F.E. and Kuhn, C.M., 1986. *Groundwater supply potential of dolomite compartments west of Krugersdorp*. Technical Report Gh3440. Directorate Geohydrology. Department of Water Affairs and Forestry, Pretoria, RSA.
- Brink, A.B.A., 1979. *Engineering Geology of Southern Africa, Volume 1*, Building Publications, Silverton.
- Brink, A.B.A. and Partridge, T.C., 1965. Transvaal karst: some considerations of development and morphology, with special reference to sinkholes and subsidences on the Far West Rand. *South African Geographical Journal*, 47, pp.11-34.
- Button, A., 1973. A regional study of the stratigraphy and development of the Transvaal Basin in the eastern and northeastern Transvaal. *Ph. D. dissertation 352p*. University Witwatersrand, Johannesburg, South Africa.
- Button, A., 1986. The Transvaal sub-basin of the Transvaal Sequence. In: Anhaeusser, C.R., Maske, S. (Eds.), *Mineral Deposits of Southern Africa*. Geological Society of South Africa, Johannesburg, pp 811-817.

- Campbell, R., 2004. Summary of the literature reviews. AVAP Steering Committee Meeting 22/9/04 Document 2. WRC Project K5/1432 [unpublished].
- Civita, M., 1994. Le carte della vulnerabilit a degli acquiferi all'inquinamento: teoria e pratica [Contamination vulnerability mapping of the aquifer: theory and practice]. Quaderni di Tecniche di Protezione Ambientale, Pitagora Editrice
- Clendenin, C.W., 1989. Tectonic influence on the evolution of the early Proterozoic Transvaal Sea, southern Africa. *Ph. D. dissertation 367p*. University Witwatersrand, Johannesburg, South Africa.
- Cornaton, F., Goldscheider, N., Jeannin, P.Y., Perrochet, P., Pochon, A., Sinreich, M. and Zwahlen, F., 2003. The VULK analytical transport model and mapping method. In Zwahlen, F. (ed), 2003. Vulnerability and risk mapping for the protection of carbonate (karst) aquifers, final report (COST action 620). European Commission, Brussels. pp 155-160.
- Daly D. and Drew, D., 2000. Irish methodologies for karst aquifer protection. – In: Beck, B. F., Pettit, A. J. and Herring, J. G. (Eds). *Hydrogeology and Engineering Geology of Sinkholes and Karst 1999*, 267-272, Balkema, Rotterdam.
- Daly, D., Dassargues, A., Drew, D., Dunne, S., Goldscheider, N., Neale, S., Popescu, C.H. and Zwahlen, F., 2002. Main concepts of the “European Approach“ for (karst) groundwater vulnerability assessment and mapping. – *Hydrogeological Journal*, 10, 2: 340 – 345.
- Daly, D. and Misstear, B.D., 2002. The groundwater protection scheme in Ireland: a risk-based tool for effective land-use planning. Proceedings of Conference ‘Protecting Groundwater’, Birmingham. Environment Agency (England and Wales), 134-144.
- De Kock, W.P., 1964. The geology and economic significance of the West Wits line. In Geology of some Ore Deposits in southern Africa. *J. Geol. Soc. S. Afr.* pp 323-386.
- Delannoy, J.J., 1987. Reconocimiento biof sico de espacios naturales de Andaluc a. AMA, Junta Andaluc a, 50p.

- Department of Water Affairs and Forestry (DWAF), 1992. Hydrology of the Upper Crocodile River sub-system. Report Number: PA200/00/1492, Volume 1 and 2. DWAF, Pretoria.
- Dreybrodt, W., 1998, Limestone dissolution rates in karst environments. *Bulletin d'Hydrogéologie*, Centre d'Hydrogéologie, Université de Neuchâtel, 16:167–183.
- Drogue, C., 1974. Structure de certains aquifères karstiques d'après les résultats de travaux de forage. (Structure of certain karst aquifers from drilling data). *CR Acad Sci Paris*, série III (278):2621–2624.
- Dunne, S., 2003a. A Localised European Approach (LEA). In Zwahlen, F. (ed), 2003. Vulnerability and risk mapping for the protection of carbonate (karst) aquifers, final report (COST action 620). European Commission, Brussels. pp 161-163.
- Dunne, S., 2003b. Appendix - Existing Vulnerability Mapping Methods. In Zwahlen, F. (ed), 2003. Vulnerability and risk mapping for the protection of carbonate (karst) aquifers, final report (COST action 620). European Commission, Brussels. pp 293-297.
- Enslin, J.F. and Kriel, J.P., 1967. The assessment and possible use of the dolomitic groundwater resources of the Far West Rand, Transvaal. International Conf. Water Peace, Washington.
- Eraso, A., 1986. Metodo de prediccion de las direcciones principales de drenaje en el karst. (Method for predicting the main directions of drainage in karst). *Kobie* 15:15 122.
- Eriksson, P.G. and Reczko, B.F.F., 1995. The sedimentary and tectonic setting of the Transvaal Supergroup floor rocks to the Bushveld Complex. *Journal of African Earth Sciences*. **21**, 487-504.
- Eriksson, P.G. and Truswell, J.F., 1974. Stratotypes from the Malmani Subgroup north-west of Johannesburg, South Africa. *Transactions Geological Society South Africa* **77**, 211-222.

- Eriksson, K. A., McCarthy, T. S. and Truswell, J. F. 1975. Limestone formation and dolomitisation in a lower Proterozoic succession from South Africa. *Journal Sedimentary Petrology* 45,604-614.
- Eriksson, P.G., Schweitzer, J.K., Bosch, P.J.A., Schreiber, U.M., van Deventer, J.L. and Hatton, C.J., 1993. The Transvaal Sequence: an overview. *Journal of African Earth Sciences*. **16**, 25-51.
- Eriksson, P.G., Hattingh, P.J. and Altermann, W., 1995. An overview of the geology of the Transvaal Sequence and Bushveld Complex, South Africa. *Mineralium Deposita* **30**, 98-111.
- Eriksson, P. G., Altermann, W., Catuneanu, O., van der Merwe, R. and Bumby, A.J., 2001. Major influences on the evolution of the 2.67-2.1 Ga Transvaal basin, Kaapvaal craton. *Sedimentary Geology*. **141-142**, 205-231.
- Eriksson, P.G., Altermann, W. and Hartzler, F.J., 2006. The Transvaal Supergroup and its Precursors. In Johnson, M.R., Anhaeusser, C.R. and Thomas, R.J. (eds), 2006. *The Geology of South Africa*. The Geological Society of South Africa, Johannesburg.
- European Water Directive, 2000. Directive 2000/60/EC of the European Parliament and of the Council of 23 October 2000 establishing a framework for Community action in the field of water policy.
- Fedra, K. and Weigkricht, E., 1995. Integrated information systems for technological risk assessment. – In: Beroggi, G.E.G. and Wallace, W.A. (Eds.). *Computer supported risk management*, 320 p., Kluwer, Dordrecht.
- Fleisher, J.N.E., 1981. *The Geohydrology of the dolomite aquifers of the Malmani subgroup in the south-western Transvaal, Republic of South Africa*. Technical Report Gh3169. Directorate Geohydrology. Department of Water Affairs and Forestry, Pretoria, RSA.
- Ford, D.C. and Williams, P.W., 1989. *Karst geomorphology and hydrology*. Academic Division of Unwin Hyman Ltd, London, 601 pp.

- Foster, M.B.J., 1984. *Steenkoppies and Zwartkrans dolomite compartments – Preliminary Geological Report*. Technical Report Gh3346. Directorate Geohydrology. Department of Water Affairs and Forestry, Pretoria, RSA.
- Foster, S.S.D., 1987. Fundamental concepts in aquifer vulnerability, pollution risk and protection strategy. –*TNO Committee on Hydrological Research, Proceedings and Information*. 38, 69-86, Den Haag.
- Foster, S.S.D. and Hirata, R.C.A., 1988. Groundwater pollution risk assessment: a methodology using available data. – WHO-PAHO-CEPIS, Technical Report, 73 p., Lima, Peru.
- Goldscheider, N., 2003. The PI method. In Zwahlen, F. (ed), 2003. Vulnerability and risk mapping for the protection of carbonate (karst) aquifers, final report (COST action 620). European Commission, Brussels. pp 144-154.
- Goldscheider, N., Klute, M., Sturm, S. and Hötzl, H., 2000a. Kartierung der Grundwasserverschmutzungsempfindlichkeit eines ausgesuchten Karstgebietes bei Engen, Baden-Württemberg. – Final report: 83 p; Karlsruhe [unpublished].
- Goldscheider, N., Klute, M., Sturm, S. and Hötzl, H., 2000b. The PI method – a GIS-based approach to mapping groundwater vulnerability with special consideration of karst aquifers. – *Z. angew. Geol.*, 46 (2000) 3: 157-166; Hannover.
- Grillot, J.C., 1977. A propos de méthodologies d'analyses quantitatives, à l'échelle régionale, de champs de fractures: premiers résultats d'une application. (Methodologies for quantitative analyses, at a regional level, of fracture fields: first results). *Revue de Géographie Physique et de Géologie Dynamique*, XIX (3):219–234.
- Gunn, J., 1986. Modelling of conduit flow dominated karst aquifers. In Günay, G. & Johnson, A.I. (eds), *Karst water resources*. IAHS, Publication 161: 587-596. Wallington, UK.
- Hälbich, I.W., Scheepers, R.S., Lamprecht, D., van Deventer, J.N. and de Kock, N.J., 1993. The Transvaal-Griqualand West banded iron formation: geology, genesis, iron exploitation. *Journal of African Earth Sciences* **16**, 63-120.

- Hartzer, F. J., 1995. Transvaal Supergroup inliers: geology, tectonic development and relationship with the Bushveld Complex, South Africa. *Journal of African Earth Sciences*. **21**, 521-547.
- Holland, M., 2007. Groundwater resource directed measures in Karst terrain with emphasis on aquifer characterization in the Cradle of Humankind near Krugersdorp, South Africa. Unpublished MSc thesis. University of Pretoria, Pretoria, South Africa.
- Hölting, B., Haertle, T., Hohberger, K.H., Nachtigall, K. H., Villinger, E., Weinzierl, W. & Wrobel, J.-P., 1995. Konzept zur Ermittlung der Schutzfunktion der Grundwasserüberdeckung. – *Geol. Jb.*, C63: 5-24; Hannover.
- International Association of Hydrogeologists [IAH] Karst Commission, 1999: Karst Groundwater. (Available from <http://www.karst-hydrogeology.de/iah-karst.html>).
- Jeannin, P.Y., Cornaton, F., Zwahlen, F. and Perrochet, P., 2001. VULK: a tool for intrinsic vulnerability assessment and validation. – 7th Conference on Limestone Hydrology and Fissured Media, Besançon 20–22 Sep. 2001, *Sci. Tech. Envir., Mém. H. S.*, 13: 185-190.
- Keefer, D.A. and Berg, R.C., 1990. Potential for aquifer recharge in Illinois. Illinois Dept Energy Nat Resources, Illinois State Geol Surv, Champaign.
- Kiraly, L., 1997. Modelling karst aquifers by the combined discrete channel and continuum approach, 6th Conference on limestone hydrology and fissured aquifers, session on modelling karst aquifers. Université de Franche-Comté, Sciences et Technique de l'Environnement, La Chaux-de-Fonds, pp 1–26.
- Kiraly, L., 2003. Karstification and Groundwater Flow. *Speleogenesis and Evolution of Karst Aquifers*, 1 (3), pp.2-26.
- Klute, M. 2000. GIS-gestützte Anwendung und Entwicklung von Methoden zur Vulnerabilitätskartierung unter besonderer Berücksichtigung der Infiltrationsbedingungen am Beispiel eines Karstgebietes bei Engen (Hegau, Baden-Württemberg). – Master thesis Univ. Karlsruhe: 130 p; Karlsruhe [unpublished].

- Kovar, K. and Nachtnebel, H. P., (Eds.) 1993. Application of Geographic Information Systems in Hydrology and Water Resources Management. IAHS Public., 235, IAHS Press, Wallingford.
- Kralik, M. and Keimel, T., 2003. The Time-Input method. In Zwahlen, F. (ed), 2003. Vulnerability and risk mapping for the protection of carbonate (karst) aquifers, final report (COST action 620). European Commission, Brussels. pp 172-180.
- Kuhn, C.M., 1986. *Geohydrological investigation of the western and central Steenkoppies compartment*. Technical Report Gh3446. Directorate Geohydrology, Department of Water Affairs and Forestry, Pretoria, RSA.
- Lobo-Ferrerira J. P., 2000. The European Union experience on groundwater vulnerability assessment and mapping. – 7 p., Internet. (Available from <http://www.teriin.org>).
- Lynch, S.D., Reynders, A.G. and Schulze, R.E., 1994. Preparing input data for a national-scale groundwater vulnerability map of southern Africa. *Water SA*, Vol 20, no. 3 pp 239-246.
- Magiera, P., 2002. GIS-gestützte Bewertung der Verschmutzungsempfindlichkeit des Grundwassers. – *Geol. Jahrb.*, Reihe C, Heft SC 3, 165 p., Hannover.
- Mangin, A., 1974. Contribution à l'étude hydrodynamique des aquifères karstiques. (Contribution the hydrodynamics of karst aquifers). *Annales de Spéléologie*, 29(3):283–332; 29(4):495–601; 30(1):21–124.
- Mangin, A., 1984. Pour une meilleure connaissance des systèmes hydrologiques à partir des analyses corrélatoire et spectrale. (For a better knowledge of hydrological systems by means of correlation and spectrum analyses). *J Hydrol* 67:25–43.
- Mangin, A., 1994. Karst hydrogeology. In: Stanford, J., Gibert, J. and Danielopol, D. (eds). *Groundwater ecology*. Academic Press. pp 43–67.
- Marker, M.E., 1972. Karst landform analysis as evidence for climatic change in Transvaal. *South African Geographical Journal*, 54, pp.152-162.
- Marker, M.E., 1980. A systems model for karst development with relevance for Southern Africa. *South African Geographical Journal*. 62, 151-163.

- Marsaud, B., 1996. Structure et fonctionnement de la zone noyée des karsts à partir des résultats expérimentaux. (Structure and functioning of the saturated zone of karsts from experimental results). Doctorate Thesis, Paris XI, Orsay, 305 pp.
- Martini, J.E.J. and Kavalieris, I., 1976. The karst of the Transvaal (South Africa). *International Journal of Speleology*, 8, pp. 229-251.
- Martini, J.E.J., Wipplinger, P.E., Moen, H.F.G. and Keyser, A., 2003. Contribution to the Speleology of Sterkfontein Cave, Gauteng Province, South Africa. *International Journal of Speleology*, 32, pp.43-69.
- Macvicar, C.N. (ed.), 1984. Land types of the maps 2626 Wes-rand 2627 Kroonstad. Memoirs on the agricultural natural resources of South Africa. No. 4. Department of Agriculture, Pretoria.
- Morris, B. L. and Foster, S.S.D., 2000. Cryptosporidium Contamination Hazard Assessment and Risk Management for British Groundwater Sources. – *Water Science and Technology*, 41/7, pp 67-77.
- Mudry, J., 1990. Les courbes flux chimique-débit et le fonctionnement des aquifères karstiques. (Chemical mass flow vs. discharge and the functioning of karst aquifers). *J Hydrol* 120 (1–4): 283–294.
- NRC (National Research Council), 1993. *Groundwater vulnerability assessment, Contamination potential under conditions of uncertainty*, Committee on Techniques for Assessing Ground Water Vulnerability, Water Science and Technology Board, Commission on Geosciences Environment and Resources, National Academy Press, Washington DC.
- Navulur, K.C.S., Engel, B.A. and Mamillapalli, S., 1995. Groundwater vulnerability evaluation to nitrate pollution on a regional scale using GIS. Applications of GIS to the modelling of non-point source pollutants in the vadose zone. ASA-CSSASSSA Bouyoucos Conf, Mission Inn, Riverside, CA, 1–3 May 1995.
- NEPC (National Environment Protection Council), 2000. Framework for the application of the Australian water quality. Schedule B (6) – Guideline on risk based assessment of groundwater contamination. – 18 p., Canberra, Australia.

- Obbes, A.M., 2000. The structure, stratigraphy and Sedimentology of the Black Reef-Malmani-Rooihogte succession of the Transvaal Supergroup southwest of Pretoria. Council for Geoscience Bulletin 127, Pretoria.
- Parsons, R. and Jolly, J., 1994. The development of a systematic method for evaluating site suitability for waste disposal based on geohydrological criteria. WRC Report No. 485/1/94, Pretoria, RSA.
- Partridge, T.C., 1994. The Land System and Land Type Classifications: Comparisons and Applications in the Southern African Context. Proceedings of the 4th Symposium on Terrain Evaluation & Data Storage, Including a Seminar on Remote Sensing Techniques; 1994 August 3-5, Midrand, Johannesburg.
- Pinault, J.L, Bakalowicz, M., Plagnes, V., Aquilina, L., 2001. Inverse modelling of the hydrological and the hydrochemical behaviour of hydrosystems: characterization of karst system functioning. *Water Resource Research*, 37, pp. 2191-2204.
- Plagnes, V., 1997. Structure and functioning of karst systems. Characterisation by means of water geochemistry. Doctorate Thesis, Université Montpellier II, Montpellier, 372 pp.
- Razack, M., 1980. Approche quantitative de l'effet d'échelle sur le relevé de la fracturation par photo-interprétation dans l'étude de la géométrie des réservoirs fissurés. (Quantitative approach of the scaling effect on fracturation analysis by interpreting aerial graphs for the study of the geometry of fissured reservoirs). *Mémoires hors série de la Société géologique de France*, 11:81-90.
- Reynders, A.G., 1994. Protection of shallow groundwater resources by means of aquifer vulnerability mapping. In: Proc Water Down Under '94 Conf, Adelaide, Australia, 21-25 November 1994, pp 631-636.
- Robb, L.J. and Robb, V.M., 1998. Gold in the Witwatersrand Basin. In: Anhaeusser, C.R., Wilson, M.G.C., (Eds.), *The Mineral Resources of Southern Africa*. Geological Society of South Africa, Johannesburg, pp 294-349.

- Robb, L.J., Brandl, G., Anhaeusser, C.R. and Poujol, M., 2006. Archaean Granitoid Intrusions. In Johnson, M.R., Anhaeusser, C.R. and Thomas, R.J. (eds), 2006. The Geology of South Africa. The Geological Society of South Africa, Johannesburg.
- Rouch, R., 1980. Les Harpacticides, indicateurs naturels de l'aquifère karstique. (Harpacticoidea, natural tracers of karst aquifers). *Mémoires hors série de la Société géologique de France*, 11:109–116.
- S.A.C.S., 1980. Stratigraphy of South Africa, Part 1. *Geol. Surv. S. Afr.* Pretoria.
- Scanlon, B.R., Mace, R.E., Barrett, M.E. and Smith, B.D., 2003. Can we simulate regional groundwater flow in a karst system using equivalent porous media models? Case study, Barton Springs Edwards aquifer. *Journal of Hydrology*, 276, pp. 137-158.
- Scholles, F., 1997. Abschätzen, Einschätzen und Bewerten in der UVP. Weiterentwicklung der Ökologischen Risikoanalyse. Weiterentwicklung der Ökologischen Risikoanalyse. *UVP-Spezial*, 13, Dortmund.
- Sililo, O.T.N., Saayman, I.C. and Fey, M.V., 2001. Groundwater Vulnerability to Pollution in Urban Catchments. Report to the Water Research Commission. WRC Project No. 1008/1/01, Water Research Commission, Pretoria, RSA.
- Sturm, S. 1999. GIS-gestützte Anwendung und Entwicklung von Methoden zur Vulnerabilitätskartierung am Beispiel eines Karstgebietes bei Engen (Hegau, Baden Württemberg) unter besonderer Berücksichtigung der Schutzfunktion der Grundwasserüberdeckung. – Master thesis Univ. Karlsruhe: 97 p.; Karlsruhe [unpublished].
- Trollip, N., 2006. *The geology of an area south of Pretoria with specific reference to dolomite stability*. MSc. thesis (unpublished),. University of Pretoria. Pretoria, South Africa.
- U.S.EPA Environmental Protection Agency, 1996. Groundwater use and value determination Guidance. A resource- based approach to decision making. – EPA, Region 1, New England, Final Draft, April 1966, Washington.

- Van Schalkwyk, A. and Vermaak, J.J.G., 2000. The Relationship between Geotechnical and Hydrogeological properties of residual soils and rocks in the vadose zone. WRC Report No. 701/1/00, Water Research Commission, Pretoria, RSA.
- Van Stempvoort, D., Ewert, L. and Wassenaar, L.I., 1993. Aquifer vulnerability index: a GIS based method for groundwater vulnerability mapping. *Can Water Resour J* 18(1):25–37.
- Vías, J.M., Andreo, B., Perles, M.J., Carrasco, F., Vadillo, I. and Jiménez, P., 2003. The COP method. In Zwahlen, F. (ed), 2003. Vulnerability and risk mapping for the protection of carbonate (karst) aquifers, final report (COST action 620). European Commission, Brussels. pp 163-171.
- Vías, J.M., Andreo, B., Perles, M.J., Carrasco, F., Vadillo, I. and Jiménez, P., 2006. Proposed method for groundwater vulnerability mapping in carbonate (karstic) aquifers: the COP method, Application in two pilot sites in Southern Spain. *Hydrogeology Journal*, 6, pp 912-925.
- von Hoyer, M. and Söfner, B., 1998. Groundwater vulnerability mapping in carbonate (karst) areas of Germany. BGR Hannover, Archive Nr. 117 854, report for EC-project COST Action 620; 38 p. [unpublished].
- Vrba, J. and Zoporozec, A., (eds.) 1994. *Guidebook on Mapping Groundwater Vulnerability*. International Contributions to Hydrogeology (IAH), 16: 131 p.; Hannover.
- Wolmarans, J.F., 1986. Some engineering-geological and hydrological aspects of mining on the West Wits Line. In: *Mineral Deposits of southern Africa*. I. Geol. Soc. S. Afr. pp. 701-796.
- Zakharova, J.V., 2001. Principles of risk assessment for groundwater contamination. – EGS, 26th Gen. Assembly, Nice 2001, Geophysical. Research Abstracts, CD-ROM edition, vol.3, 2001.
- Zwahlen, F. (ed), 2003. Vulnerability and risk mapping for the protection of carbonate (karst) aquifers, final report (COST action 620). European Commission, Brussels.